The Hong Kong Polytechnic University

Department of Building Services Engineering

Experimental and Numerical Investigation of Integration of Cooled-ceiling, Nocturnal Sky Radiative Cooling and MPCM Slurry Thermal Storage

Zhang Shuo

A thesis submitted in partial fulfillment of the requirements for the Degree of Doctor of Philosophy

June, 2012

Certificate of Originality

I hereby declare that this thesis is my own work and that, to the best of my knowledge and belief, it reproduces no material previously published or written, nor material that has been accepted for the award of any other degree or diploma, except where due acknowledgement has been made in the text.

_____ (Signed)

_____Zhang Shuo_____ (Name of student)

Department of Building Services Engineering
The Hong Kong Polytechnic University
Hong Kong SAR, China
June, 2012

Abstract

Abstract of thesis entitled: Experimental and Numerical Investigation of Integration of Cooled-ceiling, Nocturnal Sky Radiative Cooling and MPCM Slurry Thermal Storage

Submitted by : Zhang Shuo

For the degree of : Doctor of Philosophy

at The Hong Kong Polytechnic University in June, 2012.

The energy consumption of buildings for cooling purposes has increased considerably during the last decades. Especially in hot climate countries, the penetration of conventional air conditioning units is extremely important, having a serious impact on the peak electricity load. In recent years, new type phase change materials (PCM), microencapsulated phase change materials (MPCM) slurry, are investigated to be used as the thermal storage medium for building cooling applications to achieve the purpose of peak load shifting and energy saving.

In this study, paraffin was chosen as the core material of MCPM slurry. The effect of supercooling, one of the major problem for PCM application, on the thermal properties of MPCM slurry was experimental investigated. In addition, the study investigated the proper method to prevent supercooling of PCM by using carbon nanotube (CNT) particles as nucleating agent. Finally, the utilization potential of nocturnal sky radiator combined with MPCM slurry as thermal storage medium is simulated and discussed.

At the beginning of the thesis, latent heat of fusion, melting and solidification temperatures and supercooling degree of the material of PCM and MPCM slurry were investigated by using differential scanning calorimeter (DSC). An experimental test device with whole hybrid air conditioning system was also set up to measure the dynamic heat transfer performance of hybrid system combined with cooled ceiling system and MPCM slurry TES under the practical operation scheme. The water slurry of microencapsulated n-hexadecane with a melting temperature of 15.7 ℃ was cooled to 5 ℃ and heated to 25 ℃ cyclically in a storage tank of 230 litre. Melting and crystallization behaviours of MPCM slurry running in a thermal storage test system were investigated experimentally. Furthermore, supercooling and its effect on effective latent heat of MPCM slurry with different experimental conditions were also calculated and evaluated. Empirical equations were obtained to describe the relationship between the effective latent heat and the charging temperature, which can be used for determining the medium mass needed for a specified working temperature range.

Afterwards, CNT was used as the nucleating agent for prevention of supercooling. Various surfactants are firstly tested as additives to overcome the rapid aggregation and sedimentation of the nanoparticles in the organic liquid. Stable and homogenous dispersion was finally attained through surface modification of the MWCNT particles with strong acids H_2SO_4 and HNO_3, plus the addition of 1-decanol as a surfactant to hexadecane organic liquid. The average hydrodynamic diameter of MWCNT-1-decanol in hexadecane was measured by dynamic light scattering (DLS) analysis and the morphology of nano-additives was observed by transmission electron microscopy (TEM). The visible aggregation was negligible even after seven

days. Thermal analysis of the n-hexadecane with well dispersed MWCNT particles by DSC indicated that the supercooling of n-hexadecane was significantly decreased with the concentration of 0.1% and 0.5% but only slightly with the concentrations over 1.0%. It appears that well dispersed nanoparticles provided stable foreign nuclei of proper size to promote the heterogeneous nucleation process and accelerate crystallization process, thus the supercooling was significantly reduced. The obvious effects of MWCNT particles on the decrease of supercooling of n-hexadecane provide promising way of improving the performance of system energy efficiency in building cooling and heating applications.

At the end of the thesis, a mathematical model of the combined system of MPCM slurry, nocturnal sky radiator and cooled ceiling was built. The cooling energy consumption and the effect of energy-free nocturnal radiation application were simulated using the energy simulation code ACCURACY and MATLAB model based on hour-by-hour calculations in five typical cities across China. It can be drawn that MPCM slurry appears to be a good medium for the combined application of passive cooling technology and the nocturnal radiation in air conditioning system due to its relatively high working temperature. The results showed the energy saving potential in Lanzhou and Urumqi can reach 77% and 62% for low-rise buildings, which exhibits strong attractions for building energy conservation and emission reduction. Hong Kong has the weakest effect in the five typical cities under the same operating condition due to the hot and humid climate condition. The present hybrid system is recommended to be used in northern west and central China cities where the weather is dry and the ambient temperature is low at night.

Publications arising from the thesis

I. Journal Paper

- Zhang, S. and J. Niu, Experimental investigation of effects of supercooling on microencapsulated phase-change material (MPCM) slurry thermal storage capacities. Solar Energy Materials and Solar Cells, 2010. 94(6): p. 1038-1048. (Based on Chapter 3)
- Zhang, S., et al., Effective dispersion of multi-wall carbon nano-tubes in hexadecane through physiochemical modification and decrease of supercooling. Solar Energy Materials and Solar Cells, 2012. 96(1): p. 124-130. (Based on Chapter 4)

II. Manusctipt

- Zhang, S., and J. Niu, Simulation investigation of nocturnal sky radiator combined with MPCM slurry thermal energy storage for building cooling applications. (Based on Chapter 5)

III. Conference Paper

- Niu, J., et al., Prevention of Supercooling of Hexadecane as Latent Thermal Storage Materials, in 4th International Symposium on Heat Transfer and Energy Conservation. 2012: Guangzhou, China.
- Zhang, S. and J. Niu, Experimental Investigation of Effective Cooling Storage Capacity of Microencapsulated PCMs with Low Supercooling

Degrees for Building Cooling Storage Applications, in International Conference on Applied Energy. 2010: Singapore. p. 1882-1891.

- Niu, J., S. Zhang, and Y. Zhang, Developing phase-change-materials with low supercooling degrees for ther mal energy storage, in Clima 2010, 10th REHVA World Congress "Sustainable Energy Use in Buildings". 2010: Antalya, Turkey.
- Zhang, S. and J. Niu. Effective Cooling Storage Capacity Characteristics of Supercooled Phase-Change Materials for Building Cooling Applications. in 6th International Symposium on Heating, Ventilating and Air Conditioning Proceedings. 2009. Nanjing, PR. China. P.428-435.
- Niu, J. and S. Zhang. The Impact of Supercooling on The Effective Cooling Storage Capacity of Phase-Change Materials in Natural Cooling Application. in 2009 ASME Summer Heat Transfer Conference Proceedings. 2009. San Francisco, Califonia USA: American Society of Mechanical Engineers,U.S.
- Zhang.S. and J. Niu. Experimental Investigation of Microencapsulated Phase-Change Material (MPCM) Slurry Effective Thermal Storage Capacities. Proceedings of the First International Postgraduate Conference on Infrastructure and Environment, 2009. Hong Kong, China: 31-44.

Acknowledgements

I would like to take this opportunity to express my heartfelt gratitude to my supervisor, Professor Niu Jianlei. His bright and sharp academic sense, invaluable guidance and advice, and continuous and powerful support enabled me to advance along the hard road of PhD study. I appreciate the way he encouraged me to initiate my own ideas by exploring the research field, directing me to conduct investigations from research interests and steadily supporting me in finishing this work. This thesis could not have been completed without his devoted supervision.

I would like to express my appreciation to my co-supervisor, Professor Li Yi. His advice and guidance have complemented many aspects of my study, especially his help on the issue of MPCM slurry production.

I am grateful to Prof. Wu Jianyong for his kind guidance on the experiment about nanoparticle dispersion. I also would like to express my gratitude to Mr. Cheng Angus for the TES experimental rig construction, Mr. Han Yu for the heat transfer test of MPCM slurry, Mr. Tse Chi Tat for the experiment work about nanoparticle dispersion, and Ms. Song Qingwen for preparing the MPCM slurry for this study. I am thankful for their assistance. The experiments could never be completed without their help.

Last but not least, I would like to thank my husband Wu Lei and my parents for their crucial support and help. And I would like to dedicate this to my baby daughter Vivian.

Table of Contents

Certificate of Originality ..... **i**

Abstract ..... **ii**

Publications arising from the thesis ..... **v**

Acknowledgements ..... **vii**

Table of Contents ..... **viii**

List of Figures ..... **xii**

List of Tables ..... **xv**

Nomenclature ..... **xvi**

Chapter 1 Introduction **1**

1.1 Background **1**

1.2 Statement of the Problem **5**

1.3 Research Objectives **8**

1.4 Outline of This Thesis **10**

Chapter 2 Literature Review **13**

2.1 Thermal Energy Storage **13**

2.1.1 Definition and Classification of TES System 13

2.1.2 Potential of Application of TES in Building Cooling Applications ... 15

2.2 Phase Change Material as Thermal Storage Medium **19**

2.2.1 Classification and Properties of PCM 19

2.2.2 Selection of Proper PCM 22
2.2.3 MPCM Slurry Application as TES Medium 26

2.3 Supercooling and Prevention Methods 28
2.3.1 Supercooling Problem 28
2.3.2 Mechanism of Supercooling 31
2.3.3 Factors Affecting Supercooling and the Prevention of Supercooling 33

2.4 Nano Materials as Nucleation Agent 36
2.4.1 Classical Theory of Nucleation 36
2.4.2 Nucleation Agent for Supercooling Prevention 42
2.4.3 Nanoparticles as Nucleation Agent 48
2.4.4 Dispersion of Nanoparticles in Liquid 50

2.5 Nocturnal Sky Radiative cooling Applications 53
2.5.1 Passive Cooling Application 53
2.5.2 Radiator Model Investigations 55
2.5.3 Radiative Cooling Application Conditions 61

Chapter 3 Effects of Supercooling on MPCM Slurry Thermal Storage Capacities 63

3.1 Introduction 63

3.2 Experimental Approach 65
3.2.1 Microcapsule and Slurry Preparation 65
3.2.2 Slurry Properties 65
3.2.3 DSC Measurements 66
3.2.4 Experimental System Description 71

3.3 Results and Discussion 75
3.3.1 Heat Loss of the Thermal Storage Tank and Heat Balance Analysis . 75
3.3.2 Charging/Discharging Process 79
3.3.3 Supercooling and Effective Latent Heat 82

3.4 Conclusions 91

Chapter 4 Supercooling Prevention of Hexadecane by Addition of Carbon Nano-Tubes 93

4.1 Introduction 93

4.2 Experimental 94

4.2.1 Materials 94

4.2.2 Dispersion of MWCNT Nanoparticles in n-Hexadecane 95

4.2.3 Characterization and Analysis of Nanoparticles 97

4.2.4 Thermal Analysis of PCM 100

4.3 Results and Discussion 101

4.3.1 Dispersion of MWCNT in n-Hexadecane 101

4.3.2 The Particle Size of MWCNT-1-decanol 107

4.3.3 Morphology of MWCNT 108

4.3.4 Supercooling Reduction 110

4.3.5 Discussion 114

4.4 Conclusions 115

Chapter 5 Utilization Potential of Nocturnal Radiative Cooling Combined with MPCM Slurry Storage and Cooled Ceiling 117

5.1 Introduction 117

5.2 Simulation Model 120

5.2.1 Simulation Tool 120

5.2.2 Structure and Operating Strategy of Hybrid System 121

5.2.3 System Design Description 123

5.3 Mathematical Model 127

5.3.1 Nocturnal Sky Radiator Model 127

5.3.2 Storage Tank Model 139

5.4 Results and Discussion 140

5.4.1 Feasibility Analysis of Radiative Cooling Applications 140

5.4.2 Load Shifting by the Hybrid System 146

5.4.3 Energy Saving Potential of the Hybrid System 151

5.5 Conclusions 162

Chapter 6 Conclusions and Suggestions for Future Research 165

6.1 Conclusions 165

6.1.1 Effect of Supercooling on MCPM Slurry as TES Medium 165

6.1.2 Prevention of Supercooling 167

6.1.3 Nocturnal Radiative Cooling Potential with MPCM slurry Storage 169

6.2 Suggestions for Future Research 171

References 176

List of Figures

Figure 1.1 Energy consumption in commercial buildings in U.S. (U.S. Energy Information Administration 2003) 2
Figure 2.1 Possible methods of reversible storage of heat and cold (Mehling and Cabeza 2008)..... 14
Figure 2.2 Heat storage as latent heat for the case of solid-liquid phase change..... 15
Figure 2.3 Classes of materials that can be used as PCM and their typical range of melting temperature and melting enthalpy (Mehling and Cabeza 2008) 19
Figure 2.4 Physical characteristics of mixture freezing point behavior (Suppes, Goff et al. 2003)..... 22
Figure 2.5 A simple method for making MCPM proposed by Ai, Jin et al. (2007) .. 26
Figure 2.6 Thermal reliability of microcapsules (Sarı, Alkan et al. 2009) 28
Figure 2.7 Schematic temperature change during heating (melting) and cooling (solidification) of a PCM with subcooling (redrawn from Mehling and Cabeza 2008)..... 29
Figure 2.8 Microphotographs of crystallization behavior inside MC (Yamagishi, Sugeno et al. 1996)..... 30
Figure 2.9 The relationship of MPCM particle size and melting /crystallization temperatures (Yamagishi, Sugeno et al. 1996) 34
Figure 2.10 Images of entangled WMCNT a) SEM image and b) TEM image (Ding, Alias et al. 2006) 51
Figure 2.11 Dispersion stability of CNT-in-water nanofluids with 0.01 vol% CNT addition until 120 h settling time (Kim, and et al. 2010) 52
Figure 2.12 A integrated cooling system: a) Schematic flow network for the long-term cool storage mode, and b) Photo of sky radiator (Saitoh and Fujino 2001)..... 56
Figure 2.13 A lightweight metallic radiator (Mihalakakou, Ferrante et al. 1998) 57
Figure 2.14 Schematic drawing of open loop night sky radiative cooling unit (Hamza H. Ali, Taha et al. 1995)..... 57
Figure 2.15 Construction details of the radiator units (Hamza H. Ali, Taha et al. 1995) 58

Figure 3.1 A schematic diagram of a heat flux type DSC showing the heat fluxes between DSC components and the corresponding DSC thermal model. (Rady 2009) 67
Figure 3.2 Definition of DSC characteristic temperatures for a freezing curve (He, Martin et al. 2004) 68
Figure 3.3 DSC curves of heat flow versus (a) temperature and (b) time 69
Figure 3.4 Photograph of Perkin Elmer DSC7 70
Figure 3.5 DSC results of microencapsulated $C_{16}H_{34}$ 71
Figure 3.6 Schematic diagram of experimental air-conditioning system 72
Figure 3.7 Photograph of experimental system: a) chamber, b) cooled ceiling system, and c) MPCM slurry storage system 73
Figure 3.8 Charging process with water as storage medium at 3 mixer speeds: (a) 80rpm, (b) 230rpm and (c) 380rpm 78
Figure 3.9 Charging process with MPCM slurry as storage medium at 3 mixer speeds: (a)80rpm, (b)230rpm and (c)380rpm 80
Figure 3.10 Discharging process with MPCM slurry as storage medium at 3 mixer speeds: (a)80rpm, (b)230rpm and (c)380rpm 82
Figure 3.11 Ratio of freezing latent heat completion at 3 mixer speeds during charging process: (a)80rpm, (b)230rpm and (c)380rpm 87
Figure 3.12 Ratio of freezing latent heat completion at 3 mixer speeds during discharging process: (a)80rpm, (b)230rpm and (c)380rpm 88
Figure 4.1 The device of ultrasound probe used to disperse MWCNTs 96
Figure 4.2 Photograph of Nicolet Avatar 360 FT-IR instrument 98
Figure 4.3 Photograph of Malvern Zetasizer (3000 HSA) DLS instrument 99
Figure 4.4 Photograph of JEOL 2011 TEM instrument 100
Figure 4.5 Photograph of METTLER TOLEDO DSC-822e 101
Figure 4.6 The FTIR spectrum of the modified MWCNT particles 104
Figure 4.7 The schematic diagram of the interaction between 1-decanol and modified MWCNT 107
Figure 4.8 The size distribution of MWCNT-1-decanol in n-hexadecane 108
Figure 4.9 TEM micrographs of original MWCNT on different scales showing the morphology: a) 200 nm and b) 50 nm 109
Figure 4.10 TEM micrographs of well dispersed MWCNT-1-decanol on different scales showing the morphology: a) 200 nm and b) 50 nm 109

Figure 4.11 TEM micrographs of different MWCNT showing the crystal structure of MWCNT: a) original MWCNT and b) MWCNT-1-decanol 110
Figure 4.12 Change in Gibbs free energy $\triangle G$ as a function of radius r of nucleus formed in a supersaturated medium (Sangwal 2007)..... 111
Figure 4.13 DSC melting and freezing curves of the pure n-hexadecane at 5 ℃/min scanning rate and the characteristic temperatures T_m, $T_{m.peak}$, T_f and $T_{f.peak}$. 112
Figure 4.14 DSC curves of the n-hexadecane with MWCNT of different fractions as the nucleating agent (NA): a) heating process and b) cooling process . 113
Figure 5.1 Schematic diagram of the hybrid system..... 122
Figure 5.2 Construction of the nocturnal sky radiator (Erell and Etzion 2000)..... 126
Figure 5.3 A schematic diagram of nocturnal sky radiator..... 128
Figure 5.4 Heat transfer mechanism of nocturnal sky radiator..... 130
Figure 5.5 Flow chart of nocturnal sky radiator calculation 138
Figure 5.6 Typical monthly average weather data in Hong Kong 141
Figure 5.7 Monthly average sky temperature of five cities in China..... 142
Figure 5.8 Percentage annual occurrence of sky temperature of five cities in China 143
Figure 5.9 Monthly average potential cooling capacity of nocturnal sky radiator: a) in Hong Kong and b) in Urumqi 145
Figure 5.10 Potential monthly cooling energy storage supplied by nocturnal sky radiator 151
Figure 5.11 Supply-demand relationship of nocturnal sky radiator system in Urumqi 152
Figure 5.12 Actual monthly cooling energy storage by the nocturnal radiator 155
Figure 5.13 Annual cooling energy storage and radiator application hours 156
Figure 5.14 Percentage of chiller energy saving and the utilization ratio of nocturnal radiator 158
Figure 5.15 Supply-demand relationship of nocturnal sky radiator system for different types of buildings in Urumqi..... 159
Figure 5.16 Chiller energy saving percentage of the hybrid system for different types of buildings..... 161

List of Tables

Table 2.1 Examples of paraffin that have been investigated as PCM (Mehling and Cabeza 2008) 25
Table 3.1 Physical properties of MPCM slurry and its component 66
Table 3.2 Instrument accuracy 74
Table 3.3 System heat balance analysis with water 78
Table 3.4 MPCM Mass fraction of the MPCM slurry determined by heat balance analysis 85
Table 3.5 Freezing latent heat of MPCM when cooled to the temperature of 5 ℃ ... 89
Table 3.6 Regression parameters and error term 90
Table 4.1. Effects of surfactants on dispersion of original MWCNT in n-hexadecane 102
Table 4.2 Effects of surfactants on dispersion of modified MWCNT in n-hexadecane 105
Table 4.3 Melting and crystallization properties of n-hexadecane with MWCNT of different fractions as the nucleating agent (NA) 113
Table 5.1 Thermal Property of the MPCM 139
Table 5.2 Hourly operational parameters of cooling storage system with nocturnal radiator in Urumqi in spring 149
Table 5.3 Hourly operational parameters of cooling storage system with nocturnal radiator in Urumqi in summer 150
Table 5.4 Monthly cooling energy storage by radiator and chiller in Urumqi 153

Nomenclature

Variable	Description	Unit
A	area	m^2
COP	coefficient of performance	-
C_p	specific heat capacity	J/(kg.K)
C_a	cloudiness coefficient	-
ΔG	free energy change	J
h_l	latent heat of fusion	kJ/kg
m	mass	g
$\dot{m}$	mass flow rate	g/s
n	total opaque cloud amount	-
$\dot{Q}$	heat rate	W
Q	cooling energy	J
ΔQ	thermal energy difference	J
R	thermal resistance	W/K
RH	relative humidity	-
T	temperature	^oC
ΔT	temperature difference	^oC
t	time	s
ΔU	sensible heat storage	J
V	wind speed	m/s
Greek symbols		
ε	emissivity, relative approximate error	-

σ	Stefan-Boltzmann constant	$W/(m^2.K^4)$

Subscripts

amb	absolute dry bulb
ave	average
b	building
c	extrapolated end
ce	ceiling
ch	chiller
conv	convective
dew	dew point
e	end peak onset, end, effective
f	end peak, freezing point
i	initial peak, initial
in	inlet
l	liquid
lab	laboratory
loss	heat loss
m	melting point
MPCM	MPCM particle
out	outlet
w	water
p	peak
rad	radiative, radiator
room	room
s	solid
sl	MPCM slurry

sky	clear sky
t	tank
1	time range, inlet
2	time range, outlet

Chapter 1

Introduction

In this chapter, the author addresses the background of the research, starting from the thermal energy storage technology used for building energy saving. Through a brief introduction of related research, this chapter states the main research questions and objectives from the perspectives of the effect of supercooling on MPCM slurry thermal storage capacities, prevention of supercooling and the evaluation the potential of using MPCM slurry storage for nocturnal sky radiator system. At the end of this chapter, the research framework is presented outlining the structure of this thesis.

1.1 Background

The energy consumption of buildings for cooling purposes has increased considerably during the last several decades. Especially in hot climate countries, the penetration of conventional air conditioning units is extremely important, having a serious impact on the peak electricity load (Mihalakakou, Ferrante et al. 1998). As shown in Figure 1.1, in U.S., 51% energy consumed in commercial buildings is used for space heating, cooling and ventilation (U.S. Energy Information Administration 2003). For a typical U.S. home, heating and cooling account for about 56% of the energy use, making it the largest energy expense for most homes (U.S. Department of Energy website). Because of the growing power demand and the huge demand difference between day and night, the electricity supply industry is facing challenges

as never before. Therefore, reducing building cooling energy consumption would have a tremendous impact on easing power supply pressure, enhancing power supply efficiency and reducing CO_2 emissions associated with fossil fuels.

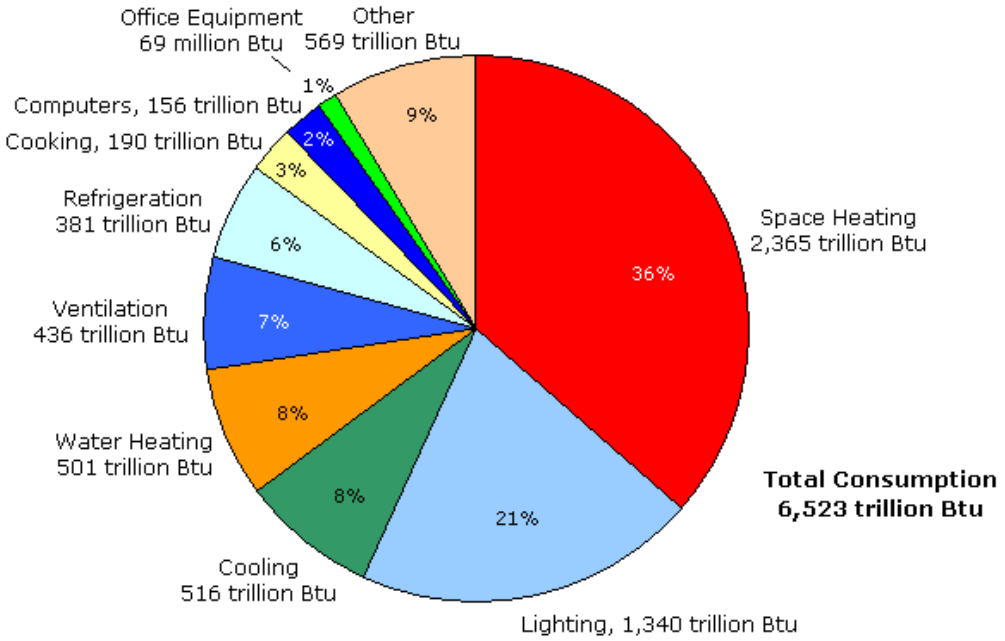

Figure 1.1 Energy consumption in commercial buildings in U.S. (U.S. Energy Information Administration 2003)

Thermal Energy Storage (TES) can be defined as the temporary storage of thermal energy at high or low temperatures for use when it is needed (Thumann and Mehta 2008). Energy storage plays a vital role in energy conservation, because it can reduce the time or rate mismatch between energy supply and energy demand. It can improve the performance of energy systems by smoothing and increases reliability (Garg, Mullick et al. 1985). TES system work best in facilities that are not fully operational at night, such as office buildings, schools, airport terminals, convention centers and sports complexes. There are many advantageous features of a well-designed and correctly operated cool thermal storage system. The installed capacity of chiller and cooling tower capacity can be reduced, and cooling production can be decoupled

from the customer demand thereby making it possible to utilize lower off-peak drive energy rates. A good storage system can provide better energy performance than a conventional instantaneous system because cooling tower runs at a lower ambient temperature at night when charging the storage tank. Increased efficiency also results from all the machinery operating nearer the design points more of their operation time than in conventional systems. Storage systems provide higher reliability since they do not totally depend on instantaneous cooling production. In cases of short shutdown of a chiller it is possible to serve critical areas for a period of time from storage.

In a building space, air is supplied and circulated for the three purposes of ventilation, humidity control and sensible heat removal. However the need for these three requirements varies over time and not necessarily in a synchronized manner (Niu, Kooi et al. 1995; Niu, Zhang et al. 2002). In addition, for sensible heat removal, a much higher temperature is needed than for dehumidification, and air transport via duct requires a significant amount of fan energy. For building cooling applications, ice-storage technology is primarily used to utilize the low tariff off-peak electricity, however the process is not energy efficient or CO_2 reducing in Hong Kong climate. When the chiller evaporation temperature has to be lowered to generate ice and the night time air temperature is not much lower than the day time temperature, the chiller system energy efficiency becomes low. If we do operate the chiller at a normal temperature of 5 ℃ to store water for day time use, the situation will be similar to that for hot water storage with solar heaters, i.e., the small sensible heat storage capacity of water will demand excessive tank sizes. In all these cases, an effective energy storage device working at proper temperature ranges will be needed.

All the following substances were studied as candidates for phase change material (PCM) as cooling storage medium: organic, inorganic and eutectic materials (Khudhair and Farid 2004). Among all the candidates, paraffin waxes have been used as PCM for many applications. This is because paraffin waxes are nonpoisonous, chemically stable, with no phase separation, and the phase change process only results in a small volume change (He, Martin et al. 2004).

With the key issues of energy storage reviewed and the understanding of the characteristics of modern air conditioning, the author's research team began working with an MPCM (microencapsulated PCM)/water slurry as the storage medium for air conditioning applications in collaboration with textile material researchers (Li and Zhu 2004). N-hexadecane, enclosed within polymer shells of melamine via microencapsulation, was used as the phase-change material. Fluid flow and heat transfer tests were conducted with slurries of MPCM mass ratios up to 30%, which good fluidity can be maintained (Wang, Niu et al. 2007; Wang, Niu et al. 2008). Convection heat transfer inside tubes was systematically investigated in collaboration with Tsinghua University, and enhancement to heat transfer in comparison with liquid water was observed and empirical heat transfer coefficient correlations were developed (Chen, Wang et al. 2008; Zeng, Wang et al. 2009).

With knowledge of these thermal dynamic and fluid flow and heat transfer behaviors, the energy saving potentials under two application scenarios (Wang, Niu et al. 2008; Wang and Niu 2009) were estimated, using a sophisticated system simulation approach. In the first scenario, a new air-conditioning system combined with cooled

ceiling and MPCM slurry storage system was proposed. The results indicate that the new system effectively achieve the target about shifting the part of cooling load from the daytime to nighttime as an energy saving and economy-favorable air-conditioning system. In the second scenario, the possibility of using evaporative cooling in combination with MPCM slurry storage was examined to shorten the period of chiller operation. The required evaporator and heat exchanger capacities, respectively in terms of the approach to the ambient wet-bulb temperature and NTU (number of heat transfer units), are reasonably estimated, and a method to determine the storage tank size was proposed. For five typical climate conditions in China, ranging from the western city Urumqi to the eastern Shanghai, the northern Beijing and the south-eastern Hong Kong, significant saving in the chiller operation can be achieved, varying from 13 to 76 %.

Based on the previous research works, there are several problems involved in intensifying the study about thermal performance of MPCM slurry for building cooling applications and the utilization potential of combining MPCM slurry storage technology with more passive cooling system using nature cooling sources.

1.2 Statement of the Problem

The first problem comes from supercooling characteristic of MPCM slurry and the effect on TES system operation condition. In the previous experimental investigations, the empirical evidence is that the two TES system operating modes - charge and discharge - are not symmetrical because of the supercooling phenomenon (Ryu, Hong et al. 1991). Most of the crystallization processes of PCM are dominated

by the heterogeneous nucleation mechanism as the phase-transition behaviour of the PCM is complicated and very sensitive to small amounts of impurities (Oliver and Calvert 1975). At the fusion temperature, the rate of nucleation is generally very low. To achieve a reasonable rate of nucleation, the solution has to be supercooled and energy must be discharged at much lower temperatures than the fusion temperature. Supercooling of more than a few degrees will interfere with proper heat extraction from the store, and supercooling by 5-10 ℃ can prevent it entirely (Sharma, Tyagi et al. 2009). The phenomenon that the latent heat can only be released at a supercooled, lower temperature is disadvantageous for energy storage applications (Zhang, Fan et al. 2005). It is believed that organic materials typically undergo congruent melting, which means melting and freezing repeatedly without phase segregation and consequent degradation of their latent heat of fusion; in addition, they crystallize with little or no supercooling and are usually non-corrosive. In contrast, most salt hydrates have poor nucleating properties resulting in supercooling of the liquid salt hydrate prior to freezing (Sharma, Tyagi et al. 2009). In general the preliminary studies and experiments indicate MPCM slurry is promising as a thermal storage medium. However, experimental investigations on the effects of supercooling on MPCM slurry thermal storage capacities appear to be limited so far. In addition, the effective cooling storage capacity at the cooling temperature range with natural cooling sources such as evaporative cooling and nocturnal radiative cooling has never been investigated.

The second question referred to the supercooling prevention by nucleation agent. As suggested by some researchers (Sangwal 2007), an effective approach for decreasing supercooling is the addition of liquid or solid nucleating agents to the PCM liquids as

the seeds and catalysts for nucleation and crystal growth. A liquid nucleating agent has a higher melting point than that of the main heat storage material, and is first solidified upon cooling to act as a nucleus of crystal formation. Several studies have been conducted on liquid nucleating agents in various liquids, such as 1-Tetradecanol (2 wt%) for microencapsulated n-Tetradecane (Yamagishi, Sugeno et al. 1996), 1-octadecanol (10 wt%) for microcapsulated n-octadecane (Zhang, Fan et al. 2005), and paraffin wax (0.8-10 wt%) for tetradecane and hexadecane paraffin-in-water emulsion (Huang, Günther et al. 2010). Solid nucleating agents, such as nanoparticles and impurity particles, acting as nucleation centers to enhance the nucleation progress have shown promising application potentials. As proposed by Oliver et al. (Oliver and Calvert 1975), the crystallization processes of most PCM liquids are controlled by the heterogeneous nucleation mechanism. The phase-transition behavior of the PCM liquids is complicated and very sensitive to small amounts of impurities. He et al. (He, Tong et al. 2007) showed that the addition of TiO_2 nanoparticles into pure water effectively reduced the supercooling of water. Zhang et al. (Zhang, Wu et al. 2010) reported that the effects of nanoparticles on supercooling of pure water are strongly dependent on their surface wettability. Among the three additive candidates, α-Al_2O_3 had more effect than γ-Al_2O_3 and SiO_2, and the effect was more notable at a lower concentration of 0.3% than at 0.5%. However, up to now, there is not a systematic method to select additive for reducing the supercooling. This is because the essential factors affecting the nucleation have not been clarified.

The last but not the least important question is about the effect of the hybrid system combined with passive cooling system, for instance, nocturnal sky radiator system,

and MPCM slurry TES. MPCM slurry provides wider application potential of nature cooling sources than conventional medium ice mainly due to its relative higher working temperature and proper thermal property. Therefore, a novel MPCM slurry storage combined with nocturnal radiative cooling and cooled ceiling system is proposed to explore the utilization of energy-free natural cooling source to replace traditional cooling power. In these years, the utilization potential and efficiency of nocturnal sky radiator system (Michell and Biggs 1979; Kimball 1985; Saitoh, Matsuhashi et al. 1985; Parker 2005) and MPCM slurry TES (Gschwander, Schossig et al. 2005; Wang and Niu 2009) has been investigated respectively, but the novel system using paraffin as the core PCM to enhance the utilization of nocturnal sky radiation for building cooling application has not been reported. In addition, the well-design of the hybrid system and the efficient control scheme of the system are also need to be studied.

1.3 Research Objectives

The first objective is proposed that the three functions of ventilation, dehumidification, and sensible heat removal can be assigned to different components in an air-conditioning system, in order to provide better energy efficiency and a better overall indoor environment quality. It is found that horizontal type ceiling panels can handle a space sensible cooling load of up to 80 watts per square meter, which should be adequate for most office buildings which comply with energy saving envelope design standards. The relatively high chilled water temperature required for the chilled ceilings, typically above 17 °C, can significantly raise the efficiency of a chiller which operates at the much higher evaporator temperature of

12 ℃, in comparison with the 5 ℃ setting of the conventional design, and extend the period of using natural cooling. With such a system, fan energy is only needed to supply the outdoor ventilation air.

The second objective is to establish an effective energy storage device working at small temperature ranges. The technology to be developed in this study will be based on petroleum derived materials, which will undergo liquid-solid phase change to store thermal energy in latent heat form at the selected working temperatures. For air conditioning applications, the phase change temperature will be around 15 to 17 ^{o}C, which will cater for removing sensible heat from a room in combination with the emerging chilled ceiling technology, while dehumidification of ventilation air will still be provided by a conventional chiller system. The TES technology to be developed will help to: a) broaden the utilization of renewable heating and cooling sources and b) raise chiller energy efficiency, via compact storage and quick charging.

The third objective is to evaluate and characterize the thermal functional performance of the PCM medium, especially the effect of supercooling on effective cooling capacity. Differential scanning calorimeter (DSC) will be used for measuring the phase change process properties of the PCM candidates and MPCM slurries, such as melting/freezing point and latent heat of fusion. An experimental test device will be set up to measure the dynamic heat transfer performance of hybrid system combined with cooled ceiling system and MPCM slurry TES under the practical operation condition.

The forth objective is using well-dispersed multi-wall carbon nano-tube (MWCNT) particles in an organic liquid n-hexadecane to decrease supercooling. Various surfactants will be tested as additives to overcome the rapid aggregation and sedimentation of the nanoparticles in the organic liquid. A transmission electron microscope (TEM) will be used to observe the morphology of nano-additives. The dispersion and stability of nano-additives in PCM will be measured under dynamic light scattering (DLS) analysis. The average particle size and the polydispersity index will also be analyzed. Thermal analysis of the n-hexadecane with well dispersed MWCNT particles will be tested by DSC to evaluate the effect of nanoparticles on the prevention of supercooling of n-hexadecane. Special recipes will be developed to formulate PCM medium which achieve good functional performances.

The final objective of this research is to assess the reduction of peak electricity demand of the combined system of MPCM slurry storage and nocturnal sky radiator using the natural cooling source, nighttime off-peak electricity refrigeration and the electricity tariff structure that will encourage the use of the combined system. Both the reduction of the peak electricity demand and annual energy consumption of the integrated system using energy-free radiative cooling are also assessed under different climate conditions in China. The optimization and proper usage of the hybrid system are also proposed to be discussed.

1.4 Outline of This Thesis

In response to the research questions and objectives, this thesis consists of six chapters.

The first chapter as presented is the introduction about the research background, purpose, method, and expected outputs.

Chapter 2 starts with the literature review covering the existing research on TES application, classification and properties of PCM, supercooling phenomenon, the common method for supercooling prevention, the classical theory of nucleation, the potential of nanoparticles using as nucleating agent and the model of nocturnal sky radiator system. Then the author addressed the motivation of the thesis, i.e. what the weaknesses of current research about MPCM slurry were and what contribution this thesis was going to make.

Chapter 3 firstly outlines the experimental apparatus and procedures used to obtain data for the heat transfer study of MPCM slurries. The DSC result of MPCM particles and the results from tests with pure water and the MPCM slurry under the practical operating conditions are reported and discussed. This chapter also proposed two correlation equations to describe the effect of supercooling on effective cooling storage capacity.

In Chapter 4, various surfactants were firstly tested as additives to overcome the rapid aggregation and sedimentation of the nanoparticles in the organic liquid. Stable and homogenous dispersion was attained through surface modification of the MWCNT particles with strong acids H_2SO_4 and HNO_3, plus the addition of 1-decanol as a surfactant to the organic liquid. In addition, the thermal performance of n-hexadecane with well dispersed MWCNT particles was measured by DSC to

evaluate the effectiveness of supercooling prevention of n-hexadecane. The obvious effects of MWCNT particles on the decrease of supercooling of n-hexadecane provide promising way of improving the performance of system energy efficiency in building cooling and heating applications.

In Chapter 5, a design of the combined system of MPCM slurry TES and nocturnal sky radiator is proposed and mathematically modeled. The annual energy consumptions of the system in five typical cities in China, and energy saving potential of the nocturnal radiative cooling for the combined are also explored and the optimal design of the MPCM slurry storage system has been made.

The final chapter, Chapter 6 addresses the conclusions and limitations of the thesis. In addition, suggestions and prospects of further steps extending this study in future are also discussed.

Chapter 2

Literature Review

In this chapter, the author reviews the theories and research related to the topic of PCM for building cooling applications. The classification and application of TES system and PCM are firstly reviewed. This part functions as the skeleton outlining the generic features of TES and PCM for building cooling application. The second part makes an effort to outline the effect of supercooling on PCM application and the potential of using nanoparticles as nucleating agents for prevention of supercooling, indicating the importance of supercooling decreasing for PCM applications in building cooling system. The final aspect reviews the application status and mathematical model of nocturnal sky radiator system to explore the potential of combine the nocturnal sky radiator to MPCM slurry system.

2.1 Thermal Energy Storage

2.1.1 Definition and Classification of TES System

TES, also commonly called heat and cold storage, allows the storage of heat or cold to be used later (Mehling and Cabeza 2008). The wide use of air-conditioning in commercial buildings increases the peak demand for electricity, and makes it difficult to tackle the global warming problem due to the CO_2 emissions that accompanying electricity generation. The use of TES as a means of managing energy demand and utilization is now accepted in many countries. Cool thermal storage

systems have been intensively studied for their ability to use stored cooling produced during off-peak hours to provide the energy necessary for daytime applications (Dinçer and Rosen 2010). Figure 2.1 shows some possible methods; they can be divided into physical and chemical processes.

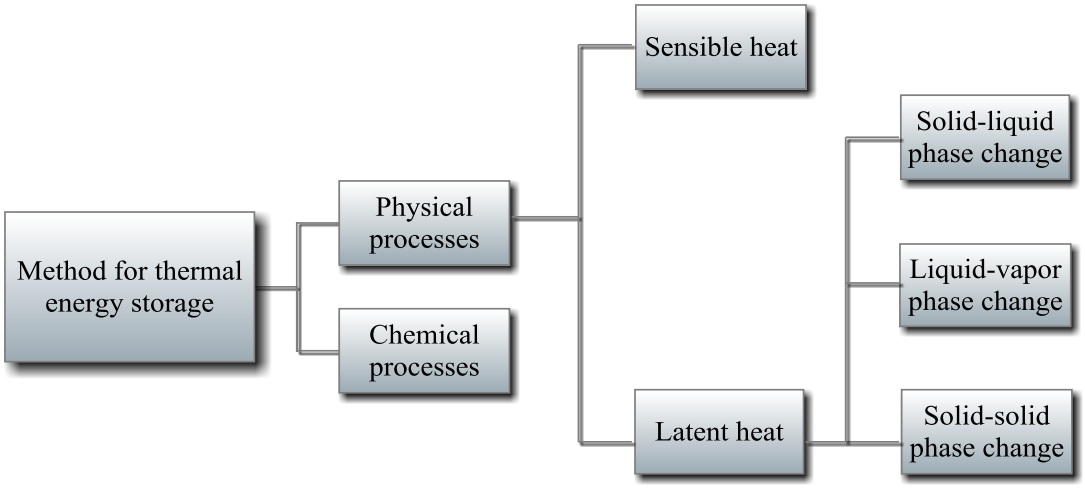

Figure 2.1 Possible methods of reversible storage of heat and cold (Mehling and Cabeza 2008)

If heat is stored as latent heat, a phase change of the storage material is used. There are several options with distinct advantages and disadvantages. The phase change solid-liquid by melting and solidification can store large amounts of heat or cold, if a suitable material is selected. Melting is characterized by a small volume change, usually less than 10 %. If a container can fit the phase with the larger volume, usually the liquid, the pressure is not changed significantly and consequently melting and solidification of the storage material proceed at a constant temperature. Upon melting, while heat is transferred to the storage material, the material still keeps its temperature constant at the melting temperature, also called phase change temperature (Figure 2.2).

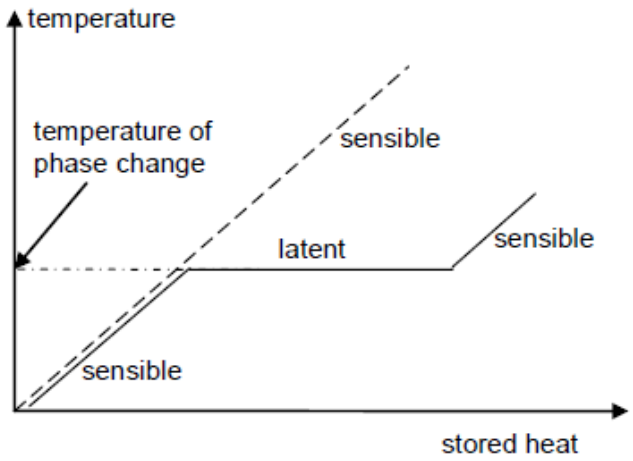

Figure 2.2 Heat storage as latent heat for the case of solid-liquid phase change

If the melting is completed, further transfer of heat results again in sensible heat storage. The storage of the heat of melting cannot be detected from the temperature, because the melting proceeds at a constant temperature. The heat supplied upon melting is therefore called latent heat, and the process latent heat storage (LHS).

2.1.2 Potential of Application of TES in Building Cooling Applications

TES technology is a matured and accepted as a proven technology to improve energy efficiency by many in the energy management and building operations fields (IEA 2002). Cool storage using water, ice or other phase-change materials as the storage medium is most widely used (thousands of installations in operation) in the USA where the summertime cooling requirements are high. It is also used in Europe, where it is also connected to heat-recovery and hot water storage systems. Cool thermal storage is also used in Australia, Canada, South Korea, Japan, Taiwan, South Africa and several other countries. Facilities that typically get the best benefit from Cool TES are those with low cooling load at night when off-peak electricity rates are

in effect. Most commercial buildings fall into this category. TES systems are suitable for individual buildings from about 10000 m^2 as well as for district-cooling systems supplying entire downtown areas. They work best in facilities that are not fully operational at night, such as office buildings, schools, airport terminals, convention centers and sports complexes.

Methods of PCM use are either passive or active. Here, the passive means that the use of PCM in the structure of buildings and the melting and freezing of PCM are realized without resort to mechanical equipment. The active means that the charging and discharging of energy in PCM storages are achieved with the help of mechanical equipment (Zhu, Ma et al. 2009). The predominant passive application in building construction is impregnation into building covering materials such as concrete, gypsum wallboard, plaster, etc., as part of building structures for lightweight or even heavyweight buildings to increase the thermal mass. Several researchers have demonstrated methods for impregnating standard gypsum board with paraffin to produce PCM building covering materials (Feldman, Banu et al. 1993; Kissock, Hannig et al. 1998; Zhang, Lin et al. 2006; Zhou, Zhang et al. 2008; Evers, Medina et al. 2010). In such applications, the PCM should have very sharp heat release characteristics at the desired room temperature. Impregnation techniques also place constraints on the material with respect to potential reactivity with chemicals like water or oxygen in the immediate environment. Impregnation methods commonly involve soaking the wallboard with the PCM chemical, for such applications salt hydrates and salts do not work (Suppes, Goff et al. 2003). The use of PCM in buildings cooling applications can provide different functions by passive method. For instance, they can be used for free cooling of buildings (Zalbaa, Marína et al. 2004;

Butala and Stritih 2006; Butala and Stritih 2009), building peak load shifting (Stovall and Tomlinson 1995; Athienitis, Liu et al. 1997; Weinläder, Beck et al. 2005), solar energy utilization (Kaygusuz 1999), waste heat recovery (Lee, Hawes et al. 2000), etc. In a pump hydro, water is pumped up a reservoir at night time and flows down to run a turbine the next day to generate electricity. However, as reviewed recently by MacCracken (2010), cooling and thermal storage may prove to be the least expensive, when measured using capital cost per unit energy ($/kWh) or per unit power ($/kW), and most energy efficient.

Several computer simulation programs have been widely developed for various energy systems. The report of Annex 14, subtask 3, has mentioned around thirty computer softwares, which can be used for the cool storage system (Annex14). The majority of these simulation programs are used to study the feasibility of the cost and energy performance of the system. A few models have also been developed to study the PCM itself. For example, Yamaha (1997) has developed a simulation model for the thermal response of a PCM installed in an air distribution system. This model was used to evaluate the performance of PCM storage systems. In the present study, a computer model has been developed to study the phase equilibrium of paraffin waxes for the design of cool storage with such materials (He 2004).

There are also a number of studies that use the experimental approach to investigate the building performance through the passive use of PCM (Zhu, Ma et al. 2009). The under-floor electrical heating system with the SSPCM storage was experimentally studied Lin, Zhang et al. (2005). The proposed system can charge heat by using nighttime cheap electricity and discharge it during daytime when necessary. The

results showed that the indoor temperature can be increased greatly. The temperature of the PCM plate can be kept at the phase transition temperature for a long period after heaters stopped working. It is worthwhile to notice that the conventional control strategies were used in these studies. There is another experimental investigation about a roof integrated solar heating system using a PCM storage (Saman, Bruno et al. 2005). This system was installed in a house in Adelaide, Australia, which utilizes the existing roof as a solar collector/absorber and incorporates a PCM storage to store heat during the day and release it to heat the living space during night or when there is no sunshine. The results showed that the effect of sensible heat was perceived in the initial periods of melting and freezing processes. A higher inlet air temperature and air flow rate can increase heat transfer rates and shortens the melting time, but a higher air flow rate increased outlet air temperatures. For freezing, a lower inlet air temperature and a higher air flow rate can increase heat transfer rates and shortens the freezing time, but a higher air flow rate reduced outlet air temperatures.

Advantageous features a well-designed and correctly operated cool thermal storage are many (IEA 2002):

- Installed chiller and cooling tower capacity can be reduced with a storage system. Cooling production can be “de-coupled” from the customer demand thereby making it possible to utilize lower off-peak drive energy rates, etc.
- A good storage system can provide better energy performance than a conventional instantaneous system because lower ambient temperatures are available to cooling towers at night when the storage is charged. Increased

efficiency also results from all the machinery operating nearer the design points more of their operation time than in conventional systems.

- Storage designs make it easy to operate variable flow systems because the storage forms a buffer between the consumption and production and reduces the need for rapid changes of chiller operation.
- Storage systems provide higher reliability since they do not totally depend on instantaneous cooling production. In cases of short shutdown of a chiller it is possible to serve critical areas for a period of time from storage.

2.2 Phase Change Material as Thermal Storage Medium

2.2.1 Classification and Properties of PCM

Because the two most important criteria of PCM, the melting temperature and the melting enthalpy, depend on molecular effects, it is not surprising that materials within a material class behave similar. Figure 2.3 shows the typical range of melting enthalpy and melting temperature of common material classes used as PCM.

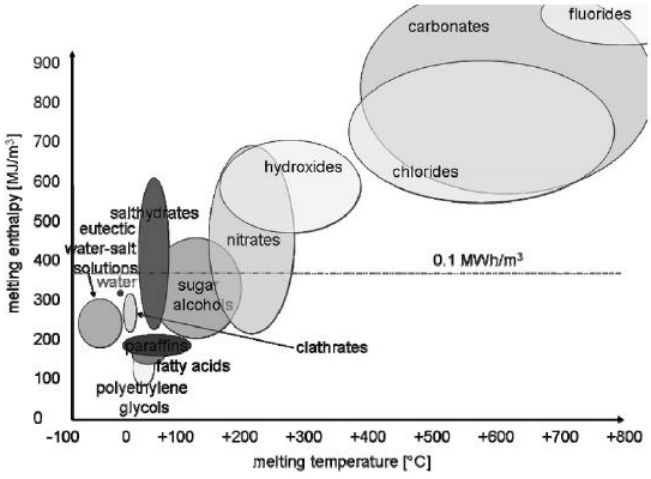

Figure 2.3 Classes of materials that can be used as PCM and their typical range of melting temperature and melting enthalpy (Mehling and Cabeza 2008)

By far the best-known PCM is water. It has been used for cold storage for more than 2000 years. Today, cold storage with ice is state of the art and even cooling with natural ice and snow is used again. For temperatures below 0 °C, usually water-salt solutions with a eutectic composition are used. Several material classes cover the temperature range from 0 °C to about 130 °C. Paraffin, fatty acids, and sugar alcohols are organic materials. Salt hydrates are salts with a large and defined amount of crystal water. Clathrates are crystalline structures in which molecules of one type are enclosed in the crystal lattice of another. When the enclosed molecule is from a gas and the surrounding crystal structure is water, the clathrate is also called a gas hydrate. They cover a temperature range from about 0 °C to 30 °C. At temperatures above 150 °C, different salts and their mixtures can be applied. In addition, the energy density is roughly proportional to the melting temperature in K. This can be understood from thermodynamics according to the theory of Richards. The theory of Richards shows that the melting enthalpy per volume is proportional to the melting temperature, the number of bonds per molecule, and the density divided by the molar mass that relates to the packing density of the molecules or atoms (Lindner 1984).

Phase change materials being marketed today rely on either a solid-solid or solid-liquid latent heat transformation. Typically, the solid-solid latent heats associated with glass transitions in polymers are lower in energy but more convenient to utilize for smaller items where material costs represent a small fraction of the final cost. Polymer PCM can be directly molded into PCM devices. Polymer PCM also tends to have reversible latent heat transitions while some solid-liquid transition tends to be

irreversible and require knowledge of the system to create viable solutions to this polymorphism. For applications involving larger heat capacities such as moderating the temperature of a building or inhibiting the tendency of a bridge to freeze, the cost of the PCM is more important; solid-liquid transition materials are preferred. Irreversibility of solid-liquid transition materials can occur with polymorphic systems. An understanding of the polymorphism can sometimes create the foundation for overcoming these otherwise detrimental irreversibility.(Suppes, Goff et al. 2003)

Except for the rare instance where an inexpensive pure material has the exact melting point needed for an application, most phase change materials are mixtures of different chemicals that provide the targeted melting point. Figure 2.4 illustrates two extremes in behavior for solid – liquid transition of mixtures. The top curve is for a system forming an ideal solid mixture where the two components are fully compatible in the same solid matrix. The bottom curve is for a system forming crystals pure in either component 1 or component 2 where the same components are not compatible. Details for applying these different forms of the freezing point depression theory can be found elsewhere (Suppes, Goff et al. 2003).

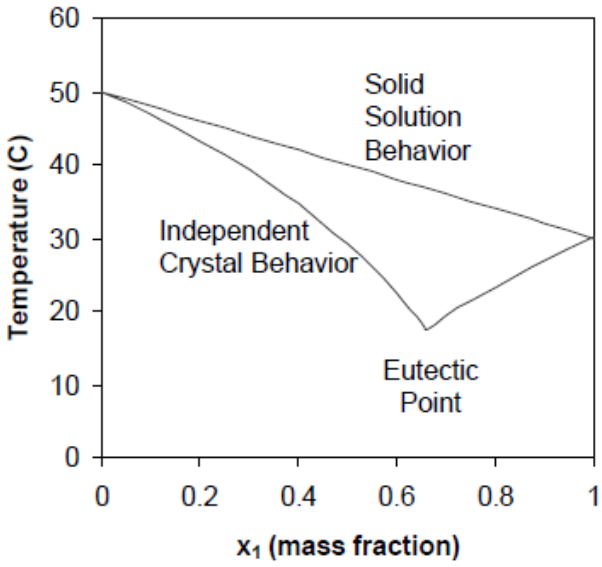

Figure 2.4 Physical characteristics of mixture freezing point behavior (Suppes, Goff et al. 2003)

2.2.2 Selection of Proper PCM

PCM should have the following properties for effective latent-heat storage: (1) a melting point suitably matched to the specific applications; (2) high storage capacity both on a volume and a weight basis; (3) reproducible crystallization without degradation; (4) little supercooling with high crystal-growth rate; (5) high thermal conductivity; (6) good chemical stability with minor corrosion; (7) it should not be hazardous, highly inflammable or poisonous; (8) little volume change with phase change; (9) low vapor pressure at the operating temperature; (10) it should be abundant and cheap (Byung Chul, Sang Done et al. 1989).

Control of melting points, similar melting and freezing points, and high latent heats are all desirable for a good PCM chemical. Targeted melting points will depend upon

the application. Proximity of melting to freezing points should be as close as possible-preferably within 3 ℃ between the peaks, at the heating and cooling rates found in typical applications of about 0. 1℃/min. Latent heats are preferably >180J/g. These three properties are necessary but not sufficient when identifying a good PCM material; therein requiring additional information, such as the sharpness of the latent heat transitions, to fully characterize performance. An index measure of performance is discussed in the results section.(Suppes, Goff et al. 2003)

In many cases, the temperature of cooling air to be blown from an indoor cooled ceiling is generally 18 ℃ and no higher than 22 ℃, in the cooled ceiling system. If it is higher than that temperature, unless the air blowing quantity to the space to be air-conditioned is increased, it is difficult to cause the air conditioning effect to the same level and rather, the air conditioning efficiency is decreased. Therefore, the latent heat storage agent which supplies cold to the cooling air is required to be those which can store latent heat at 20 ℃ or lower in consideration of the temperature difference (about 2 ℃) needed for heat exchange with air (Zalba, Marin et al. 2003; Farid, Khudhair et al. 2004). In the case of ice, a typical example of a latent heat storage agent for air conditioning, since it is required to be cooled at 0 ℃ or lower, there is a problem that COP of a refrigerator is lowered and accordingly the energy needed for cooling becomes so high to make energy saving difficult. To keep COP high as it is and to save energy, the latent heat storage agent for air conditioning is required to be those which can store heat at 5 ℃ or higher and at lowest 3 ℃ or higher. For the above-mentioned reasons, it is desired to make a latent heat storage agent for air

conditioning which can store heat at a temperature in the range of 3 °C to 16 °C available (Tomura and Kawasaki-shi 2010).

Paraffin shows good storage density with respect to mass, and melts and solidifies congruently with little or no subcooling (Mehling and Cabeza 2008). Their thermal conductivity is however comparatively low. Regarding the stability of a container, their vapor pressure is usually not significant. Their volume increase upon melting is in the order of 10 vol.%; this is similar to that of many inorganic materials, but less critical as paraffin are softer and therefore build up smaller forces upon expansion. Paraffin is insoluble in water as they are water repellent. They do not react with most common chemical reagents; in fact, the name "paraffin" originates in the Latin and means that they are little reactive. At elevated temperatures, paraffin bonds can crack and the resulting short chain molecules evaporate. Paraffin is combustible and people often conclude that paraffin burn easily. The fact that candles do not burn as a whole shows is not correct. The compatibility of paraffin with metals is very good; with plastics however, paraffin can cause softening of the plastic. Paraffin has very few safety constraints. Table 2.1 shows examples of paraffin. It indicates that with rising number of C atoms in C_nH_{2n+2} the melting temperature increases. By mixing different paraffins, melting points between those of the pure paraffins can be obtained (Gschwander, Schossig et al. 2005).The limit is Polyethylene with thousands of C atoms. At very low numbers of C atoms, methane C_1H_4, ethane C_2H_6, and propane C_3H_8 are gasses at ambient conditions. Tetradecane is the smallest n-alcane that melts above 0 °C. They are hydrocarbons or alkanes with different numbers of C-atoms in their chain.

Table 2.1 Examples of paraffin that have been investigated as PCM (Mehling and Cabeza 2008)

Material	Melting temperature (℃)	Meilting enthalpy (kJ/kg)	Thermal conductivity (W/mK)	Density (kg/m3)
n-Tetradecane	6	230	-	760(liquid,20 ℃)
C14H30			0.21(solid)	-
n-Pentadecane	10	212	-	770(liquid,20 ℃)
C15H30			-	-
n-Hexadecane	18	210,238	-	760(liquid,20 ℃)
C16H34			0.21(solid)	-
n-Heptadecane	19	240	-	776(liquid,20 ℃)
C17H36			-	-
n-Octadecane	28	200,245	0.148(liquid,40 ℃)	774(liquid,70 ℃)
C18H38			0.358(solid,25 ℃)	814(solid,20 ℃)
n-Eicosane	38	283	-	779
C20H42			-	-
n-Triacontane	66	-	-	775
C30H62			-	-
n-Tetracontane	82	-	-	-
C40H82			-	-
n-Pentacontane	95	-	-	779
C50H102				-
Polyethylene	110-135	200	-	-
CnH2n+2	-	-	-	870-940(solid,20 ℃)
n up to 100000				

2.2.3 MPCM Slurry Application as TES Medium

In recent years, a new approach has been proposed, in which the PCM is microencapsulated and suspended in a single-phase heat transfer fluid to form the solid-liquid MPCM slurry (Kasza and Chen 1985). A simple method to make MPCM has been proposed by Ai, Jin et al. (2007). The particularity of this method is to use casein as the protein multilayer to protect the microparticles from re-coalescencing before MPCM is finally stabilized. The fabrication process is shown in Figure 2.5. They used n-hexadecane as the core material. It was shown that the casein was very effective in protecting the agglomeration of emulsion. Further measurements indicated that the melting temperature of MPCM was increased and latent heat of MPCM was smaller than the bulk material which they attributed to the presence of the impurity. The decrease of the latent heat was always a drawback of MPCM because of the presence of the shell.

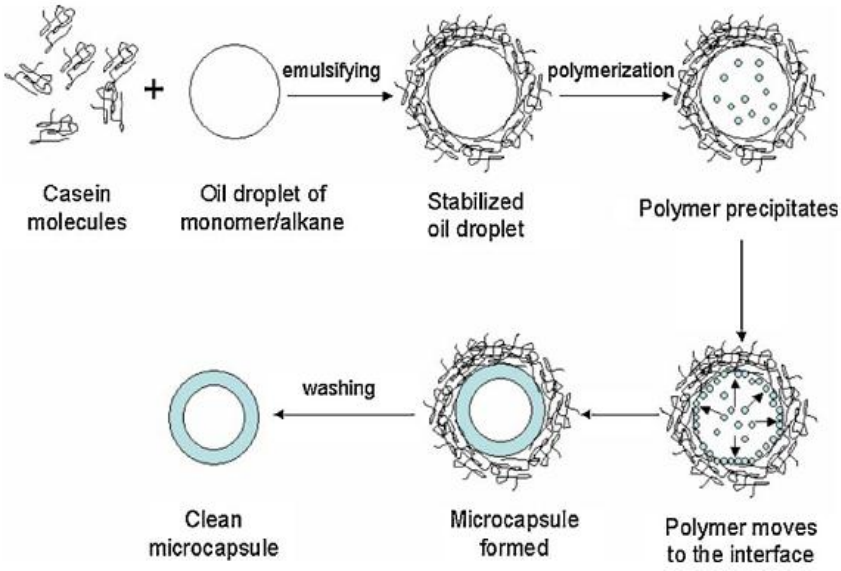

Figure 2.5 A simple method for making MCPM proposed by Ai, Jin et al. (2007)

Due to the microencapsulation of PCM particles in a thin plastic shell, the core material is always separated from the carrier fluid, which makes MPCM slurry behave like a liquid, while the latent heat effect associated with phase change significantly increases the heat capacity of the carrier fluid. In addition, the heat transfer coefficient between the fluid and heat transfer surface may be greatly increased because of the latent heat effect and the particle to particle interactions (Sohn and Chen 1981; Kasza and Chen 1985). The flow and heat transfer characteristics of MPCM have been experimentally and theoretically investigated by a number of researchers (Yamagishi, Sugeno et al. 1996; Regin, Solanki et al. 2008). The experimental results show that the MPCM flow enhanced the local heat transfer coefficient relative to the single heat transfer fluid with only small increases in the pressure drop; pressure drops were even lower than those for pure water under some conditions (Yamagishi, Sugeno et al. 1996; Yamagishi, Takeuchi et al. 1999; Inaba, Kim et al. 2004). To understand the mechanism of the heat transfer enhancement of an MPCM flow, a theoretical model was developed for laminar MPCM flow in a circular duct with constant temperature or heat flux. The results predicted that the heat fluxes were about 2-4 times higher than for single-phase fluids (Charunyakorn, Sengupta et al. 1991). Modifications were made by accounting for the microcapsules' crusts, initial subcooling and degree of phase change range, which brought predictions closer to the experimental results (Zhang and Faghri 1995; Hu and Zhang 2002).

Thermal reliability of microcapsules has also been checked by researchers. Sarı, Alkan et al. (2009) did DSC measurement of PMMA/octacosane microcapsules after

5000 thermal cycling. The results (Figure 2.6) showed that the melting point of the PMMA/octacosane microcapsules changed in range of 51.1 ^{o}C and 52.3 ^{o}C when its freezes point changed in range of 53.7 ^{o}C and 55.2 ^{o}C after 5000 cycling, respectively. Based on these results, it is worth noting that the PMMA/octacosane microcapsules have good thermal reliability in term of the changes in its phase change temperatures. Also, the average latent heats of melting and freezing of the PCM after repeated 5000 thermal cycling were measured as 79.9 J/g and 81.7 J/g, respectively. It is clear that, there is no significant temperature or enthalpy change observed for latent heat thermal energy storage applications after thermal cycling.

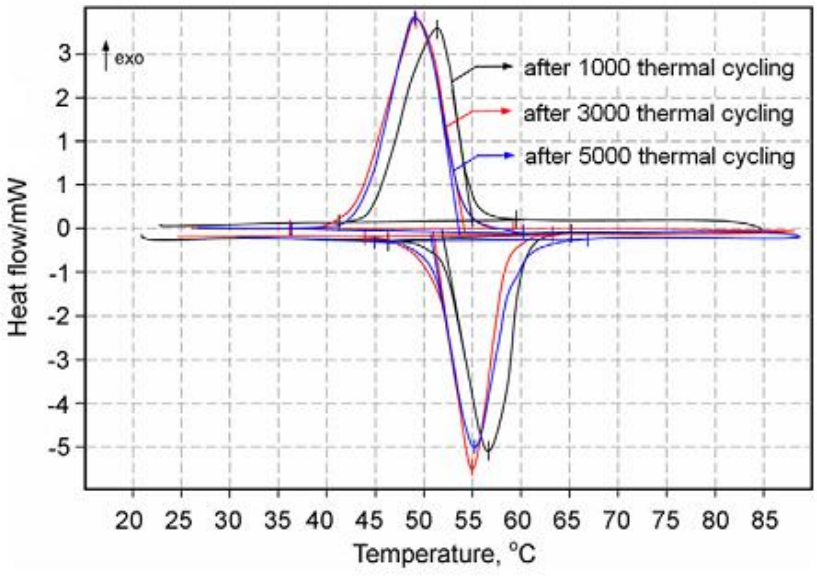

Figure 2.6 Thermal reliability of microcapsules (Sarı, Alkan et al. 2009)

2.3 Supercooling and Prevention Methods

2.3.1 Supercooling Problem

The main feature of crystallization is its stochastic character, i.e. samples which are apparently identical will not transform at the same temperature during the cooling

process. It is only possible to determine a probability of transformation per unit time and a statistic method is needed to analyze the experiments.(Clausse, Dumas et al. 1987)

One of the major problems in using the PCM as thermal storage material is supercooling, i.e., when a PCM liquid is cooled, freezing usually occurs at a lower temperature than the melting point (see Figure 2.7). As the latent heat is only released below the supercooled temperature, large temperature difference between charging and discharging is needed to fully utilize the latent heat, which is undesirable for the energy efficiencies of energy storage applications (Zhang, Fan et al. 2005).

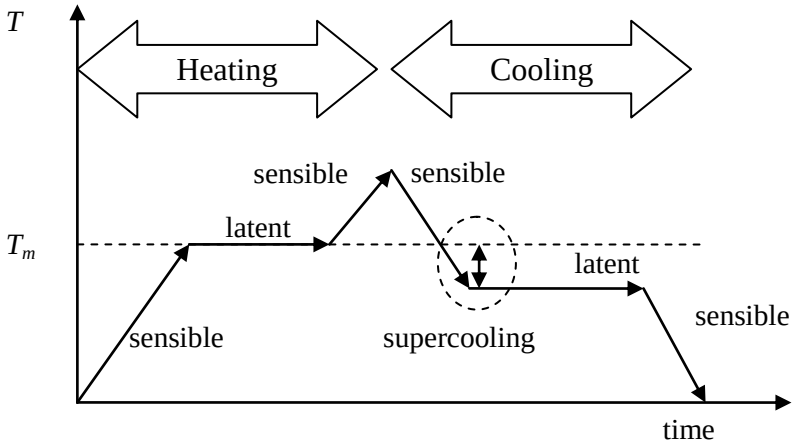

Figure 2.7 Schematic temperature change during heating (melting) and cooling (solidification) of a PCM with subcooling (redrawn from Mehling and Cabeza 2008)

Yamagishi, Sugeno et al. (1996) did series DSC test and found a shape of two peaks due to the two different nucleations are shown in the DSC cooling curves, and DSC samples of different size-distributions have the same: shape as the two peaks. The crystallization inside a droplet starts from the generation of small crystalline nuclei.

There are two processes to form the nuclei; the nuclei forms inside the liquid (homogeneous nucleation) or on the interface of solid substances (heterogeneous nucleation). Yamagishi, Sugeno et al. used high-speed video camera to observe the crystallization in MC (Yamagishi, Sugeno et al. 1996), and the microphotographs clearly showed It is also observed in MCs samples that the crystallization behaviors occurred after either of the above-mentioned nucleation. When the nuclei form in a MC, it grows until the core material has entirely crystallized. Figure 2.8 (a) shows the heterogeneous nucleation; the nuclei forms on the interface between the core material and the MC wall. Figure 2.8 (b) shows the homogeneous nucleation; the nuclei forms inside the core material. It is also observed the two nucleation processes and the heterogeneous nucleation occurred at a higher temperature as compared with the case of homogeneous nucleation. That's why there are always two peaks during the crystallization process.

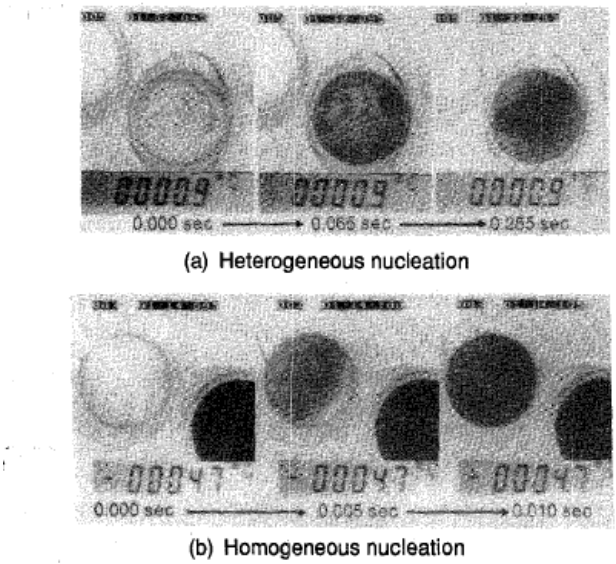

Figure 2.8 Microphotographs of crystallization behavior inside MC (Yamagishi, Sugeno et al. 1996)

According to the research (Clausse, Dumas et al. 1987), the process of crystallization inside the emulsion is not thermodynamic equilibrium nature, i.e. the nuclei appear at the metastability breakdown of supercooling. The number of crystallized emulsions per unit time during steady cooling are proportional to the 4 probability to have a nuclei per unit time and per the volume (in the case of homogeneous nucleation) or per unit area of favorable site (in the case of heterogeneous nucleation). Although this probability of nucleation is also a function of the temperature, the character of crystallization is stochastic, i.e. emulsions which are apparently identical will not crystallize at the same temperature. The process of MGs crystallization can be seem as an similar feature to that of emulsion.(Clausse, Dumas et al. 1987).

2.3.2 Mechanism of Supercooling

The cause for supercooling is complicated. It is believed that organic materials typically undergo congruent melting, which means melting and freezing repeatedly without phase segregation and consequent degradation of their latent heat of fusion, and they crystallize with little or no supercooling and usually non-corrosiveness. By contrast, most salt hydrates have poor nucleating properties resulting in supercooling of the liquid salt hydrate prior to freezing (Sharma, Tyagi et al. 2009). Alvarado et al. (2006) presented an experimental study on characterization of supercooling suppression of MPCM slurry, and indicated that the initiation of freezing point is inversely proportional to cooling rate. Yamagishi et al (Yamagishi, Sugeno et al. 1996) studied the melting and crystallization processes of microencapsulated n-tetradecane and n-dodecane of different mean diameters ranging from 5 to 1000 μm. The DSC results showed the degrees of supercooling were constant in the range of

100-1000 μm, however, in the range of 5-100 μm, the crystallization temperatures lowered as the microcapsule sizes decreased. For PCM emulsion, Huang et al (Huang, Günther et al. 2010) investigated the paraffin-in-water emulsions with droplet size in the range of 0.2 to 12.5 μm, and indicated droplet size and their distribution play a vital role both in the melting and nucleation temperature. With droplet size reducing, nucleation temperature decreased significantly faster than melting temperature, so the supercooling increased.

The formation of the nuclei is associated with a change in the free energy of the system (Sangwal 2007). In homogeneous systems, nuclei of the new phase are not formed as soon as the system becomes supersaturated even though thermodynamically such a situation is possible. The system is said to be in a state of metastable equilibrium, and it can remain in that state without attaining the minimum free energy corresponding to the equilibrium state. In other words, in such cases nucleation of the new phase sets in after some period (called the induction period), the value of which depends on such factors as the temperature and pressure of the system, the presence of chemical phases (impurities) different from the nucleating phase and mechanical disturbances. Introduction of seeds of the nucleating phase and increased supersaturation level facilitate the process of nucleation of the new phase. This supersaturation level corresponds to the upper limit of the state of metastable equilibrium and defines the width of the metastable zone width. (This is the true cause of supercooling, also the microcosmic factors affecting supercooling in 2.3.3, the words are also in 2.4.1)

2.3.3 Factors Affecting Supercooling and the Prevention of Supercooling

There are several researchers (Clausse, Dumas et al. 1987; Yamagishi, Sugeno et al. 1996; He 2004; Lee 2004) investigated and reported the supercooling phenomenon and the factors affecting supercooling, including the sample volume and the cooling rate.

- **Sample volume**

Clausse, Dumas et al. (Clausse, Dumas et al. 1987) addressed that the supercooling increasing when the sample volume decrease. In their experiment, water samples whose volumes are a few cubic millimeters crystallize around 259K, otherwise microsize samples freeze around 234K. (Clausse, Dumas et al. 1987)

Lee (2004) reported that the supercooling phenomenon becomes rapidly heavier in the process of reducing the size of the microcapsule to the order of micrometer, particularly, 100 micrometers or less. It is known that this is because the droplets of molten liquid are reduced in size and the number of crystallization nuclei in each droplet of molten liquid is simultaneously decreased when the molten liquid is phasechanged to the solid state again.

Yamagishi, Sugeno et al (1996) did series DSC test of the MC samples of different mean diameters ranging from 5 to 1000 μm, and the conclusion can be drawn from Figure 2.9: the degrees of supercooling, which were defined as the difference between the temperatures of both melting and crystallization, were constant in the

range of 100- 1000μm. In the range of 5 - 100μm, the crystallization temperatures lowered as the MC sizes decreased. Yamagishi, Sugeno et al (1996) gave the conclusion that it was confirmed that there was no effect of the MC size on the measured values of either the melting temperature or the latent heats of fusion. By contrast, it is well-stated that the crystallization temperature of a liquid droplet lowered with reducing its size, because the number of nuclei in each droplet decreases as the droplet size reduces.

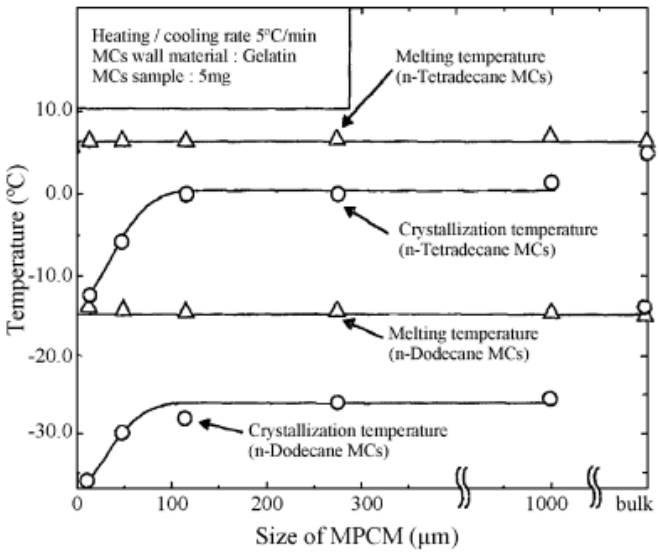

Figure 2.9 The relationship of MPCM particle size and melting /crystallization temperatures (Yamagishi, Sugeno et al. 1996)

In the research of Zhang et al (2005), the DSC cooling curves of mC_{18} are mainly affected by the average diameters. Adding 10.0 wt% of 1-octadecanol to the microcapsules as a nucleating agent decreases the degree of supercooling of microencapsulated n-octadecane from 26 ℃ to approximately 12 ℃ at a heating and cooling rate of 10.0 ℃/min.

- **Cooling rate**

The deviation between the theoretical model, the temperature sensor measurements, and the DSC measurement is partly a result of the systematic influences from the instruments, and the inherent error sources, also from experimental conditions. In every case, a slow heating/cooling rate during the DSC measurements should be used to ensure approximate thermodynamic equilibrium at every moment during the experiment. This will avoid a "coring" of the DSC curve, and thus will avoid incorrect temperatures. The phenomenon of "coring" means non-equilibrium freezing in which each solidified unit has a higher-melting centre surrounded by layers of material of increasingly lower melting point. The melting process will tend to retrace the path of the freezing process, if the system is at a uniform temperature (Lane 1983). The phenomenon of "coring" will result in large deviations if the DSC scanning rate is not slow enough. (He 2004)

Alvarado et al. (2006) presented an experimental study on the characterization of supercooling suppression of MPCM slurry. They studied the key parameters influencing MPCM slurry supercooling and indicated that the initiation of freezing point is inversely proportional to the cooling rate.

He, Martin et al. (2003; 2004) did series experiment about the effect of supercooling DSC measurement results by different cooling rate. The experimental result shows that characteristic temperatures depend very much on the DSC heating/cooling rate. In the melting process, there is an enlarged temperature range as compared to the freezing process at the same rate. Result also indicates that a higher scanning rate

gives the result of a wider temperature range. He, Martin et al. have reported that when DSC runs at slower scanning rate, the results agree better with theoretical modeling of the system's equilibrium behavior. In He's DSC result of $C_{14}H_{30}$, it can be seen that the temperature range reached 16.5 ℃ for the freezing process, and 18 ℃ for the melting process at a 5 ℃/min scanning rate. When the scanning rate is slower, 2 ℃/min, the temperature range is 11 ℃ for the freezing and 14 ℃ for the melting. However, with a DSC scanning rate of 0.5 ℃/min, two peaks appear and the temperature range of the high temperature peak is only 3.9 in the freezing process and 5 ℃ from melting process, respectively. As discussed by He, Martin et al. (He, Martin et al. 2003), the low temperature peak is presumably due to a solid-solid phase transition.

2.4 Nano Materials as Nucleation Agent

2.4.1 Classical Theory of Nucleation

Crystal morphology analysis should be one of the theory methods to explain the nucleating agent working mechanism, which is continued to be considered.

The formation of the nuclei is associated with a change in the free energy of the system (Sangwal 2007). In homogeneous systems, nuclei of the new phase are not formed as soon as the system becomes supersaturated even though thermodynamically such a situation is possible. The system is said to be in a state of metastable equilibrium, and it can remain in that state without attaining the minimum free energy corresponding to the equilibrium state. In other words, in such cases

nucleation of the new phase sets in after some period (called the induction period), the value of which depends on such factors as the temperature and pressure of the system, the presence of chemical phases (impurities) different from the nucleating phase and mechanical disturbances. Introduction of seeds of the nucleating phase and increased supersaturation level facilitate the process of nucleation of the new phase. This supersaturation level corresponds to the upper limit of the state of metastable equilibrium and defines the width of the metastable zone width.

Nuclei, which can attain a size greater than that of a critical nucleus, develop into crystals of visible size by the attachment of growth species (i.e. molecules, atoms or ions) at energetically favorable growth sites such a kinks in the ledges of surface. At a given supersaturation and temperature, there is a critical value of the free energy when stable 3D nuclei of critical size are formed. Thus, the process of growth of crystals of visible size involves at least two stages: (1) formation of stable 3D nuclei and (2) development of the stable 3D nuclei into crystals with well-developed face.

2.4.1.1 Driving Force for Phase Transition

The driving force for the processes of crystallization (i.e. nucleation, precipitation, growth. deposition, etc.) is the difference in the free energy of supersaturated or spercooled mother phase and the free energy of the newly forming phase. Under constant temperature and pressure condition, any change in a system proceeds from a state of higher to a state of lower Gibbs free energy. Consequently, the Gibbs function G is taken as a thermodynamic potential, and the change in the system as a passage from a state of higher to a state of lower potential.

2.4.1.2 Tree-Dimensional Nucleation of Crystals

The formation of three-dimensional (3D) nuclei from atomic or molecular entities xi ling in the volume of a growth medium involves their aggregation in an ordered phase. The details of the process of aggregation of atoms or molecules in the supersaturated medium and the order in the structure of the nuclei are not well known. However, the process is usually envisaged to occur as a result of collision of individual atoms or molecules in such a way that the collision yields a sequence of aggregate of increasing size such as dimers, trimers. Tetramer, etc., according to the reactions:

$$\begin{aligned} A + A &= A_2 \\ A_2 + A &= A_3 \\ &\cdots\cdots \\ A_{n-1} + A &= A_n \end{aligned} \qquad (2.1)$$

where A_2, A_3, … A_n are the resulting aggregate formed by the additions of individual atoms/molecule to the preceding ones. Aggregates such as A_2, A_3, … A_n are usually called embryos, sub-nuclei or clusters. The formation of sub-nuclei of large size is, therefore, a statistical process and the formation of such sub-nuclei by the collision f a large number of atoms/molecules simultaneously is highly improbable. Since the surface tension of a sphere is the lowest the sub-nuclei prefer to attain a rounded shape. Since the process of formation of sub-nuclei is in dynamic equilibrium, some of them grow larger whereas others imply disintegrate with time. However, the statistical addition of individual atoms/molecules to some of the sub-nuclei leads to

their development into a size when they no longer disintegrate. Such nuclei are said to attain a critical size and are called three-dimensional Pstable nuclei.

The above treatment of heterogeneous 3D nucleation considers only changes in the interfacial energy of the nucleus, and does not take into account the process of integration of growth species into the embryos during nucleation on foreign particles. Figure 2.7a shows this effect (the process of integration of growth species into the embryos during nucleation on foreign particles). It can be seen that nucleation on a foreign substrate body of radius Rs reduces the effective surface of collision of embryos, where growth species are incorporated into embryos.

At low supersaturations, the nucleation barrier is very high; the nucleation rate is controlled by heterogeneous nucleation. However, at higher supersaturations, the pre-exponential term involving factors associated with effective collisions becomes dominant over the exponential term.

It can be seen that nucleation on foreign particles with small $\Phi(m, R')$, and $\Phi'(m, R')$, corresponding to a large m and/or a large radius Rs, is dominant at low supersaturations. In contrast, nucleation on particles with large $\Phi(m, R')$, and $\Phi'(m, R')$,corresponding to a small m and/or a small radius Rs, is governed by kinetics at high supersaturations. It may be concluded that, for a given system, different foreign particles having distinct surface properties and/or different sizes control nucleation in different supersaturation regimes. Homogeneous nucleation occurs only when $\Phi(m, R') = \Phi'(m, R') = 1$, and this occurs at very high supersaturations.

2.4.1.3 Nucleation and Transformation of Metastable Phases

Under the same conditions several phases can coexist, but the phase which is characterized by the lowest free energy $G=H-TS$ at a given temperature T is the stable one. This may be explained in terms of the thermodynamic stability of different phases.

Overall crystallization of a phase in a closed system occurs by nucleation and growth of crystallites in the volume. The overall crystallization may occur by a mononuclear or polynuclear mechanism involving the formation of one or many nuclei in the volume, respectively. There are two routes to the formation of many nuclei in the volume. In the first case, the nuclei may be formed in the system at the initial moment t=0 and thereafter they grow irreversibly until the completion of crystallization in the entire volume. In the second case, the nuclei form continuously during the crystallization process. These two processes are known as instantaneous and progressive nucleation mechanisms, respectively. However, during progressive nucleation the nucleation rate can be time independent (stationary nucleation) or time dependent (nonstationary nucleation).

As discussed above, nucleation may be homogeneous or heterogeneous. Homogeneous nucleation occurs in ideally pure liquids, whereas heterogeneous nucleation occurs when the system contains nanoparticles (e.g. Seeds) and/or impurity particles.

During crystallization, it is frequently observed that the newly formed phase in the supersaturated mother phase is a metastable one rather than the thermodynamically most stable one. However, under conditions favorable for the formation of a metastable phase, with time the system tends to attain the minimum free energy state by transformation of the metastable crystallization phase into the thermodynamically stable phase. The process of transformation occurs by nucleation and growth of the thermodynamically stable crystallites in the metastable phase rather than in the old mother phase. This means that when direct formation of the stable phase is not possible, the overall crystallization becomes a two-stage process in which the formation of the first stage precedes the appearance of the second stage. This is described by the Oswald rule of stages (also called Oswald step rule).

In general, the transformation of a metastable phase into a stable phase is determined by temperature, ionic strength (i.e. supersaturation ratio S), and medium composition, including additives.

2.4.1.4 Induction Period for Crystallization

As discussed in Section 2.4.1.3, there are two possibilities for the formation and growth of nuclei in the mother phase. In the first case, one nucleus is formed in the system within a time t and then it grows to visible dimensions at an infinitely fast growth rate R. in the second case, while the first nucleus grows to visible dimensions, new nuclei have time to form. These cases are referred to as the mononuclear (MN) and polynuclear (PN) mechanisms, respectively.

2.4.2 Nucleation Agent for Supercooling Prevention

Any foreign substance other than the crystallizing compound is considered as an impurity. Thus, a solvent used for growth and any other compound deliberately added to the growth medium or inherently present in it is an impurity. Different terms, such as additive, admixture, inhibitor and poison, are used in the literature for foreign substances other than the solvent used for obtaining supersaturated solutions. Irrespective of its concentration, a deliberately added impurity is called an additive, but by the term admixture we mean an impurity added in relatively large amounts (up to several percent). A surfactant may be any chemical compound active on the surface in changing its growth behavior. An impurity can accelerate or decelerate the growth process. The impurity that decelerates growth is called a poison or an inhibitor, while one that accelerates growth is said to be a growth promoter.

The thermodynamic basis of solubility of organic substances in the solid state has frequently been discussed in the literature. Briefly summarised, these discussions state that the formation of solid solutions of organic compounds can occur if the mixed molecules are similar in form and dimensions. However, a mutual solubility of such compounds over the entire concentration range is only possible if the crystal symmetry of the pure components is the same (W.M 1957; Mnyukh 1960; Turner 1971; Dirand, Bouroukba et al. 2002). Whether such solid solutions approach ideal behaviour or exhibit varying degrees of non-ideality depends how well the compounds match with regards to the lattice dimensions and the chemical similarity of the compounds. An ideal solution results if the “guest” component does not disrupt the attractive-repulsive forces within the crystal lattice of the “host”

component. Such disruption may cause positive deviations from ideality due to repulsive tendencies, or negative deviations caused by attractive force (Lane 1983). Positive deviations are the most common (He 2004).

Previous work has indicated that additives have a profound effect on the course of nucleation, crystal growth, aggregation, and phase transformation (Sangwal 2007). The additives offer the necessary seeds inside the main PCM to start the nucleation and thus are acting as a nucleating catalyst. Both liquid and solid nucleating agents could be used as the nucleating agent.

For liquid nucleating agent, the melting point of nucleating agent is higher than that of the heat storage main material, and the crystal structure of agent and main PCM material is similar. So when the heat storage main is cooled, the nucleating agent is first solidified and works as a nucleus. Yamagishi et al (Yamagishi, Sugeno et al. 1996) selected 1-Tetradecanol (2 wt %) as the nucleating agents for microencapsulated n-Tetradecane. Zhang et al. (Zhang, Fan et al. 2005) added 10wt% of 1-octadecanol inside the microcapsulated n-octadecane and the supercooling decreased from 26 ℃ to 12 ℃. Huang et al (Huang, Günther et al. 2010) selected 0.8-10 wt% paraffin wax with a freezing peak point of 50 ℃ as the nucleating agent for tetradecane and hexadecane paraffin-in-water emulsion, and the supercooling was reduced by about 12 ℃.

For solid nucleating agent, when the system contains nanoparticles and/or impurity particles, which act as nucleation centre, to enhance nucleation progress. Nanoparticles working as nucleating agent was investigated by some researchers, and

showed an appreciable application potential. In Oliver et al 's (Oliver and Calvert 1975) opinion, most of the crystallization processes of PCM are dominated by the heterogeneous nucleation mechanism, the phase-transition behavior of the PCM being complicated and very sensitive to small amounts of impurities. He et al. (He, Tong et al. 2007) found that by putting nanoparticles into pure water, the supercooling of water was obviously decreased. Moreover, the TiO_2-$BaCl_2$-H_2O nanofluids had a much lower supercooling degree than the $BaCl_2$ – H_2O nanofluids, which implied that the different additives have different nucleation effects. Zhang et al. (Zhang, Wu et al. 2010) indicated the different effect on decreasing supercooling by adding different nanoparticles into pure water strongly lie on wettability and the crystal structure. In the three additive candidates, α-$Al2O_3$ has better effect than γ-$Al2O_3$ and SiO_2, and the effect of lower additive concentration of 0.3% is more obvious than 0.5%. However, up to now, there is not a uniform standard yet to select additive for reducing the supercooling. This is because the essential factors affecting the nucleation have not been clarified.

In the very recent work reported by Huang et al (Huang, Petermann et al. 2009; Huang, Doetsch et al. 2010; Huang, Günther et al. 2010; Huang, Noeres et al. 2010) and Gunther et al (Günther, Schmid et al. 2010; Günther, Huang et al. 2011), it was found that paraffins in emulsified form as finely dispersed droplets behave significantly different than in the bulk. Especially, strong subcooling for droplet sizes below 20 µm was observed. It was also be drawn that subcooling worsens with decreasing emulsion droplet size, and the supercooling of hexadecane emulsions can be decreased with the addition of a paraffin of a higher-melting temperature as the nucleating agent. In addition, it is shown that many different effects can play a role in

the nucleation of PCM emulsions. Both deactivation and creation of nucleation sites have to be expected when dividing a PCM volume into small droplets. The nucleation rate in small droplets could be dominated by homogeneous nucleation, which again depends on the droplet volume. It is shown clearly that the surfactant used to stabilize the emulsion has a strong impact on the nucleation of the sample, too. Finally, it is lined out that not only the nucleation, but also the melting and the solidification temperature are affected by the emulsification of the PCM.

Fan (2003) indicated the study of crystal morphology is helpful to choose proper nucleating agent for promoting crystallization of n-alkane and to understand the thermal storage and temperature regulation mechanism of PCM capsules. Fan (2003) also indicated that C18 is the triclinic crystalline phase by using X-ray Diffraction analysis. Other researchers showed while the stable phase observed for C_{16}, C_{18}, and C_{20} is the triclinic crystalline phase, nucleation proceeds through a transient metastable rotator phase. The odd n-alkanes from C_{13}-C_{41} crystallize is an orthorhombic system (Zhang, Fan et al. 2005). Paraffin is the homologue of C_{18}, and the triclinic crystalline in paraffin is the same as C_{18}, so it is possible using paraffin as the nucleating agent to promote the crystallization of C18 and to prevent supercooling of PCM capsules (Fan 2003).

Hwang, Y., et al.(Hwang, Park et al. 2006; Hwang, Lee et al. 2007) have made series experiments on various nanoparticles of multi-wall carbon nano tubes, C_{60}, CuO and SiO_2. As base fluid DI water, ethylene glycol, oil, silicon oil and poly-a-olefin oil (PAO) was used. They indicated thermal conductivity enhancement depends on the

volume fraction of the suspended particles, thermal conductivities of the particles and basefluids.

There are several US patents supply different nucleating agents to prevent supercooling of PCM. Most of the nucleating agents were liquid additives which have higher freezing temperature and will crystallize before the main PCM.

Tomura, K. (Tomura and Kawasaki-shi 2010) used tri-n-butylalkylammonium salt or its aqueous solution as the supercooling-preventive agent added to a heat storage main agent, such as tetraalkylammonium compound hydrate. When a tetraalkylammonium compound which forms a hydrate having a melting point higher than that of a heat storage main agent by at least 5 ℃ is added to the heat storage main agent as a supercooling preventive agent, the hydrate of the tetraalkylammonium compound is produced at first to give a nucleus for the hydrate formation of the heat storage main agent. If the difference in the melting points is smaller than 5℃, the supercooling preventive effect cannot be obtained sufficiently. Tomura, K. suggested 1 to 20 wt% ratio of supercooling preventive agent is preferable and accordingly supercooling can be reliably prevented. If the addition amount is lower than 1%, the effect of preventing supercooling by forming a nucleus for hydrate production of the heat storage main agent is insufficient. On the other hand, if the addition amount exceeds 20%, the melting point of the mixture of the heat storage main agent and the supercooling preventive agent is affected and increased, resulting in undesirable consequence.(Tomura and Kawasaki-shi 2010) The latent heat quantity ratio is considerably decreased if the addition ratio of the aqueous tetra-n-butylammonium fluoride solution with the congruent concentration

exceeds 20%, but if the addition ratio is up to 16%, the decrease of the latent heat quantity ratio is little. The supercooling releasing capability is insufficient if the addition ratio is 4% or lower. Accordingly, it is preferable to adjust in the range of 7 to 16% for the addition amount of the aqueous tetra-n-butylammonium fluoride solution with the congruent concentration at which latent heat quantity is not decreased and the supercooling releasing capability is sufficient even if the difference between the cooling temperature and the melting point is about 3℃ (Tomura and Kawasaki-shi 2010).

Salyer, I.O.'s patent (Salyer 2002), the phase change composition comprised a eutectic mixture of water and sodium chloride and the nucleating agent comprised calcium oxide, calcium hydroxide, or pentaerythritol. The amount of from about 0.1 to 5 weight percent was suggested. Preferably, the phase change composition included about 1% by weight of the nucleating agent.

In Lee, Won-mok's work (Lee 2004), the specific phase change materials were paraffin hydrocarbons with the number of carbon from 13 to 28. Lee also suggested the nucleating material could be added to the phase change material by the amount of about 0.1 to 15% with respect to the weight of the phase change material. However, the amount of the nucleating agent may be varied depending on temperature, and it was preferred that the nucleating agent be used within a range of about 1 to 6%. Lee's final suggestion was, as for the size of the microcapsule of the present invention produced as such, its diameter was within a range of 0.1 to 1,000 micrometers, preferably 0.1 to 300 micrometers. When the phase change material was produced in the form of the aforementioned microcapsule having the size of the

order of micrometers, a surface area thereof on which heat transfer occurs was increased so that the phase change material can be efficiently used.

2.4.3 Nanoparticles as Nucleation Agent

Ding, Y., et al. (Ding, Alias et al. 2006) made experiments on aqueous suspensions of multi-walled carbon nanotubes (CNT nanofluids), and obtained that the effective thermal conductivity increased with increasing temperature and CNT concentration; the viscosity of CNT nanofluids increased with increasing CNT concentration and decreasing temperature; and significant enhancement was observed of the convective heat transfer depends on the flow condition, CNT concentration and the pH level.

The crystallization behavior of n-alkanes has been well investigated (Marie, Chevalier et al. 2005). Depending on their length and evenness, pure n-alkanes crystallize in monoclinic (even0carbon n-alkanes with n>26), triclinic (even-carbon n-alkanes with n<26), or orthorhombic (odd-carbon n-alkanes) structure. n-Alkane mixtures crystallize as orthorhombic or hexagonal phases. The thermodynamic behavior of n-alkane mixture solutions resembles eutectics. Needle-shaped crystals are formed when the cooling rate of the mixture solution is fast, but plates are formed when the cooling rate is slow. The larger, flat faces of plates usually exhibit spiral growth (Sangwal 2007).

Paraffin wax consists of a mixture of mostly straight-chain (normal) n-alkanes, CH3-$(CH_2)_n$-CH_3. In the solid state, pure n-alkanes form single crystals of four crystal systems. The type of system depends on the temperature and the number of carbon atoms in the molecule. There are the hexagonal (α-phase), rhombic (β-phase),

monoclinic (γ-phase) and triclinic (δ-phase) system (Broadhurst 1962). n-Alkanes with n=12, 14, 16, 18 and 20 form triclinic crystals below their melting point, and n-alkanes with n=11-43 form hexagonal crystals. Furthermore, Agafonov, Garkushin et al. (1999) have also reported a consideration of component structural characteristics which reveals that the interaction of components having similar structures (α-α, β-β, γ-γ and δ-δ) results in the formation of continuous solid solutions (He 2004).

Nanoparticles have been extensively investigated for the effective enhancement of thermal conductivity and latent heat storage capacity for TES application. Nanoparticles working as supercooling preventive agents were also investigated by some researchers (Liu 2005; Okada, Watanabe et al. 2007), and their use showed an appreciable application potential. One of the main assignments in the use of nanoparticles was to investigate effective dispersion technique to avoid the aggregation phenomenon (Rastogi, Kaushal et al. 2008; Song, Jiang et al. 2008). In addition to bulk PCM and MPCM slurries, additives were also used to enhance solidification of O/W (oil-in-water) emulsions (Sakamoto, Ohba et al. 2004).

There are various researches (Abu-Nada 2008; Kakaç and Pramuanjaroenkij 2009) showed nanoparticles have significant effect on heat transfer enhancement. In addition to the study of effect of CNT on supercooling, a brief analysis of effect of CNT on heat transfer enhancement could be considered. Wang, Xie et al. (2009) prepared and investigated the thermal properties of heat storage nanocomposites consisting of paraffin wax (PW) and multi-walled carbon nanotubes (MWNTs). DSC results revealed that the melting point of a nanocomposite shifted to a lower temperature compared with the base material, with increasing the mass fraction of

MWNTs. With the addition of MWNTs, the latent heat capacity was reduced. The enhancement ratios in thermal conductivities of nanocomposites increase both in liquid state and in solid state with the increasing with the mass fraction of MWNTs when compared to the pure PW. For the composite with a mass fraction of 2.0%, the thermal conductivity enhancement ratios reach 35.0% and 40.0% in solid and in liquid states, respectively.

2.4.4 Dispersion of Nanoparticles in Liquid

A major problem with the use of nanoparticles as nucleating agents is the poor dispersibility of nanoparticles in the liquid. Because of their high aspect ratios, large specific surface area, and substantial van der Waals attractions, carbon nano-tubes tend to self-aggregate into bundles spontaneously. In addition, the high flexibilities increase the possibility of nano-tubes entanglement and close packing (Vaisman, Wagner et al. 2006; Sun, Chen et al. 2009). Ding, Alias et al. (2006) got SEM and TEM image of the entangled WMCNT if these nanoparticles are directly put in distilled water. Figure 2.10 clearly shows that the nanotubes are entangled and some are in the format of agglomerates.

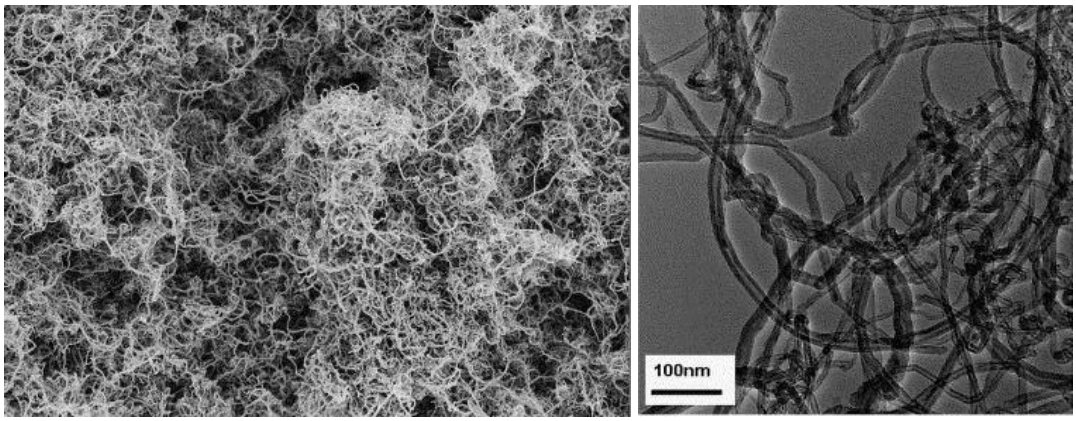

a) **b)**

Figure 2.10 Images of entangled WMCNT a) SEM image and b) TEM image (Ding, Alias et al. 2006)

The structure of MWCNT particle plays an important role on its poor solubility and dispersivity in either water or organic solvents (Vaisman, Wagner et al. 2006). The carbons on the tubular part are joined with three neighbor carbons (120 °) to form the hexagonal structure hence the hybridization state is sp^2, while the carbons on the end caps are pentagons and heptagons which are sp^3 hybridized. The sp^2 hybridized carbons stay in the pz orbital and are responsible for π–π interactions causing aggregation between MWCNT particles. But these π-electrons also promote adsorption of various chemicals on the MWCNT particle surface via π–π stacking interactions (Zhang, Zou et al. 2003; Vaisman, Wagner et al. 2006). n-hexadecane is a straight chain alkane with 16 carbon atoms. As it only consists of carbon and hydrogen atoms only and none of other functional group presented, these structural characters cause it quite inert and immiscible with water.

Two common approaches are available for dispersion of MWCNT: the use of external mechanical forces and physicochemical modification of the particle surface

properties (Rastogi, Kaushal et al. 2008). Mechanical approach can only temporarily break the interactions between MWCNT particles and the particles will aggregate again after the force is removed. Physicochemical approaches can be classified into physical and chemical methods. Physical methods mostly involve the adsorption of chemical surfactants onto the MWCNT surface which do not change the chemical properties of the MWCNT surface. Chemical methods involve the surface modification or functionalization of the particles with various chemical reagents to improve their dispersibility in the liquid and to increase the resistance to aggregation.

Kim, and et al. (2010) used plasma-treatment method to disperse CNT in water and made stable nanofluid. Different recipes were used and compared to get plasma-treated CNTs including argon, oxygen and methane/oxygen mixtures. The dispersion stability result can be shown in Figure 2.11.

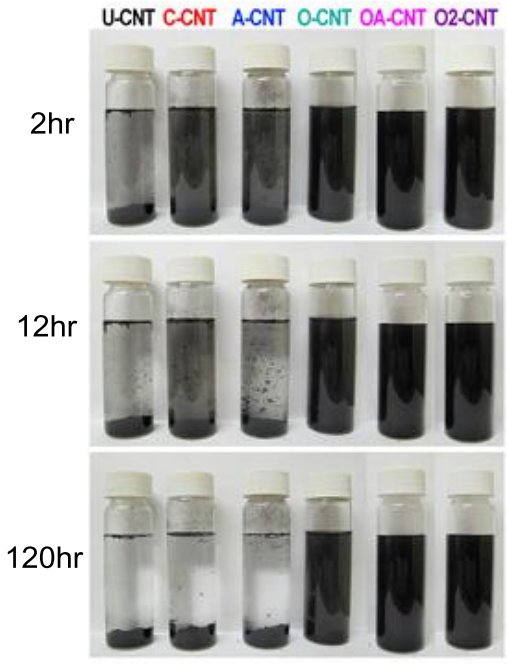

Figure 2.11 Dispersion stability of CNT-in-water nanofluids with 0.01 vol% CNT addition until 120 h settling time (Kim, and et al. 2010)

2.5 Nocturnal Sky Radiative cooling Applications

2.5.1 Passive Cooling Application

The energy consumption of building has been increasing in recent year and occupies a large portion of total energy consumption. For example, in American building consumes 33 % of annual energy consumption. HVAC system consumes a large portion of the building energy use. Hence, it is very important to explore innovative cooling strategy.

Passive cooling of buildings can be defined in several ways. One way is to consider any treatment of the building which reduces its cooling load, such as solar control, minimizing internal heat gain, etc., as passive cooling techniques (Santamouris 2006). These techniques include such subjects as lowering the urban temperatures, shading of windows, and envelope's exterior colors of low solar absorptivity. Another way is to consider all the above mentioned subjects as elements of proper architectural and urban design, responsive to the climate and aiming to improve thermal comfort in hot periods even when the building is not mechanically conditioned, or to lower the equipment size and energy consumption in air-conditioned buildings (Givoni 2011). Passive cooling of buildings from this viewpoint comes after appropriate design has been applied, and can be defined as the use of renewable sources of energy to enhance heat loss from the building.

Lowering of indoor temperatures by passive systems can be provided through the utilization of several natural heat sinks: the ambient air, the upper atmosphere, water evaporation, and the under-surface cooled soil. A list of passive cooling systems defined in this way includes (Givoni 2011):

- Naturally ventilated buildings: Enhancing comfort and/or lowering indoor temperature by daytime ventilation when the indoor temperature in closed buildings is too high.
- Nocturnal ventilative cooling: Lowering the indoor daytime temperature by ventilating the building at night.
- Direct evaporative cooling: Lowering the temperature while raising the humidity of the ventilation air by water evaporation.
- Indirect evaporative cooling: The primary cooling is derived from evaporation but the building is cooled indirectly, without elevating the indoor humidity.
- Radiant cooling: Utilizing nocturnal longwave radiant heat loss to the sky.

Long-wave radiation emissions is a continuous day and nighttime phenomenon. However, during the daytime the long-wave radiation emitters are exposed to solar radiation. The objects absorbing solar radiation are heated and that in most cases outweighs the cooling effect produced by the emission of long-wave radiation. For this reason, the net cooling effect of the radiators can be obtained only during the nighttime (nocturnal radiation) (Mihalakakou, Ferrante et al. 1998).

The fundamental of the nocturnal radiation is that the upper atmosphere is near absolute zero, about 4 K (Bliss 1961), and thus it can be utilized as a heat sink. The radiative cooling of a surface exposed to sky at night can be used to lower the

temperature of a fluid beneath the radiator below that of the surrounding ambient temperature. Using such a nocturnal cool sink is an attractive subject for researchers due to its ultimate goal of keeping the environment out of contamination. Under clear sky conditions, the downward radiation has two distinct peaks at wavelength values of about 7 and 15 μm, respectively. It also has a clearly evident deep drop in radiation value between wavelength values of 8 and 13 μm, called the atmospheric window, since the atmosphere is almost transparent to ground radiation within this latter range (Hamza H. Ali, Taha et al. 1995).

In the case of building cooling applications, the cooled body is the building or the nocturnal radiator and the heat sink is the sky. This effect is especially evident on a clear night with low humidity (Saitoh and Fujino 2001).

2.5.2 Radiator Model Investigations

There are two method of applying radiative cooling in buildings (Mihalakakou, Ferrante et al. 1998). The first method is called direct, or passive, radiative cooling. In this case the building envelope radiates towards the sky and gets cooler. The second method is called hybrid radiative cooling. In this case the radiator is not the building envelope but usually a metal plate.

There are several design options for applying passive radiative cooling in buildings which involve three basic types of nocturnal radiators (Mihalakakou, Ferrante et al. 1998): (1) a movable insulation system which can be moved over the high mass roof

of the building, (2) a lightweight, usually metallic radiator which cools the ambient air below its initial temperature, and (3) an unglazed water-type solar collectors.

For the first type radiator, Saito and Fujino (2001) constructed an energy-independent residential house (Figure 2.12) incorporating sky radiative cooling, solar thermal, and photovoltaic energies.

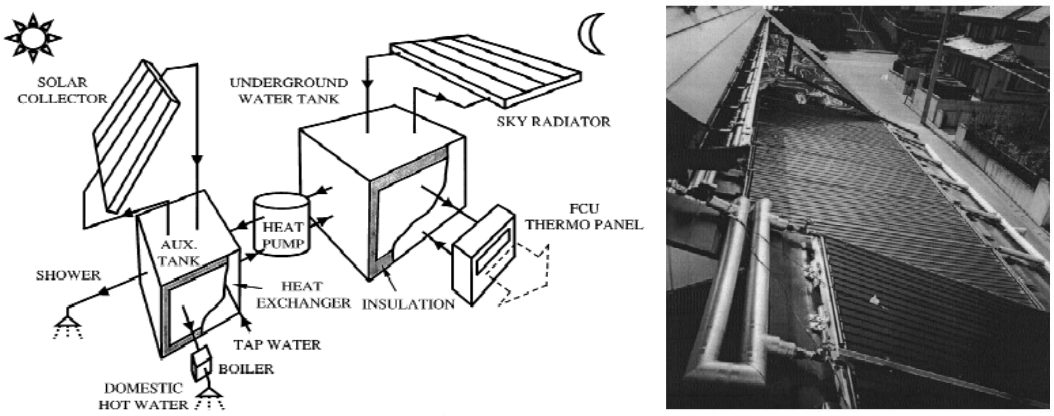

a) **b)**

Figure 2.12 A integrated cooling system: a) Schematic flow network for the long-term cool storage mode, and b) Photo of sky radiator (Saitoh and Fujino 2001)

For the second type radiator, Mihalakakou, Ferrante et al. (1998) investigated a lightweight metallic radiator with an air space and ambient air flow (Figure 2.13). The operation of such a radiator is the opposite of an air flat plate solar collector. Air is cooled by circulating under the metallic surface of the radiator before being directed into the building to provide instantaneous cooling during the night and to cool the interior mass of the building by convection, creating a cold storage for the following day. The main two differences between a lightweight metallic radiator and

an air flat plate solar collector are firstly the different operating period during the day and secondly the radiator is not equipped with glazing material since ordinary glazing used in solar systems is not transparent to long-wave radiation.

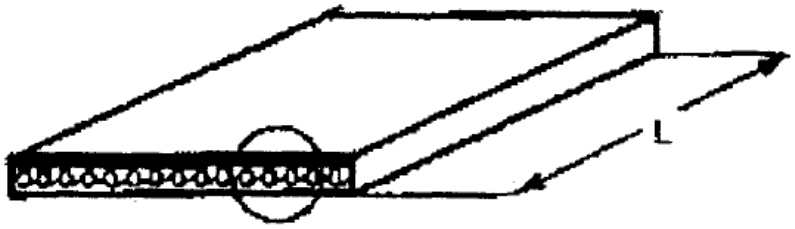

Figure 2.13 A lightweight metallic radiator (Mihalakakou, Ferrante et al. 1998)

For the third type radiator, Hamza HHH. Ali, Taha et al. (1995) used a two parallel plates night sky radiator with the top one (radiator) being a painted black aluminum plate. The radiator plate was covered by a polyethylene windscreen cover. The schematic of the system unit and the construction details of the radiator unit are shown in Figure 2.14 and Figure 2.15.

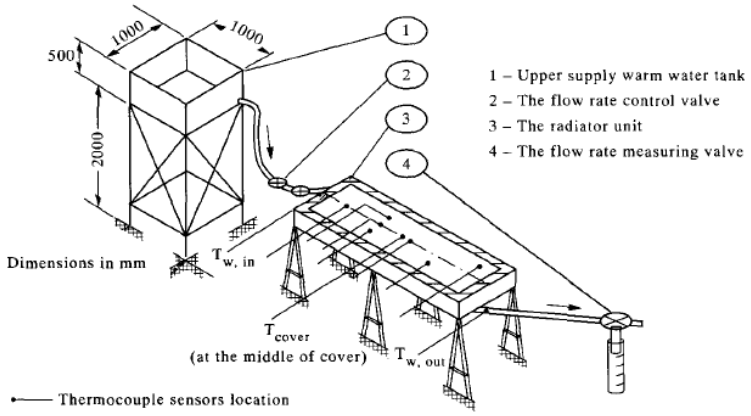

Figure 2.14 Schematic drawing of open loop night sky radiative cooling unit (Hamza H. Ali, Taha et al. 1995)

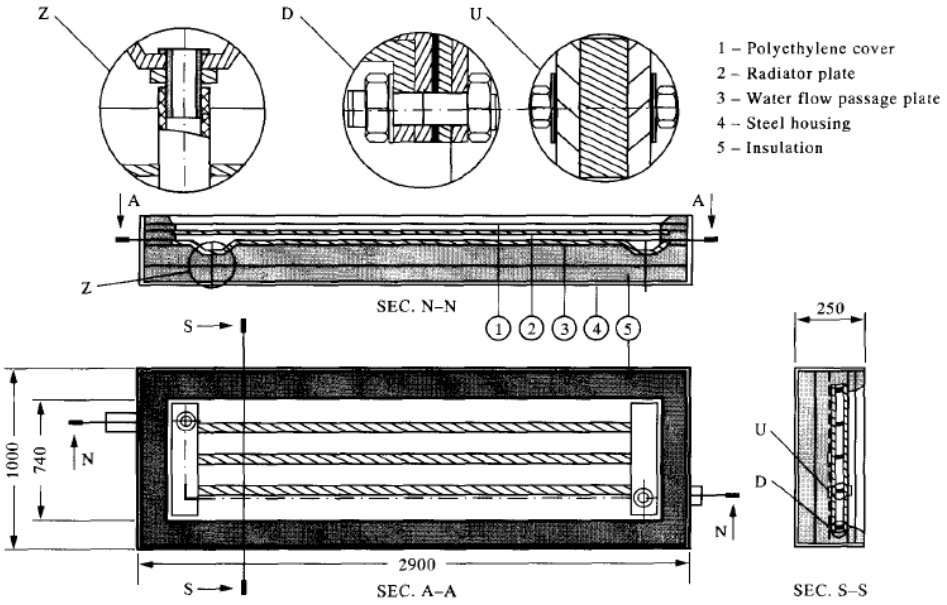

Figure 2.15 Construction details of the radiator units (Hamza H. Ali, Taha et al. 1995)

Radiator was investigated by several researchers by experimental method (Hamza H. Ali, Taha et al. 1995; Saitoh and Fujino 2001) and numerical method (Argiriou, Santamouris et al. 1994; Hamza H. Ali, Taha et al. 1995; Mihalakakou, Ferrante et al. 1998).

Saitoh and Fujino (2001) proposed an energy-efficient house incorporating solar thermal and sky radiation. The HARBEMAN house has two major features: one is a large heat/cool storage tank (30-60m^3) which makes it possible to store energy seasonally. Another feature is to utilize seasonal sky radiative cooling. This difficulty was overcome by changing the period of sky radiator operation: the water of the underground tank is chilled in advance in spring when the ambient temperature and humidity are relatively low. The temperature of the tank is cooled down to 4 ℃ with the aid of a small capacity heat pump (600 W) that utilizes night-time electricity. Based on 3 years monitor, the experiment results indicated the house consumes only

one-sixth of fossil energy compared with the conventional house. It also emits very low amounts of carbon dioxide and other pollutant gases.

Argiriou, Santamouris et al. (1994) use 12 years of hourly weather data to assess the radiative cooling potential in Athens. The model has been used to calculate the sky-temperature depression and the outlet air temperature for a flat-plate radiative air cooler using hourly values of the following weather data: ambient temperature, relative humidity, wind velocity. The performance results for a simple radiator are also presented. The radiative cooling potential for Athens is promising and simple radiators can be used to estimate the cooling potential. Argiriou, Santamouris et al. also indicated sky temperature depression is the difference between the ambient air temperature and the sky temperature. While the sky-temperature depression quantities the potential for radiative cooling as a function of weather data at a particular site, the stagnation temperature takes into account not only weather data but also the characteristics of the radiator. The stagnation temperature is the lowest temperature attainable by a radiator for specific weather and operational parameters and indicates the cooling efficiency. Argiriou, Santamouris et al. drew the conclusion that the radiative cooling is useful in Athen, and the performance evaluation of natural cooling techniques should be based on detailed climatic data.

Hamz H. Ali, Taha et al. (1995) carried out both experimental and theoretical studies of nocturnal cooling of water flowing through a night sky radiator unit. The experimental study was conducted for a gravity flow open loop system. The parameters studied include the effect of average water mass flow rate, uncovered from the ambient versus covered supply warm water tank, and windscreen cover

thickness on the performance. A new definition of the performance was expressed by an overall efficiency. A comparison between nocturnal cooling of stagnant and flowing water was also done. In the theoretical study a thorough radiation model was developed which calculates the radiation heat losses from both the cover and the radiator plate considering multiple reflections and absorptions between cover and plate. Energy balance was then applied on the cover, the radiator plate and the water. The cover and insulation were considered one lump each, while each of the radiator plate and the water were divided into discrete number of lumps. Energy storage in the radiator frame and insulation, and water elements was considered. Experimental results were also used for verification of the theoretical model.

Wind screens are used in radiative cooling systems to reduce convective heat gain from the ambient transparent. This system has been researched by several researchers (Mostrel and Givoni 1982; Argiriou, Santamouris et al. 1994; Hamza H. Ali, Taha et al. 1995; Mihalakakou, Ferrante et al. 1998). Mostrel and Givoni (1982) give experimental and simulation investigations on the radiator thermal transfer fundamentals, the influence of humidity, the dew formation and cloudiness to the radiation effect, the effect of different structures, colors and materials of wind screens, and the influence of other factors like the dust. On the other side, some researchers do not suggest using wind screen in radiative cooling system. In the research of Mihalakakou, Ferrante et al. (1998), the nocturnal radiator was covered with a thin polyethylene wind-screen which reduces the convective heat gains from the warmer ambient air to the radiator, thus improving the efficiency of the system. Taking into account that wind-screens have to be transparent to longwave radiation, thin polyethylene films (60-100/zm) can be used in these radiators. On the contrary,

Argiriou, Santamouris et al. (1994) indicated that the contribution of the wind screen to reduction of the stagnation temperature seems not to be significant. For optimal weather conditions, the stagnation temperature of the unprotected radiator ranges from 22 ℃ in September to 27 ℃ in July for 80 % of the time. For the wind-screened radiators, it ranges from 19 ℃ in September to 23 ℃ in July. But he did not suggest use wind screen in Athens because of the high cost, short life and limited effect.

2.5.3 Radiative Cooling Application Conditions

As is well known, sky radiative cooling appears most significantly (Saitoh and Fujino 2001) : (1) under a clear weather condition, (2) in low relative humidity, (3) low wind speeds. The high efficiency depends on the large temperature difference between the sky and the cooling collector, the nocturnal radiator. Therefore, the performance evaluation of natural cooling techniques should be based on detailed climatic data (Argiriou, Santamouris et al. 1994). The weather in summer in Hong Kong and other tropical cities are not appropriate for sky radiation to be effectively used because of high ambient temperature and high humidity (80–90 %). On contrast, there is more potential in the north, west and central cities in China to be developed due to the relatively low temperature and low humidity.

In this study, the integrated system of MPCM slurry storage, coiled ceiling system, and the nocturnal sky radiator system was studied. Because the efficiency and the energy consumption saving of nocturnal sky radiator system depend on the weather conditions, MPCM slurry with relative high melting temperature has great potential to be combined with the nocturnal radiation system. If water is used as the storage

medium as convention, the working temperature of the heat transfer medium in radiator have to be decreased below 0 ℃. The operating time will obviously decrease because the sky temperature is always higher than this temperature 0 ℃. Using water as the storage medium almost makes the using of nocturnal radiator infeasible. Using the high melting temperature MCPM slurry as the storage medium can rise the working temperature of the water, the heat transfer medium, to nearly 15℃ in the radiator. It becomes possible that the cooling can be still obtained in summer, because of using the radiator with a relative high temperature, 15 ℃, and the temperature difference still exist when the sky temperature rise according to the ambient temperature and humidity around radiator.

Chapter 3

Effects of Supercooling on MPCM Slurry Thermal Storage Capacities

This chapter presents the experimental investigation of microencapsulated paraffin slurry as a cooling storage medium for building cooling applications. The microencapsulated n-hexadecane particles are first measured by a differential scanning calorimeter (DSC) to check the thermal properties of the phase change point and latent heat capacity. Then MPCM slurry is measured using a small-scale thermal storage test system to simulate the practical operating situations of an air conditioning system. MPCM slurry is cooled to 5 ℃ and heated to 25 ℃ cyclically in a 230 liter storage tank with three stirring conditions. The thermal process and properties of MPCM slurry tested under the practical operating conditions are reported and discussed. This chapter further proposes two correlation equations that can be used to describe the effect of supercooling on the effective cooling storage capacity observed in the tests.

3.1 Introduction

PCM has long been used as thermal storage materials because of the large amount of heat absorption/release during the phase change processes, with only small temperature variations (Dinçer and Rosen 2010). In recent years, alternative phase change materials with higher melting temperature which is proper to HVAC applications are most desirable and have been investigated by several researchers

(Zalba, Marin et al. 2003; Farid, Khudhair et al. 2004; Gschwander, Schossig et al. 2005). In addition, a new approach was also proposed, in which the PCM was microencapsulated and suspended in a single-phase heat transfer fluid to form the solid-liquid MPCM slurry (Kasza and Chen 1985). Therefore, the utilization of MPCM slurry with controllable working temperature offers a great chance of employing natural cooling resources in traditional building cooling applications to reduce the energy consumption and CO_2 emission.

Supercooling is one of the major problems associated with MPCM slurry as cooling storage medium. The phenomenon that the latent heat can only be released at a supercooled, lower temperature is disadvantageous for energy storage applications (Zhang, Fan et al. 2005). In general the preliminary studies and experiments indicate MPCM slurry is promising as a thermal storage medium. However, experimental investigations on effects of supercooling on the MPCM slurry thermal storage capacities appear to be limited so far. In our earlier work, Wang et al. (2007; 2009) studied the flow and heat transfer behaviors of phase change material slurries in a horizontal circular tube and the performance of a cooled-ceiling operating with MPCM slurry, disregarding the supercooling for simplification.

In this chapter, we present our experimental investigation of microencapsulated paraffin slurry as a cooling storage medium for building cooling applications, in particular, we focus on establishing the effective cooling storage capacity at the cooling temperature range with natural cooling sources such as evaporative cooling and nocturnal radiative cooling, which can be used to estimate the realistic ability to cool these natural cooling sources under different climatic conditions.

3.2 Experimental Approach

3.2.1 Microcapsule and Slurry Preparation

MPCM slurry is made by microencapsulating phase change material with a thin film as a shell and dispersing the microencapsulated PCM into an aqueous solution as a carrier fluid. Hexadecane ($C_{16}H_{34}$), for which the melting temperature is 18 ℃ and the latent heat is 234 kJ/kg (Lane 1983), was chosen as the core material, and Amino Plastics was chosen as the shell material. The core-shell ratio was controlled to be about 7:1 by weight during the preparation process, meaning the thickness of the shell was approximately 0.3μm. Pure water was chosen as the carrier fluid. The initial reason for this is that water is easy to handle and has no chemical effect on either the phase change material or the shell wall. Another important reason is that the original form of slurry is in aqueous form and can be easily diluted with pure water to obtain different concentrations according to various engineering applications. The solid content of the emulsion used in this study is about 23%.

3.2.2 Slurry Properties

Flow and heat transfer characteristics are associated with the following properties: density, thermal conductivity, melting/freezing point and latent heat of fusion of the PCM, as well as the properties of the carrier fluid, the particle size, and the concentration of the slurry. The thermal property model, which has been applied by various researchers (Charunyakorn, Sengupta et al. 1991; Wang, Niu et al. 2007) to

phase change slurries, was used in the present study to calculate the properties of the slurry, which are given in Table 3.1 (Wang and Niu 2009).

Table 3.1 Physical properties of MPCM slurry and its component

	Density $kg.m^{-3}$	Specific heat $J.kg^{-1}.{}^{o}C^{-1}$	Thermal conductivity $W.m^{-1}.{}^{o}C^{-1}$	Latent Heat $kJ.kg^{-1}$
N-hexadecane (solid)	780	1805	0.4	224
(liquid)	770	2221	0.21	
Urea-formaldehyde	1490	1675	0.433	
Water (at 20 ^{o}C)	998	4183	0.599	
MPCM particle (solid)	829	1789	0.382	196
(liquid)	819	2153	0.203	
MPCM slurry (mass fraction)				
Φ=0.2	976	3707	0.551	39.2

3.2.3 DSC Measurements

DSC is one of the most frequently-used testing methods in the development of PCMs (He 2004). Figure 3.1 shows the schematic of a heat flux type DSC describing the heat fluxes between DSC components and the corresponding DSC thermal model. The various scanning rates have been employed in these DSC measurement processes. DSC has been used for selecting a PCM from candidates for the evaluation of PCM prototypes and to investigate the reproducibility of PCM thermal characteristics (He and Setterwall 2002; Yamazaki, Sasaki et al. 2002; Suppes, Goff

et al. 2003; Genovese, Amarasinghe et al. 2006; Cai, Song et al. 2008; Rady 2009). For example, Banu, Feldman et al. (1998) reported that DSC was running at a heating/cooling rate of 2 and 0.2 ℃/min to determine the thermal characteristics of PCM wallboards. Marinkovic, Nikolic et al. (1998) used DSC at a 5 ℃/min scanning rate to determine the melting temperature, the enthalpy of fusion and the heat capacity of the two binary mixtures of $Ca(NO_3)_2 \cdot 4H_2O+CaCl_2 \cdot 6H_2O$ and $CH_3CONH_2+Ca(NO_3)_2 \cdot 4H_2O$ for an agricultural greenhouse application. Sari and Kaygusuz (2001) used DSC at 10 ℃/min scanning rate to test the thermophysical properties of palmitic and stearic acid as PCMs for TES.

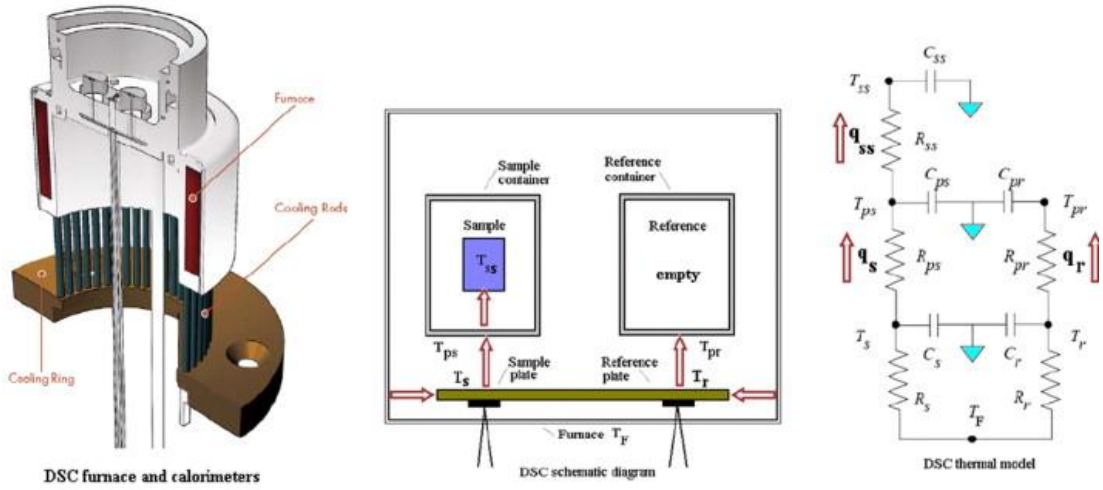

Figure 3.1 A schematic diagram of a heat flux type DSC showing the heat fluxes between DSC components and the corresponding DSC thermal model. (Rady 2009)

The characteristic temperatures from DSC measurements are: the initial peak temperature (T_i), the extrapolated peak onset temperature (T_e), the extrapolated end temperature (T_c), the peak temperature (T_p) and the end peak temperature (T_f). All of these are shown in Figure 3.2, which demonstrates a typical freezing curve. Not all

the characteristic temperatures can be reproduced with equal accuracy. The use of T_e, T_c and T_p is recommended by Hetakeyama and Quinn (1999) for both the melting and freezing peak characteristics. The extrapolated peak onset temperature is defined as the intersection between the tangent to the maximum rising slope of the peak and the extrapolated sample baseline (He, Martin et al. 2004).

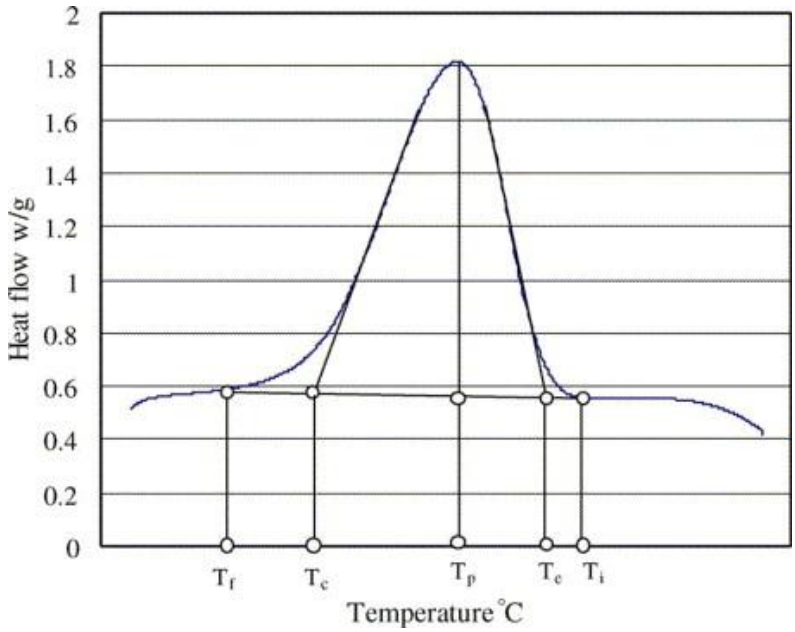

Figure 3.2 Definition of DSC characteristic temperatures for a freezing curve (He, Martin et al. 2004)

The enthalpy change of the phase transition process (storage density) can also be determined by DSC measurements (He, Martin et al. 2004). The area of a DSC peak can be used to estimate the enthalpy change of phase transition. From theoretical modeling, it can be calculated using the equation below:

$$Q_{pc} = \int_{t1}^{t2} \left(\frac{\delta Q}{dt}\right)_{pc} dt \qquad (3.1)$$

Here $(\frac{\delta Q}{dt})_{pc}$ is the heat flow in unit w/g and t is time. The software automatically calculates the total peak area, i.e. the total enthalpy change (Q_{pc}) of the phase transition. However, the enthalpy change (storage density) in any temperature range within the phase transition temperature range cannot be obtained directly. There are two ways to get the enthalpy change in any temperature range according to Equation(3.1). The first way is to utilize the DSC curves (Figure 3.3) that give the heat flow versus temperature (a) to obtain the value of heat flow [$(\frac{\delta Q}{dt})_1$ and $(\frac{\delta Q}{dt})_2$] in any temperature range (T_1 and T_2). Then, based on the heat flow [$(\frac{\delta Q}{dt})_1$ and $(\frac{\delta Q}{dt})_2$], the time range (t_1 and t_2) is obtained from the curve of the heat flow versus time (b). Finally, Equation (3.1) is used to calculate the enthalpy change at any temperature range.

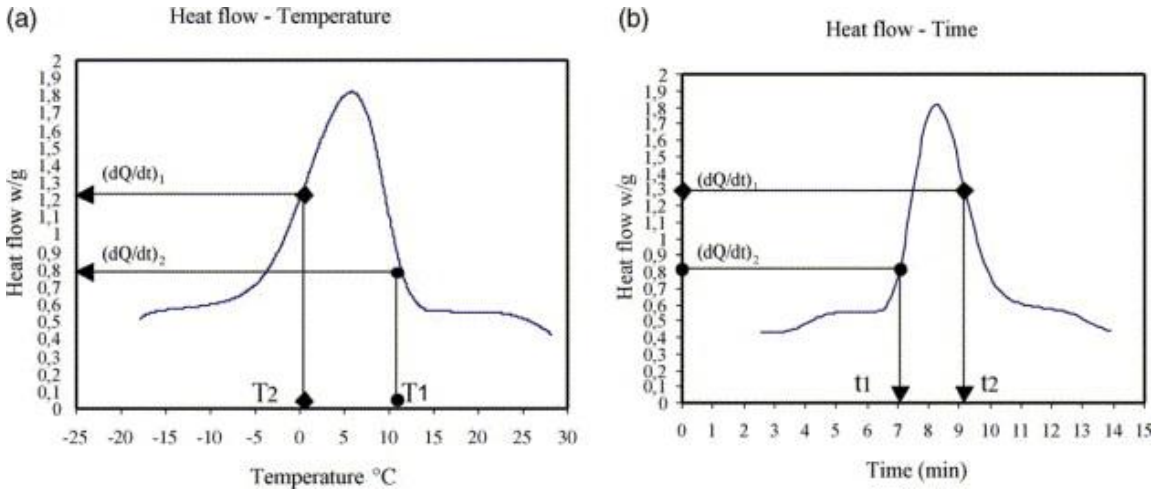

Figure 3.3 DSC curves of heat flow versus (a) temperature and (b) time

In PCM cooling storage applications, the storage density and phase transition temperature determine the storage system capacity, size and application. The study of the phase equilibrium and phase diagram becomes very important and useful. A

phase diagram can give the correct phase transition temperature range and present the energy storage density. If incorrect values are utilized for a cool storage system design, it will result in a lower cooling capacity and economic losses. Therefore, the phase equilibrium study is invaluable to PCM thermal energy storage researches and developers. Combining phase equilibrium considerations with DSC measurements makes it possible to interpret the DSC data properly. This gives a reliable method that incorporates both the heat of phase change and the temperature range.

In this study, the phase transition point and the latent heat of microencapsulated $C_{16}H_{34}$ were measured using a differential scanning calorimeter (Perkin Elmer DSC7, Figure 3.4) with a heating/cooling rate of 5 ℃/min. Perkin Elmer software was used to analyze and plot the thermal data.

Figure 3.4 Photograph of Perkin Elmer DSC7

Figure 3.5 shows the DSC results of microencapsulated $C_{16}H_{34}$ particles. From the DSC results, the diagram showing the key thermal performance of microencapsulated $C_{16}H_{34}$ particles can be drawn, with the melting temperature T_m=15.7 ℃, freezing temperature T_f=12.5 ℃, supercooling degree $\triangle T$=3.3 ℃, and latent heat of melting h_l=178 kJ/kg. However, it can also be observed that two peaks occur in the freezing process, each associated with a latent heat of freezing of 57

kJ/kg and 83 kJ/kg respectively. This indicates that, for the total latent heat of freezing to reach the value of 140 kJ/kg, supercooling to a temperature of around 5 ℃ would be required.

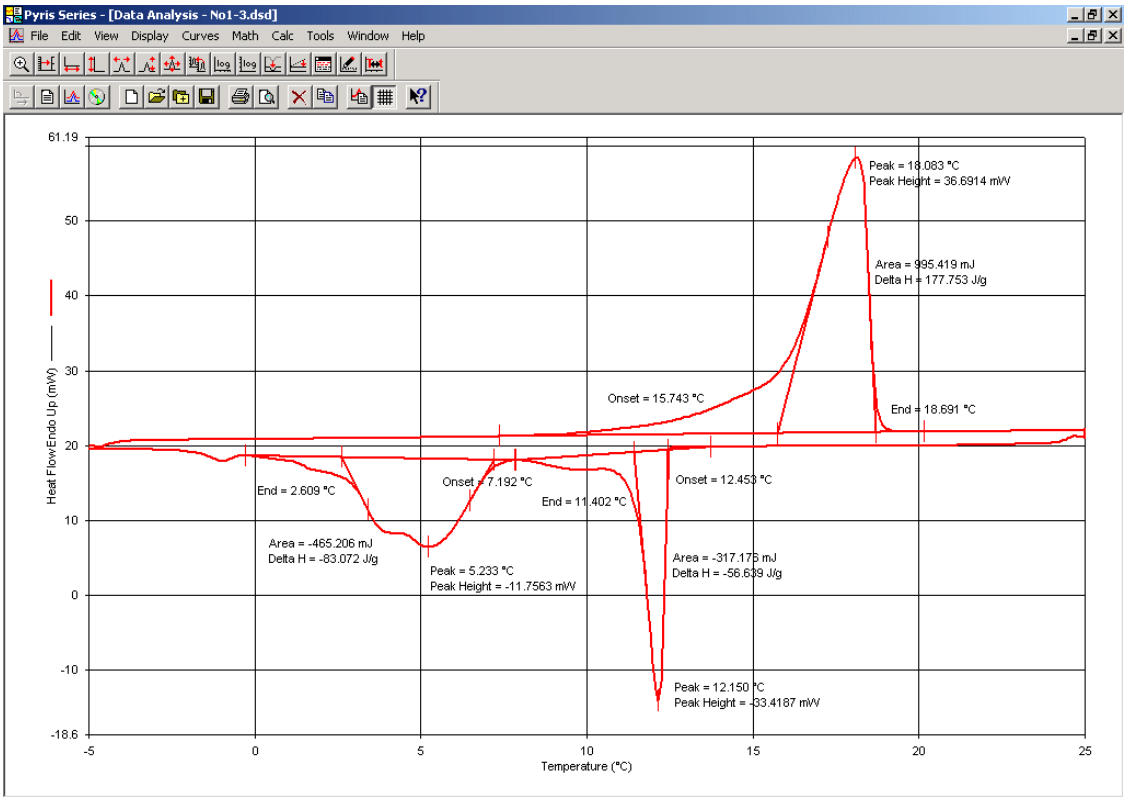

Figure 3.5 DSC results of microencapsulated $C_{16}H_{34}$

3.2.4 Experimental System Description

To investigate the effects of supercooling under realistic operating conditions in air-conditioning applications, we constructed a small-scale system which employs a cooled-ceiling supplied with MPCM slurry to cool an office room which could be occupied by two persons. The system will be used as the experiment platform to observe the cyclic cooling storage (or charging) and release (or discharging)

processes, in complement to the DSC measurements. The schematic diagram of the whole system is given in Figure 3.6 and the photograph of the experimental system is shown in Figure 3.7.

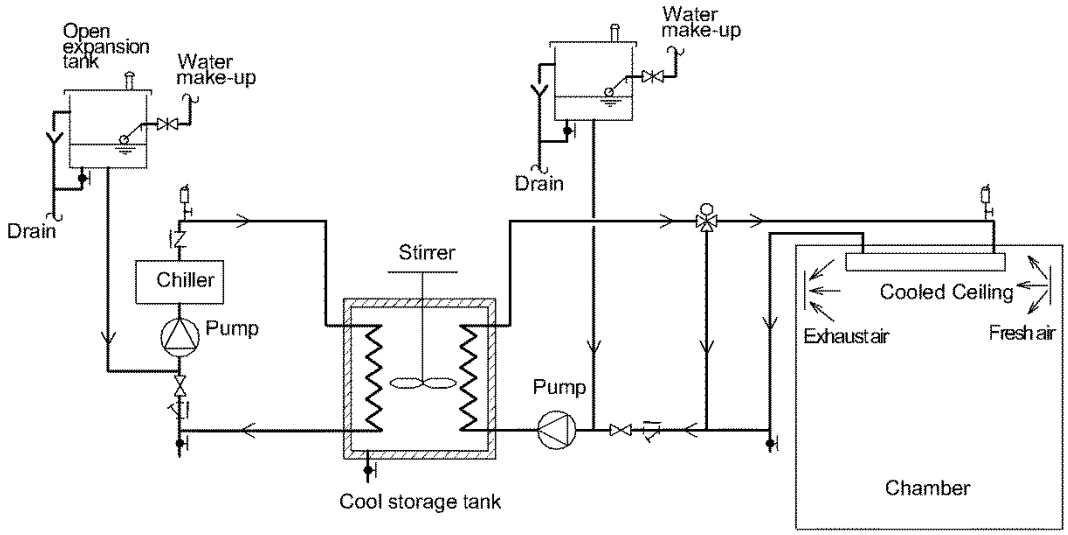

Figure 3.6 Schematic diagram of experimental air-conditioning system

The dimensions of the chamber are 2.7m (w) x 4m (l) x 3m (h). Four water-type ceiling panels are installed in the chamber to extract the sensible load. Fresh air is cooled and dehumidified by a conventional air handing unit (AHU), and then supplied to the chamber at the minimum ventilation rate for ventilation purposes.

The cool storage tank is a cylindrical stainless steel tank, with an insulation layer of 40 cm glass wool clad with a stainless steel sheet. The diameter of the tank is 0.6m, the height is 0.8m, and the internal volume is 0.23m^3. Two coil heat exchangers are set in the tank, both are Φ 20x15m(l) and made of titanium alloy. There is a variable-speed stirrer in the tank to enhance the heat transfer, which is controlled by an electronic controller.

a)

b) **c)**

Figure 3.7 Photograph of experimental system: a) chamber, b) cooled ceiling system, and c) MPCM slurry storage system

During charging, the chiller runs and supplies chilled water to cool the MPCM slurry in the cool storage tank via a heat exchanger. The compressor of the chiller operates with an on/off control, with a set-point temperature for the supply chilled water of

5 ℃. The cooling was stored mostly in the form of latent heat in the MPCM particles, with a small portion as sensible heat in the MPCM particles and water.

During the discharging, water is cooled by the cool storage tank via the other heat exchanger, and then circulated through the cooled ceiling panels in the chamber. A bypass pipe and a three-way modulating control valve are installed to vary the flow rate of the chilled water through the ceiling panel. A variable-speed mixer in the storage tank runs to enhance the heat transfer of the two heat exchangers during both the charging and discharging process.

Eight T-type thermocouples, four bourdon manometers, two turbine flowmeters, and four watt transducers were installed to measure the system's operational parameters. All the data were collected and transferred by a real-time data acquisition system (DAS), and then stored on a computer. The instrument accuracies are shown in Table 3.2, in compliance with ASHRAE 94-77 (Lane 1983).

Table 3.2 Instrument accuracy

Type of measurement	Instrument accuracy
Temperature difference	±0.1℃
Liquid flow	±1.0% of reading
Pressure difference	±25Pa
Time	±0.20%
Mass	±0.20%

3.3 Results and Discussion

3.3.1 Heat Loss of the Thermal Storage Tank and Heat Balance Analysis

Pure water is generally used in water-storage and ice-storage systems; this is one of the most conventional thermal storage systems, and has been used in many practical commercial and industrial applications. In this research project, pure water is used for the calibration of the heat balance of the new system using MPCM slurry. Pure water in the tank was first cooled to 8.8 ℃, and then kept in the laboratory, where the room temperature is around 20 ℃, for 18 hours. At the end of this time, the water temperature had raised to 10.8 ℃. The heat loss of the storage tank is given by:

$$Q_{t.loss} = m_w C_{p.w}(T_e - T_i) \tag{3.2}$$

where m_w is the mass of pure water in the storage tank, T_e and T_i are the end and initial water temperatures in the storage tank (℃), $C_{p.w}$ is the specific heat capacity of pure water [J/(g. K)].

Therefore the total thermal resistance of the storage tank can be given by:

$$R_t = \frac{Q_{t.loss}}{t(T_{lab\cdot ave} - T_{w.ave})} \tag{3.3}$$

where R_t is the total thermal resistance of the storage tank, *t* is the test period, $T_{lab\cdot ave}$ is the average laboratory temperature, and $T_{w.ave}$ is the average water temperature.

The calculation results are $Q_{t.loss}$=1709kJ over the 18 hour test period, and R_t=2.69W/℃. In this way it was ascertained that the heat losses to the surroundings are small, a maximum 3% of the total cooling storage.

Based on the calculation about the heat loss of the thermal storage tank, the heat balance was then checked when running with water. Theoretically， the cooling supplied by chiller Q_{ch} will be totally stored in the water, acting as sensible heat storage ΔU_w. Considering the heat loss of the tank, the difference between the amount of heat coming into and leaving the thermal storage tank ΔQ is defined as:

$$\Delta Q = Q_{ch} - \Delta U_w - Q_{t.loss} \tag{3.4}$$

The mixer in the tank runs at 3 different speeds (80rpm, 230rpm, 380rpm). The charging process results with water as the medium are shown in Figure 3.8. It is observed that on-off operation of the chiller caused unwanted temperature fluctuations of the chilled water.

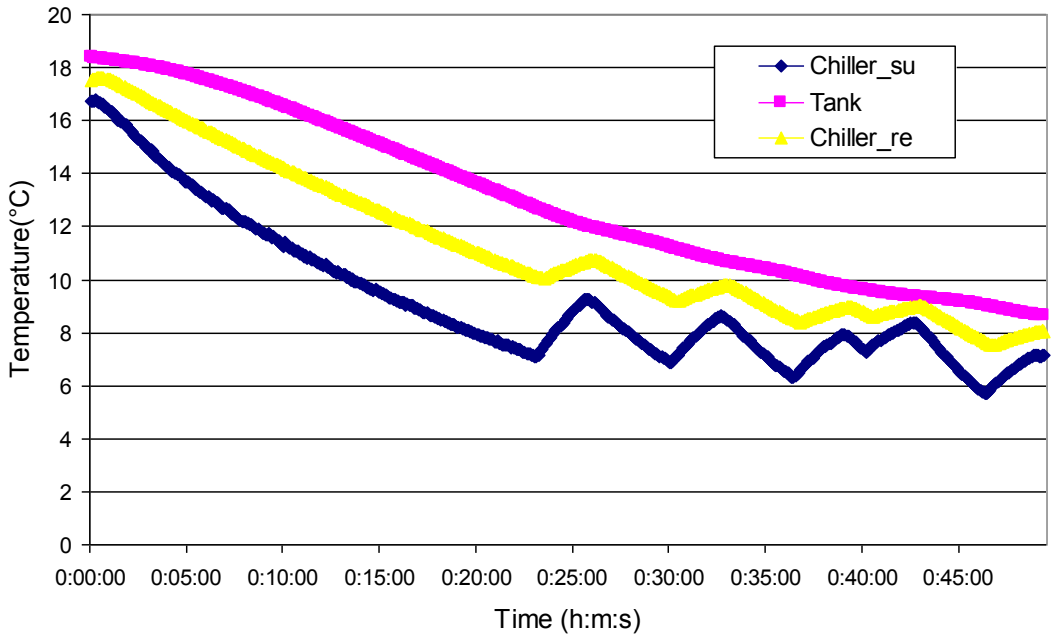
Chiller_su
Tank
Chiller_re
Temperature(°C)
Time (h:m:s)
0
2
4
6
8
10
12
14
16
18
20
0:00:00
0:05:00
0:10:00
0:15:00
0:20:00
0:25:00
0:30:00
0:35:00
0:40:00
0:45:00

a)

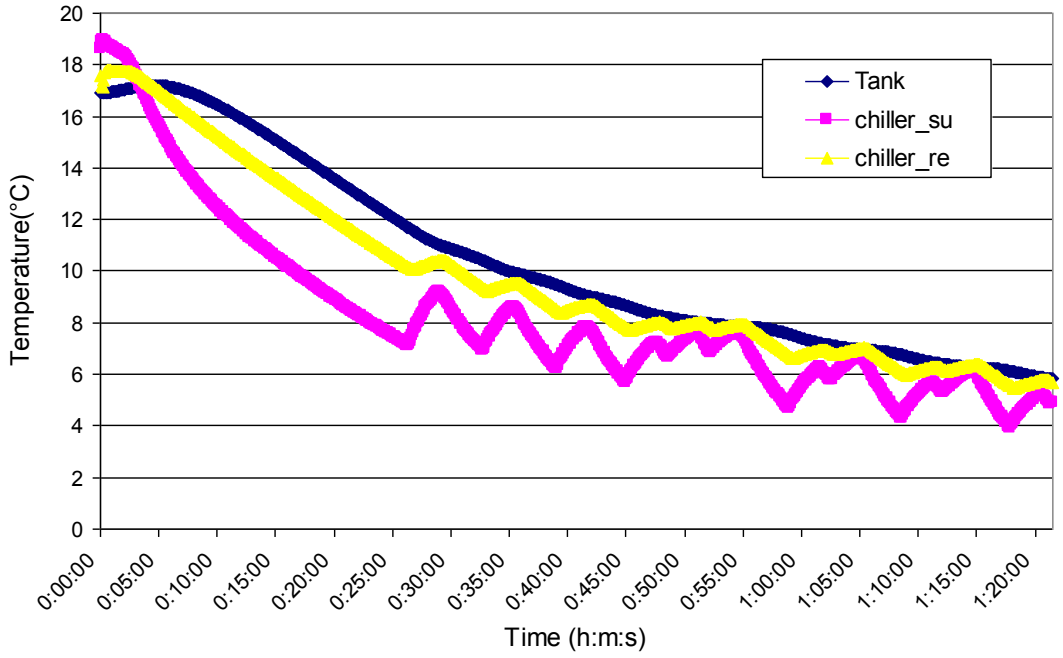
Tank
chiller_su
chiller_re
Temperature(°C)
Time (h:m:s)
0
2
4
6
8
10
12
14
16
18
20
0:00:00
0:05:00
0:10:00
0:15:00
0:20:00
0:25:00
0:30:00
0:35:00
0:40:00
0:45:00
0:50:00
0:55:00
1:00:00
1:05:00
1:10:00
1:15:00
1:20:00

b)

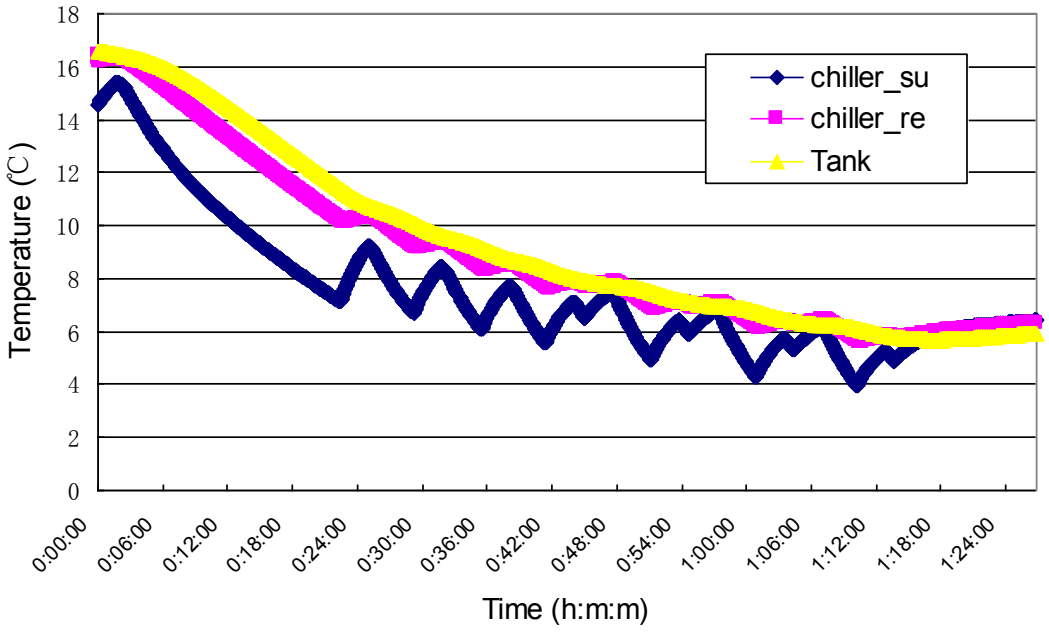

c)

Figure 3.8 Charging process with water as storage medium at 3 mixer speeds: (a) 80rpm, (b) 230rpm and (c) 380rpm

The heat balance calculation results based on Equations (3.2) - (3.4) are shown in Table 3.3.

Table 3.3 System heat balance analysis with water

	Q_{ch} kJ	ΔU_w kJ	$Q_{t.loss}$ kJ	ΔQ kJ	$\Delta Q / Q_{ch}$ %
80rpm	7597	7366	53	179	2.4%
230rpm	9731	9027	125	579	5.9%
380rpm	8664	7892	103	669	7.7%

Based on the test and calculation results, it is ascertained that the error in the heat balance is less than 8% of the total input cooling energy.

3.3.2 Charging/Discharging Process

The pure water in the storage tank was replaced with the MPCM slurries, which were cooled to 5 ℃ and heated to 25 ℃ cyclically at 3 different tank mixer speeds (80rpm, 230rpm, 380rpm); the test was repeated 5 times at every mixer speed. One set of charging/discharging process results with MPCM slurry as the medium at 3 different mixer speeds (80rpm, 230rpm, 380rpm) are shown in Figure 3.9 and Figure 3.10. The sensible thermal storage process and the latent heat storage process can be observed via the slope of the slurry temperature change over time. It can also be observed that variation of the temperature slope with the discharging is more obvious than with the charging process since melting occurs at one distinct temperature while solidification occurs over a wider temperature range.

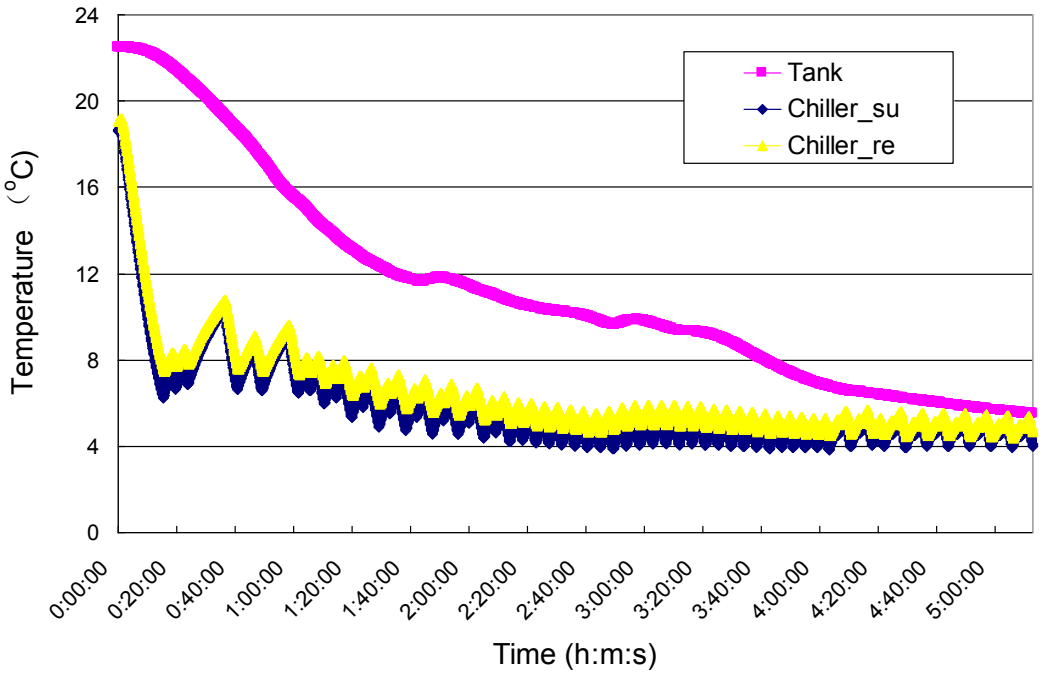

a)

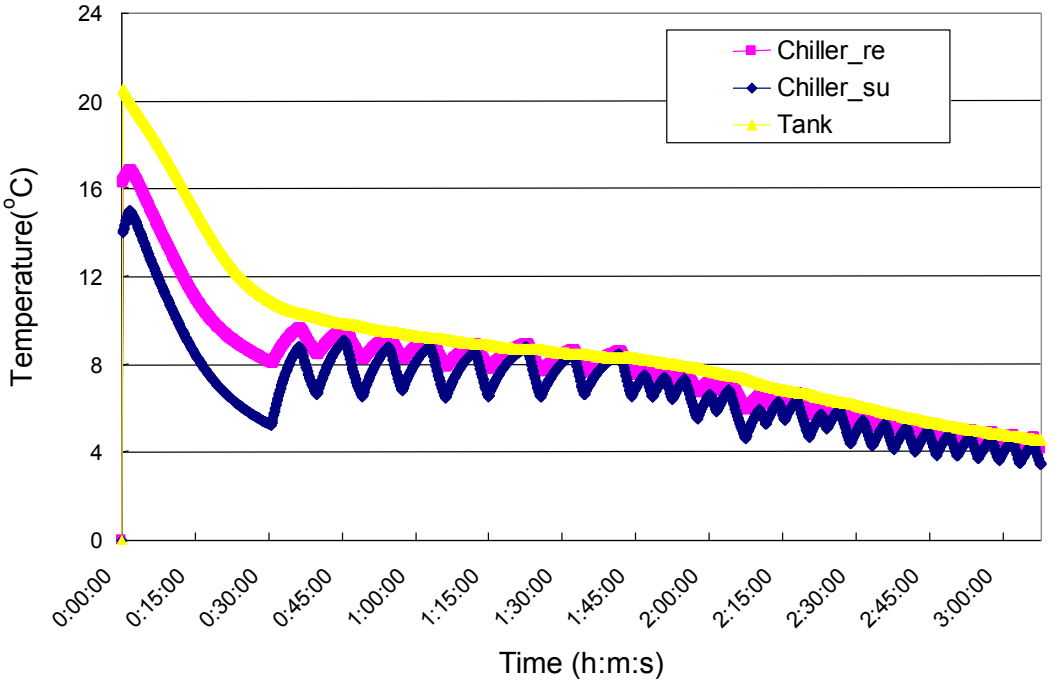

b)

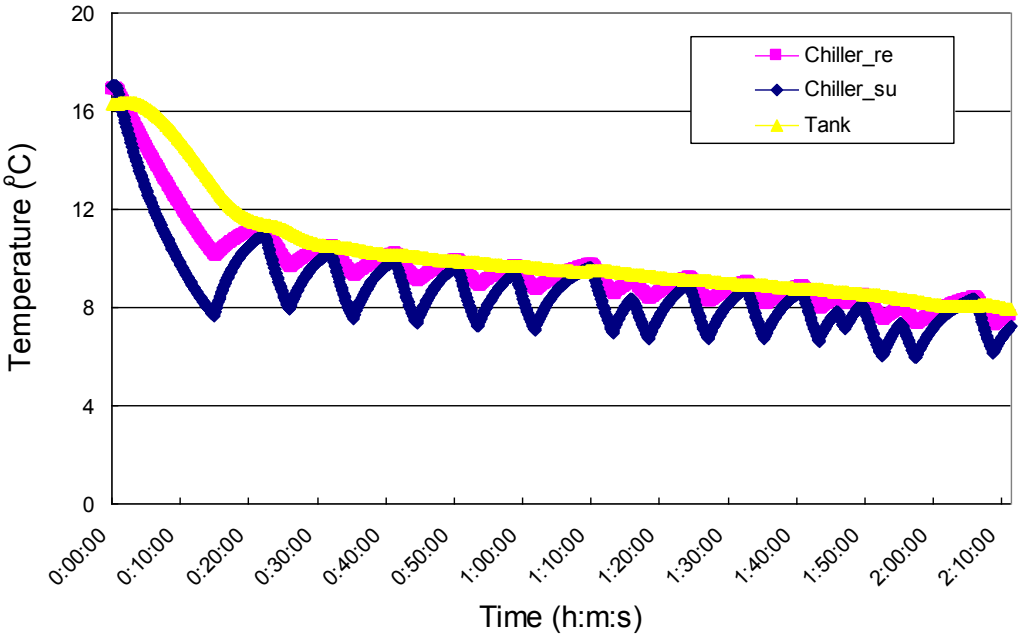

c)

Figure 3.9 Charging process with MPCM slurry as storage medium at 3 mixer speeds: (a)80rpm, (b)230rpm and (c)380rpm

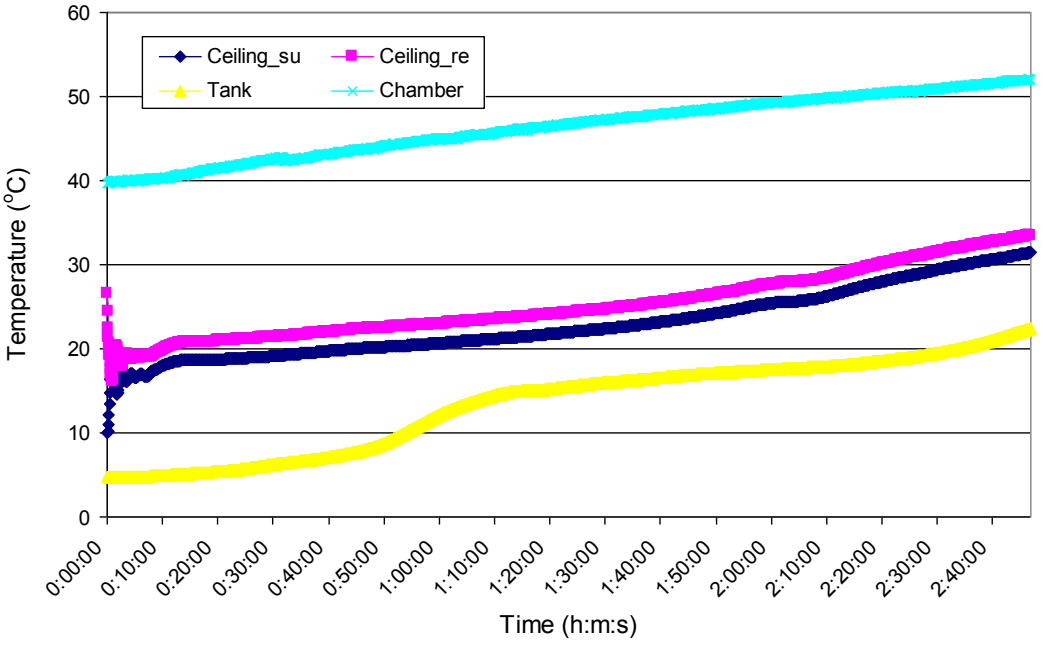
Ceiling_su
Ceiling_re
Tank
Chamber
Temperature (°C)
Time (h:m:s)
0
10
20
30
40
50
60
0:00:00
0:10:00
0:20:00
0:30:00
0:40:00
0:50:00
1:00:00
1:10:00
1:20:00
1:30:00
1:40:00
1:50:00
2:00:00
2:10:00
2:20:00
2:30:00
2:40:00

a)

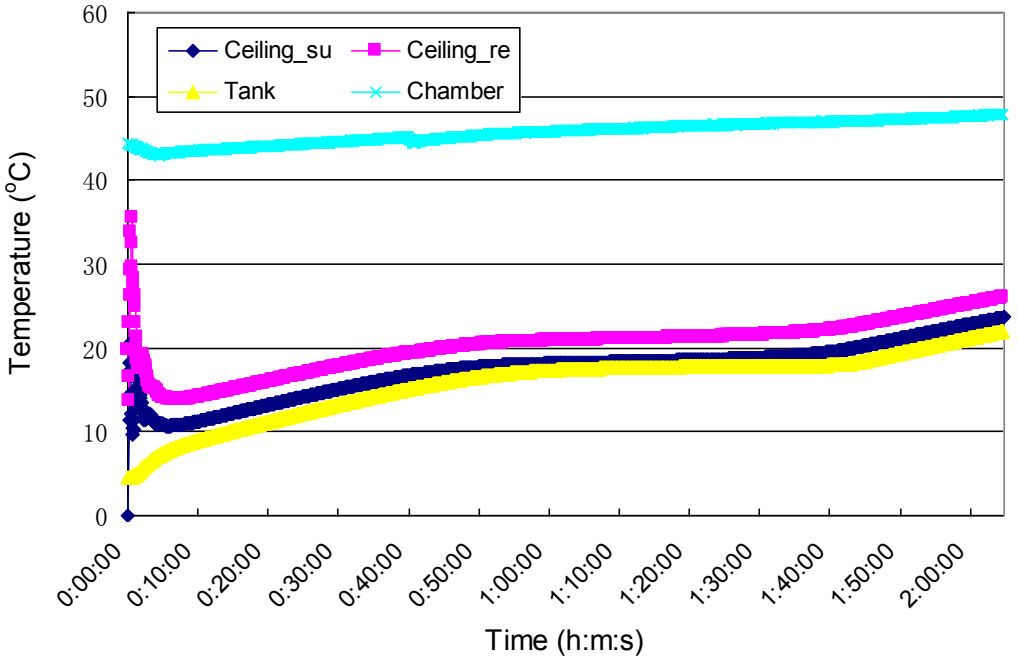
Ceiling_su
Ceiling_re
Tank
Chamber
Temperature (°C)
Time (h:m:s)
0
10
20
30
40
50
60
0:00:00
0:10:00
0:20:00
0:30:00
0:40:00
0:50:00
1:00:00
1:10:00
1:20:00
1:30:00
1:40:00
1:50:00
2:00:00

b)

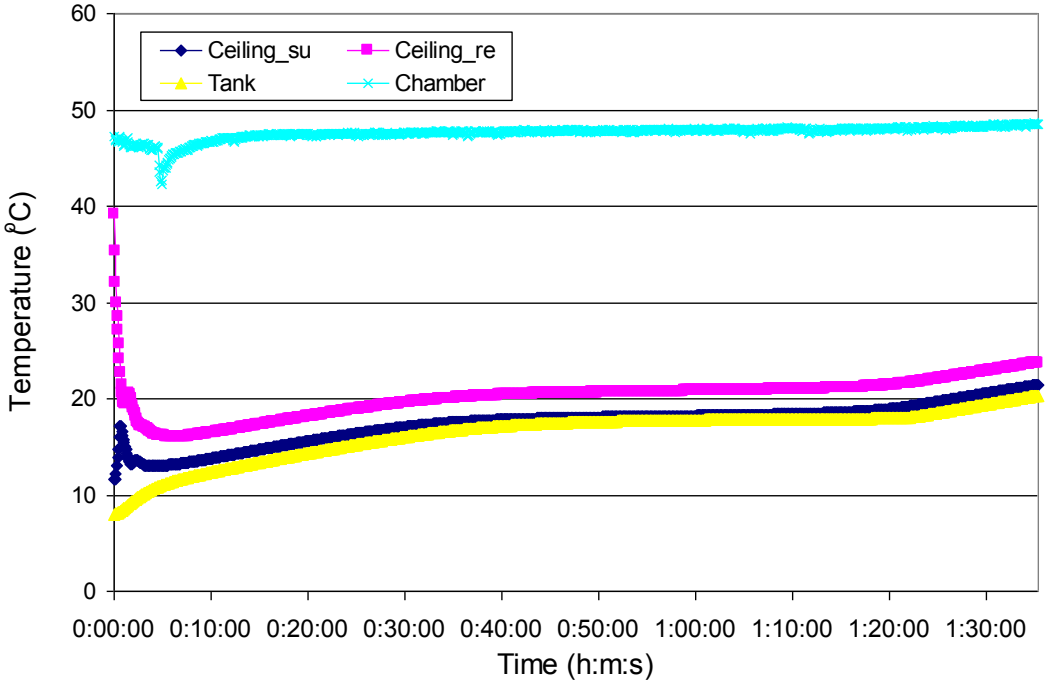

c)

Figure 3.10 Discharging process with MPCM slurry as storage medium at 3 mixer speeds: (a)80rpm, (b)230rpm and (c)380rpm

3.3.3 Supercooling and Effective Latent Heat

As mentioned above, latent heat, melting / freezing points and supercooling degree of MPCM are key parameters that determine the cooling storage tank size, the operating temperature range and the energy efficiency of mechanical cooling storage or cooling ability of a natural cooling storage. Some studies (Zhang, Hu et al. 1996; Alvarado, Marsh et al. 2006) show that the initiation of freezing point is inversely proportional to the cooling rate with a linear trend, which means the supercooling degree is proportional to the cooling rate. Due to the accurate measuring range of the DSC equipment and the experimental efficiency, cooling rates of between 3 ℃/min

and 15 ℃/min (He and Setterwall 2002; Suppes, Goff et al. 2003; Alvarado, Marsh et al. 2006) are generally used to measure the thermal characteristics of PCM/MPCMs. In our experiments, microencapsulated $C_{16}H_{34}$ was measured using DSC with a heating/cooling rate of 5 ℃/min. However, when MPCM slurry is used in a practical air-conditioning system, it generally operates with a much lower heating/cooling rate, and so the key thermal characteristics of microencapsulated $C_{16}H_{34}$ tested in the practical air-conditioning system are expected to be different from the DSC results. In our experiment system, a 0.4 ℃/min cooling rate was eventually used for thermal characteristic testing.

In practice, latent heat storage systems also make use of some sensible heat capacity in the system, so the total thermal storage can be defined as (Lane 1983):

$$\Delta Q_{sl} = m_{sl} C_{p.sl} (T_i - T_m) + m_{MPCM} h_{l.MPCM} + m_{sl} C_{p.sl} (T_m - T_e) \tag{3.5}$$

where m_{sl} is the mass of MPCM slurry in the storage tank; m_{MPCM} is the mass of MPCM particles in the storage tank; $h_{l.MPCM}$ is latent heat of fusion per unit of mass of MPCM particles; $C_{p.sl}$ is specific heat capacity of MPCM slurry; T_e and T_i are the end and initial slurry temperatures in the storage tank; and T_m is the melting temperature of MPCM slurry. However, in Equation (3.5), it is assumed that phase change is completed at T_m and so no supercooling is considered. A different calculation of the storage heat is needed when supercooling is considered, as illustrated below.

In every measurement interval of 5 seconds, the heat balance of the MPCM slurry system charging/discharging process can be defined as:

$$Q_{ch} = \Delta Q_{sl} + Q_{t.loss} \tag{3.6}$$

$$Q_{ce} = \Delta Q_{sl} - Q_{t.loss} \tag{3.7}$$

where, Q_{ch}, Q_{ce} can be calculated using Equation (3.8) respectively.

$$Q = \dot{m}_w C_{p.w}(T_{out} - T_{in}) \tag{3.8}$$

where $\dot{m}_w$ is the mass flow rate in cycle pipe; T_{out} and T_{in} are outlet and inlet water temperature.

$Q_{t.loss}$ can be calculated using Equation (3.3), so ΔQ_{sl} is related to the sensible and latent heat change, and can be calculated using Equation (3.9) as follows:

$$\Delta Q_{sl} = \Delta U_{sl} + \Delta Q_{sl.l} = m_{sl} C_{p.sl}(T_e - T_i) + \Delta m_{MPCM} h_{l.MPCM} \tag{3.9}$$

where Δm_{MPCM} is the mass of MPCM particles which have changed phase. $h_{l.MPCM}$ is determined using the DSC technique, and so the actual phase change quantity Δm_{MPCM} can be obtained:

$$\Delta m_{MPCM} = \frac{\Delta Q_{sl} - \Delta U_{sl}}{h_{l.MPCM}} = \frac{Q_{ch} - Q_{t.loss} - m_{sl} C_{p.sl}(T_e - T_i)}{h_{l.MPCM}} \tag{3.10}$$

Then we can define the effective latent heat $h_{l.e}$ as:

$$h_{l.e} = \frac{\Delta m_{MPCM}}{m_{MPCM}} h_l \tag{3.11}$$

where Δm_{MPCM} is the mass of MPCM particles which have changed phase, m_{MPCM} is the total mass of MPCM particles, and h_l is latent heat of fusion per unit mass.

Furthermore, the mass fraction of MPCM particles in the slurry was double-checked, based on the heat balance for the discharging process.

$$\Delta m_{MPCM} = \frac{\Delta Q_{sl} - \Delta U_{sl}}{h_{l.MPCM}} = \frac{Q_{ce} + Q_{t.loss} - m_{sl} C_{p.sl} (T_e - T_i)}{h_{l.MPCM}} \tag{3.12}$$

The results are shown Table 3.4, and agree with the initial mass ratio when the slurry was prepared.

Table 3.4 MPCM Mass fraction of the MPCM slurry determined by heat balance analysis

Mixer speed	Mass fraction
80rpm	21.2%±1.2%
230rpm	24.7%±0.3%
380rpm	24.1%±0.6%

Using the methodology above, the ratio of latent heat completion, defined as $h_{l.e}/h_l$ for each cooling temperature, can be acquired, as shown in Figure 3.11 and Figure 3.12.

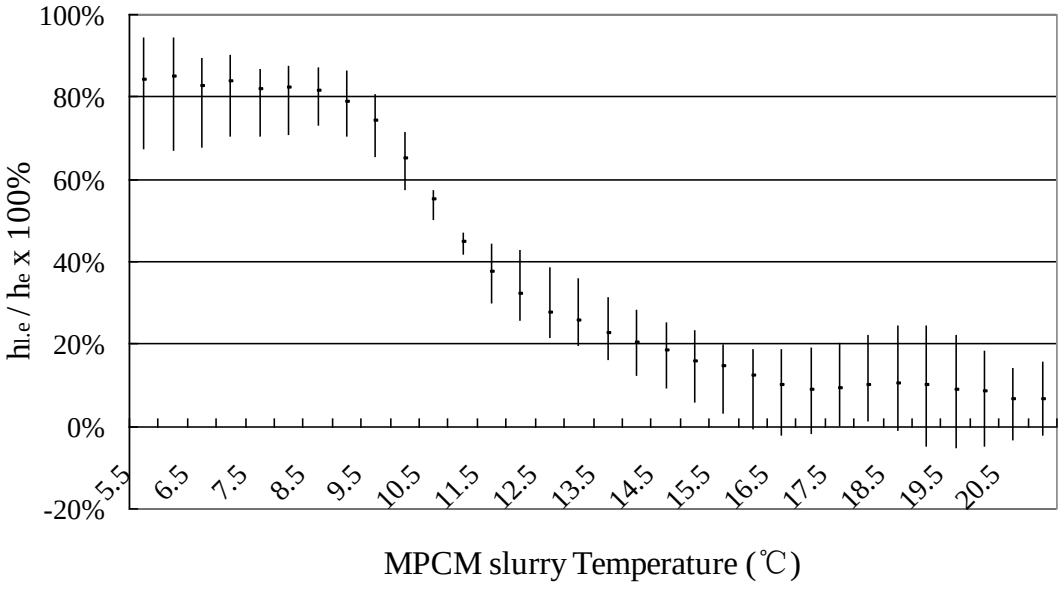

a)

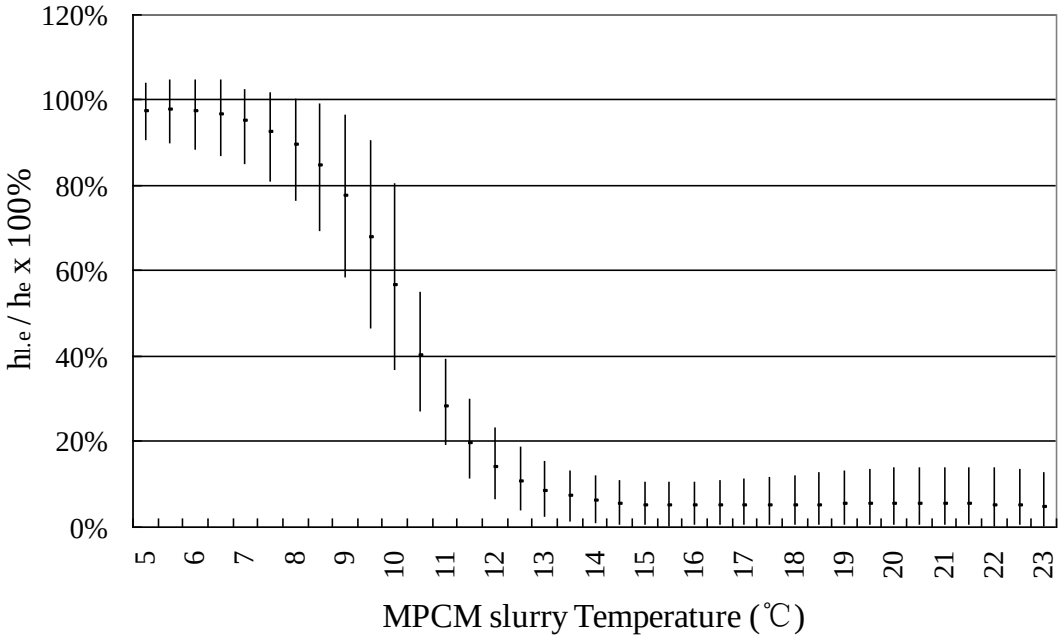

b)

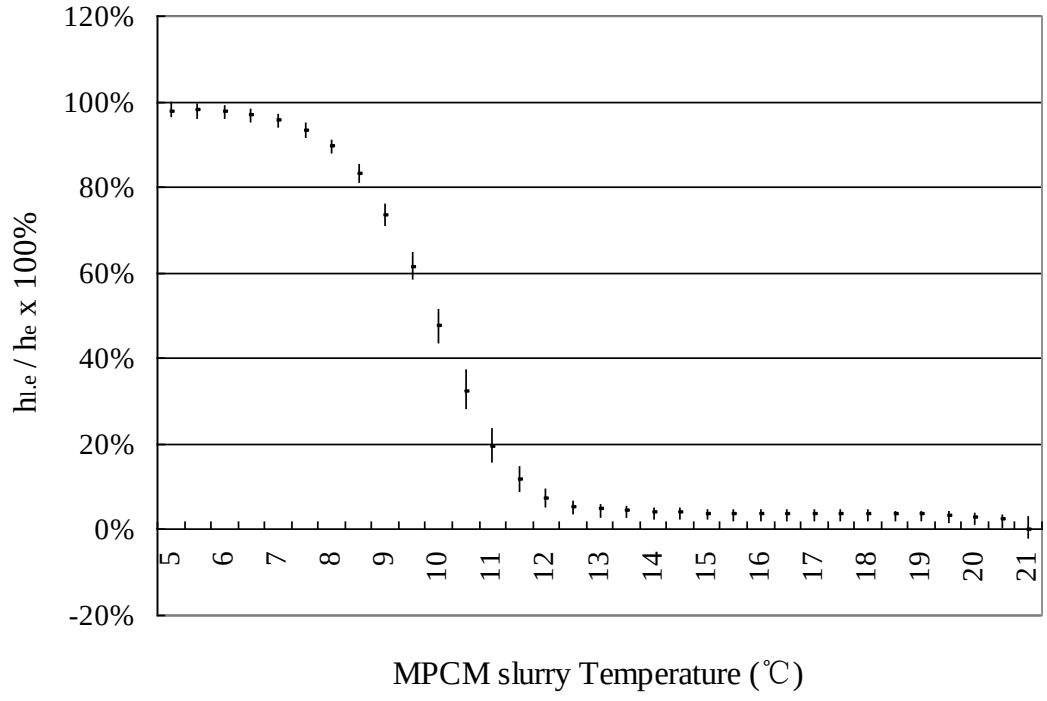

c)

Figure 3.11 Ratio of freezing latent heat completion at 3 mixer speeds during charging process: (a)80rpm, (b)230rpm and (c)380rpm

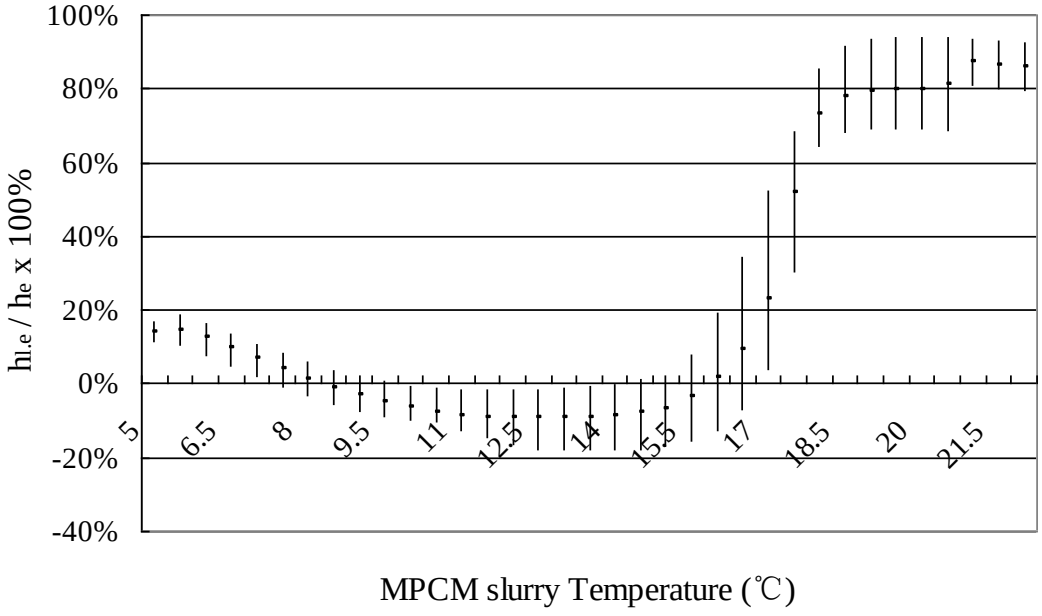

a)

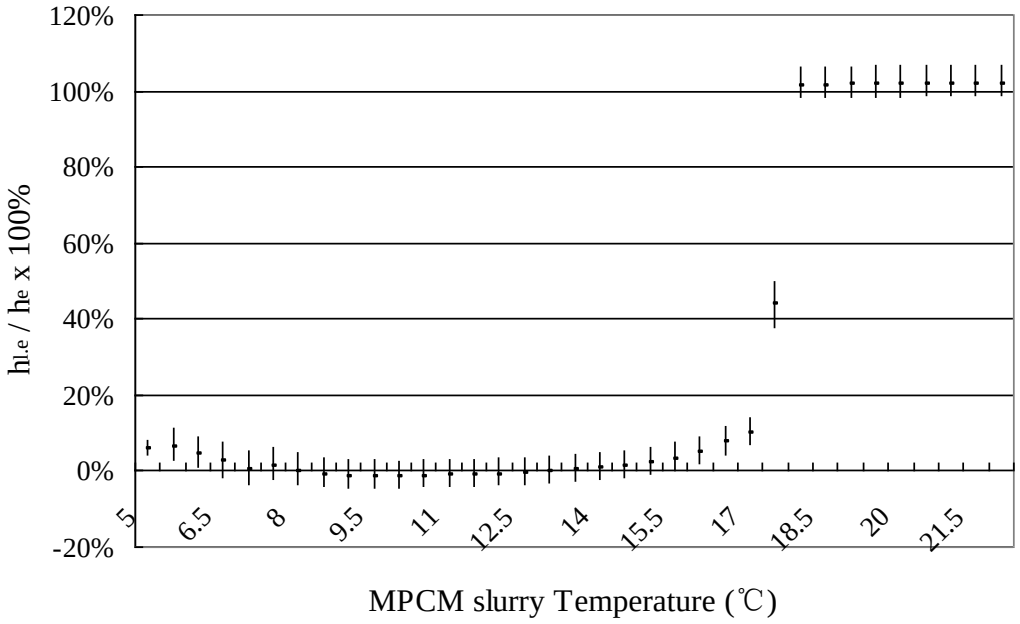

b)

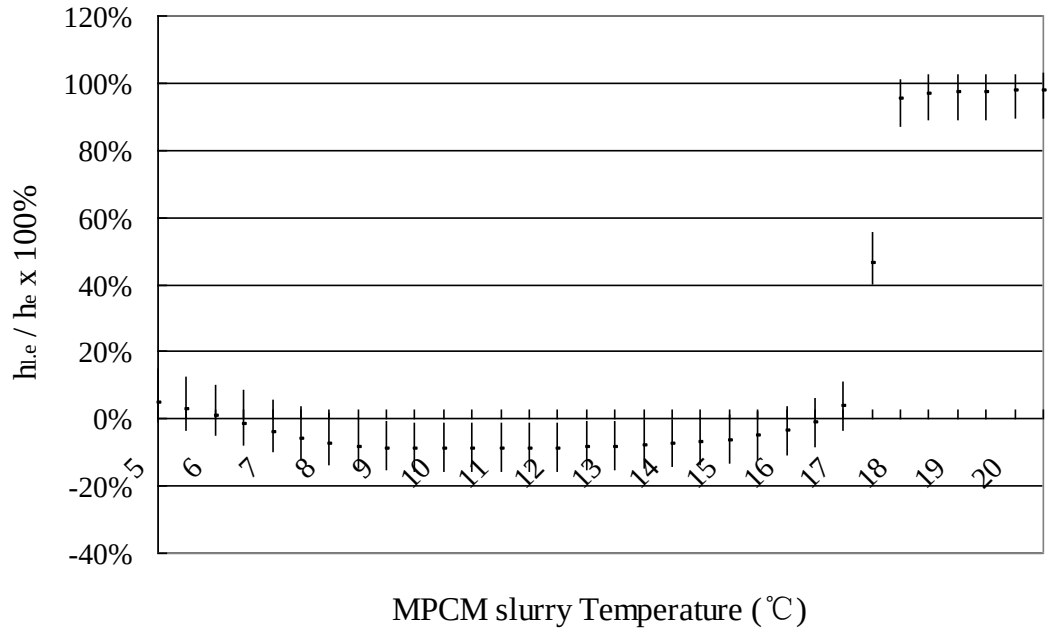

c)

Figure 3.12 Ratio of freezing latent heat completion at 3 mixer speeds during discharging process: (a)80rpm, (b)230rpm and (c)380rpm

In Figure 3.11 and Figure 3.12, each of the vertical lines in the diagram represents the distribution range of the ratio of latent heat completion obtained in the corresponding experiment and the dot on the line represents the average value. Judging from the transition points of the curves in Figure 3.11 and Figure 3.12, the freezing starts at a temperature of 13 ℃, and the corresponding supercooling degree is about 3 ℃. On the other hand, the latent heat conversion is not complete even at the end temperature of 5 ℃. As shown in Table 3.5, the end effective freezing latent heats of the MPCM vary with the stirring conditions of the slurry.

Table 3.5 Freezing latent heat of MPCM when cooled to the temperature of 5 ℃

Mixer speed	$h_{l.e}$ (kJ/kg)
80rpm	149±26
230rpm	166±15
380rpm	179±9

The functions in the form of polynomial obtained via regression analysis, describing the relationship of the ratio of latent heat completion and MPCM slurry temperature can be written as follows:

For the charging process:

$$\frac{h_{l.e}}{h_l}=\begin{cases}0 & T\geq 15\\ c_0+c_1I+c_2I^2+c_3I^3+c_4I^4+c_5I^5+c_6I^6 & 5.5<T<15\\ 0.9 & T\leq 5.5\end{cases} \tag{3.13}$$

where $I=\dfrac{T-15}{5.5-15}$

And for the discharging process:

$$\frac{h_{l.e}}{h_l} = \begin{cases} 0 & T \le 14 \\ c_0 + c_1 I + c_2 I^2 + c_3 I^3 + c_4 I^4 + c_5 I^5 + c_6 I^6 & 14 < T < 18 \\ 1 & T \ge 18 \end{cases} \qquad (3.14)$$

$$where \qquad I = \frac{T - 14}{18 - 14}$$

The results of a regression analysis for the charging and discharging process are shown in Table 3.6.

Table 3.6 Regression parameters and error term

	Charging			Discharging		
	80rpm	230 rpm	380 rpm	80 rpm	230 rpm	380 rpm
c_0	0.10	0.00	0.07	-0.10	0.01	-0.02
c_1	2.93	2.54	1.60	1.32	-1.53	-2.72
c_2	-25.75	-26.34	-13.67	-15.28	17.95	30.87
c_3	98.63	103.39	36.48	70.31	-81.47	-136.18
c_4	-160.97	-167.48	-16.80	-142.06	173.81	280.61
c_5	118.97	123.50	-25.19	131.97	-174.04	-270.71
c_6	-33.05	-34.68	18.59	-45.42	66.40	99.15
R^2	0.91	0.90	0.99	0.76	0.99	0.97

Equations (3.13) and (3.14) describe the charging and discharging process in realistic building cooling application conditions. In the practical air-conditioning utilizations, the slurry would be cooled to 7-8 ℃, in order to optimize the efficiency and cost of the operation of the chiller and the whole air-conditioning system. Based on this operation condition, the latent heat transition is completed to about 80% according to Figure 3.11 and Equations (3.13) and (3.14). However, to utilize natural cooling sources such as evaporative cooling for building cooling, a higher storage temperature of around 17 ℃ would be desirable. In this respect, the MPCM used in this study would offer very limited cooling storage capacity at this temperature due to the supercooling that occurred, but it would work effectively in climates where natural cooling, such as nocturnal sky radiative cooling, can cool the slurry to around 7 ℃. This analysis demonstrates that developing a PCM working at a temperature of around 17 ℃ with small supercooling can greatly maximise the opportunities for using natural cooling sources for building cooling applications.

3.4 Conclusions

The melting and crystallization behaviours of MPCM slurry running in a thermal storage test system are investigated experimentally. Supercooling and effective latent heat of MPCM slurry with different experimental conditions are also investigated. The experiment's results show that in a practical air conditioning system with thermal storage the latent heat transition is not entirely complete. For the specific MPCM investigated, the utilization ratio of the latent heat is related to the end temperature, and is around 80% when cooled to around 8 ℃.

Due to the phenomenon of supercooling, it is necessary to utilize the latent storage capacity or only part of the storage capacity can be used at a limited cooling temperature. With electrically-driven cooling storage, this supercooling will lower the COP of the cooling storage process. For passive cooling schemes, this would mean reduced utilization hours of natural cooling sources such as evaporative cooling and reduced per-volume storage capacities.

Chapter 4

Supercooling Prevention of Hexadecane by Addition of Carbon Nano-Tubes

This chapter presents the stable and homogenous dispersion that was attained through surface modification of the MWCNT particles with strong acids H_2SO_4 and HNO_3, plus the addition of 1-decanol as a surfactant to the organic liquid. This physiochemical process was identified as an effective method by which to prevent MWCNT particles aggregating and sedimentating rapidly in the organic liquid, n-hexadecane. The thermal performance of n-hexadecane with well dispersed MWCNT particles was measured by DSC to evaluate the effectiveness of supercooling prevention of n-hexadecane and a significant decrease in supercooling was confirmed, which indicates that introducing MWCNT particles into hexadecane is a promising method that may lead to more efficient energy usage in building cooling and heating storage applications.

4.1 Introduction

In previous chapter, the new hybrid system using MPCM slurry as the TES medium is designed and tested under the practical operating status. It is clearly shown, for the specific MPCM investigated, the effective latent heat relates to the end temperature, and is around 80% of the thermodynamic latent heat when cooled to around 8 ^{o}C. The results demonstrated that although the paraffin type MPCM slurry provides great

opportunities of using natural cooling sources for building cooling applications, the supercooling still decrease the utilization ratio. Therefore, it is indeed an imperative issue to find an effective method to prevent supercooling of PCM.

As the statement of the research problem, the addition of liquid or solid nucleating agents to the PCM liquids as the seeds and catalysts for nucleation and crystal growth is an effective approach for decreasing supercooling (Sangwal 2007). However, up to now, there is not a systematic method to select additive for reducing the supercooling. This is because the essential factors affecting the nucleation have not been clarified.

In this chapter, MWCNT nanoparticles are used as the nucleating agent to decrease the supercooling of bulk organic liquid PCM n-hexadecane. A great effort was made to solve the problem of poor dispersibility and self-aggregation of nanoparticles. The addition of various chemical surfactants and the chemical modification of the particle surface were attempted to attain a stable and well dispersed suspension of nanoparticles in the organic liquid. The effectiveness of well-dispersed MWCNT particles as a nucleating agent to decrease supercooling was evaluated by DSC at various concentrations.

4.2Experimental

4.2.1 Materials

In this study, n-hexadecane $C_{16}H_{34}$ (99%) was chosen as the PCM liquid (purchased from International Laboratory USA), and multi-walled carbon nano-tube (MWCNT)

as the nucleating agent. The MWCNT had an outer diameter of 10-20 nm, length of 0.5-2 μm and >95% purity (purchased from Chengdu Organic Chemicals Co. Ltd, Chinese Academy of Sciences, China). Several surfactants were tested as additives for dispersing the MWCNT particles in n-hexadecane, including sodium dodecyl sulfate (SDS), cetyl trimethylammonium bromide (CTAB), polyvinylalcohol (PVA), polyethylene glycol (PEG), tetramethylethylenediamine (TEMED), Triethylamine (TEA), glacial acetic acid (AcCOOH), 1-decanol (decan-1-ol), salicylic acid (SA), Tween-80 (polysorbate 80) and Triton X-100 ($C_{14}H_{22}O(C_2H_4O)_n$), which were all of analytical grade.

4.2.2 Dispersion of MWCNT Nanoparticles in n-Hexadecane

Two methods were attempted to improve the dispersion of MWCNT particles in the PCM liquid, the addition of a chemical surfactant into the PCM liquid and the surface-modification of the nanoparticles with the addition of a surfactant. All the dispersion experiments were performed in glass test tubes using the ultrasonication technique. For dispersion with surfactants, the MWCNT particles were added at 30-50 mg/L to n-hexadecane in each test tube, and one of the surfactants mentioned above was added to the tube at 1 % (w/v). The tubes were ultrasonicated by an ultrasound probe (Sonics Vibra-Cell^{TM}, model VCX130) for 5 min at 30% amplitude of power. The dispersion devices are shown in Figure 4.1.

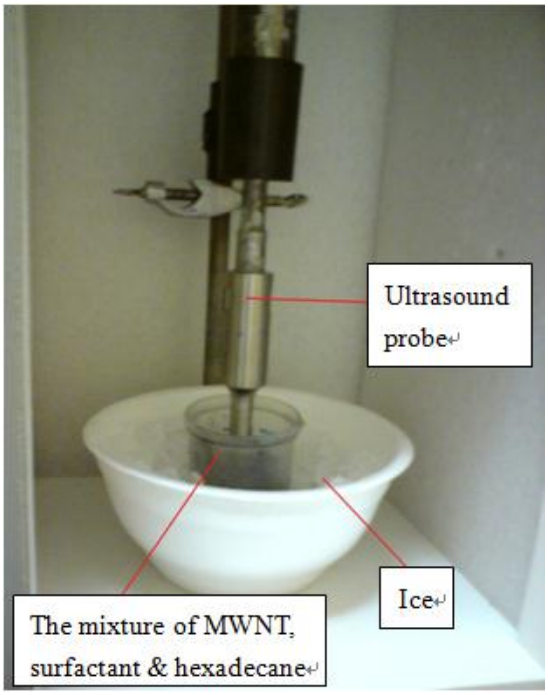

Figure 4.1 The device of ultrasound probe used to disperse MWCNTs

Surface modification of the MWCNT particles was performed in a mixture of two strong acids, concentrated H_2SO_4 (98%) and HNO_3 (70%) at a 3:1 volume ratio. MWCNT particles were added to H_2SO_4-HNO_3 in a test tube and sonicated in an ultrasounic bath for 6 hours and then heated with reflux at 65 ℃ for 4 hours. After cooling down to room temperature, the acid liquid was diluted with deionized water and the MWCNT particles were spun down at 18000 rpm for 2 hours. After removal of the liquid, the solid particles were dried at 80 ℃ in an oven for about 24 hours.

The surface-modified MWCNT particles were re-dispersed in n-hexadecane by ultrasonication by using an ultrasound probe with a 30% amplitude of power for 5 min. Each of the surfactants was added to the dispersion and the dispersion was sonicated in an ultrasound bath for 20 minutes. Based on the experimental results as shown later in section 3.1, surface-modification plus the addition of 1-decanol to the PCM liquid was the most effective method for the stable dispersion of the

nanoparticles. Therefore, the surface-modified MWCNT particles were dispersed in 1-decanol by ultrasonication for 10 minutes to attain an excess amount of 1-decanol being coated on the MWCNT particles. This yielded a stock of 1-decanol-coated, surface-modified MWCNT particles, which was applied to generate the final MWCNT-hexadecane slurry at various concentrations from 0.1 wt% to 10 wt% for the following studies.

4.2.3 Characterization and Analysis of Nanoparticles

4.2.3.1 Fourier Transform Infrared Spectrometry (FTIR)

The surface properties of the modified MWCNT particles were analyzed by Fourier transform infrared (FTIR) spectrometry on a Nicolet Avatar 360 FT-IR instrument (Figure 4.2) by using the KBr pellet method. Infrared spectrometers are used to measure the light absorption of samples in the infrared range (~1 to 100 micrometer). The wavelength range of ~1 to 100 micrometer (μm) is usually referred to as the infrared range. The range of 2.5 to 25 μm (400 to 4000 cm^{-1}, in terms of frequency) or the mid-infrared range is very useful to organic chemists as absorption of light in this range is usually caused by the vibration of chemical bonds. The position and intensity of the absorption bands are useful in speculating on the structure of organic molecules.

Figure 4.2 Photograph of Nicolet Avatar 360 FT-IR instrument

The infrared spectrometer is a tool commonly used in chemistry laboratories for obtaining the infrared transmission/absorption spectra of samples. The position and intensity of the absorption bands provide information on the chemical structure of the material. The infrared absorption intensity can also be used to determine the concentration of the target material in a mixture. Traditional infrared spectrometers employ wavelength/frequency scanning to provide the spectrum (plot of transmission/absorption intensity against wavelength/frequency). Modern spectrometers employ the Michelson interferometer or its variants to provide the same information in a much shorter time without scanning. However, the data collected has to be treated mathematically (by a computer) to yield the familiar spectrum. The mathematical tool used is known as Fourier transformation, and IR spectrometers that apply this technique are known as FT-IR spectrometers. All the IR spectrometers in our laboratories are FT-IR spectrometers.

4.2.3.2 Dynamic Light Scattering (DLS)

The size distribution of nanoparticles dispersed in n-hexadecane was measured by dynamic light scattering (DLS) analysis by using a Malvern Zetasizer (model 3000 HSA) (Figure 4.3) at a 90° scattering angle and at 25 ^{o}C. Each sample was scanned 100 times and the average particle size (nm) and the polydispersity index were computed by the Zetasizer 3000HSA-Advanced Software 15.

Figure 4.3 Photograph of Malvern Zetasizer (3000 HSA) DLS instrument

4.2.3.3 Transmission Electron Microscopy (TEM)

The morphology of the original and modified MWCNT particles was examined with transmission electron microscopy (TEM) by using a JEOL 2011 instrument (Figure 4.4) at a high voltage of 200 kV and a point resolution of 0.23 nm. The TEM was operated by the Jeol Fas TEM software and the images were processed using Gatan Digital Micrograph.

Figure 4.4 Photograph of JEOL 2011 TEM instrument

4.2.4 Thermal Analysis of PCM

Thermal analysis of the PCM with the modified MWCNT as the nucleating agent was performed on a differential scanning calorimeter (DSC) (METTLER TOLEDO DSC-822e, Figure 4.5) equipped with a thermal analysis data station. Samples (10 mg each) were placed into hermetically sealed aluminum pans and treated with the following temperature program: the sample was first cooled to the initial temperature of -5 ℃ for at least 15 minutes for stabilization, then heated from -5 ℃ to 30 ℃ at a rate of 5 ℃/min, held for 5 minutes at 30 ℃, and finally cooled from 30 ℃ to -5 ℃ at a rate of 5 ℃/min. STARe software was used to analyze and plot the thermal data.

Figure 4.5 Photograph of METTLER TOLEDO DSC-822e

4.3 Results and Discussion

4.3.1 Dispersion of MWCNT in n-Hexadecane

4.3.1.1 Dispersion of Original MWCNT by Surfactants

Table 4.1 shows the suspension time, i.e. the period for complete sedimentation of the original MWCNT particles in hexadecane supplemented with the eleven surfactant chemicals. A longer time period leads to the surfactant enhancing the suspensions with greater effectiveness; the suspensions can be listed in descending order as: Tween 80 < Triton X-100< control ~ AcCOOH ~ SDS ~ CTAB < PVA ~ PEG < SA < TEA < 1-decanol < TEMED.

Table 4.1. Effects of surfactants on dispersion of original MWCNT in n-hexadecane

Surfactant	Suspension time (min)	Surfactant	Suspension time (min)
Control	30	TEA	60
SDS	25	AcCOOH	30
CTAB	25	SA	40
PVA	35	1-decanol	70
PEG	35	Tween-80	15
TEMED	85	Triton X-100	25

Compared with that of the control (30 min), the suspension period of MWCNT in hexadecane was decreased by the addition of several of the surfactants, most significantly the two nonionic surfactants, Tween 80 and Triton X-100. It appears that these surfactants accelerated the aggregation and sedimentation of MWCNT particles in the organic liquid. The ionic surfactants, including SDS and CTAB, had only a slight effect on the dispersion of MWCNT, probably because the hydrophobic tails of these surfactants had a stronger interaction with the hexadecane than with MWCNT. The polymeric surfactants, including PVA and PEG, greatly increased the suspension period, probably by their attachment or adsorption onto the MWCNT particles creating steric resistance to aggregation. However, their higher molecular weight and low solubility in the hexadecane may be unfavorable for the dispersion. In comparison, the amines, including TEA and TEMED, were more favorable. Their amino groups perhaps initially attached to the MWCNT surface through electron donation of NH group and the steric tail, increasing the resistance to aggregation, though not sufficient to overcome the strong π–π interaction among MWCNT

particles. As for the polar molecules, 1-decanol had a remarkable effect on enhancing the dispersion, though AcCOOH and SA only had a slight effect. 1-decanol may interact with the nanoparticles through the electro-static force of its negatively charged OH group, as the NH group does in the amines. Of all the surfactants tested, TEMED and 1-decanol were the most effective at enhancing the dispersion.

4.3.1.2 Surface modification of MWCNT

Surface modification of the MWCNT particles was performed in a mixture of two strong acids: concentrated H_2SO_4 and HNO_3. The results of surface properties of the modified MWCNT particles were analyzed according to their FTIR spectroscopy, as shown in Figure 4.6. There is a peak in the FTIR spectrum of the acid-treated MWCNT particles at around 1764 cm^{-1}, which is assigned to the C=O bond stretching. The peak at around 2922 cm^{-1} is the anhydrous O-H bond stretching. The peaks at around 1341 cm^{-1} and 1050 cm^{-1} are O-H bonds bending. The peak around 1195 cm^{-1} is the C-O bond stretching. These peaks indicate that COOH groups were introduced at the end or the side of the MWCNT particles, thereby having functionalized or modified surfaces of MWCNT particles. The peak around 1107 cm^{-1} is the C-O stretching in acid anhydride, which may be caused by the acid group polymerizing during the drying process in the oven.

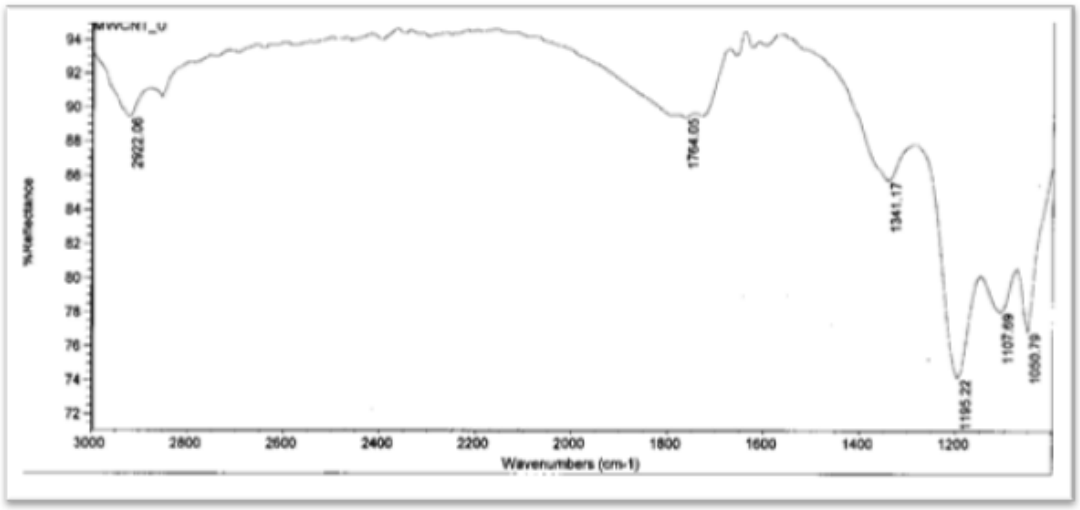

Figure 4.6 The FTIR spectrum of the modified MWCNT particles

It took a longer time to disperse the modified MWCNT particles than it took with the original MWCNT particles 110 min versus 45 min. The steric effect of carboxylic acid group and the irregularity of the modified MWCNT particle surface presented themselves in lower effectiveness of packing and a slower rate of aggregation. The aggregation of modified MWCNT particles eventually appeared, probably due to low solubility of COOH in n-hexadecane, the hindrance provided by small size of the acid group, and the hydrogen bonding interaction among acid groups in modified MWCNT particles.

4.3.1.3 Dispersion of modified MWCNT by surfactants

The effects of the tested surfactants on the dispersion of the modified MWCNT in n-hexadecane are shown in Table 4.2 Their effectiveness can be presented in descending order as: Tween 80 ~ Triton X-100 < AcCOOH < TEMED ~ PEG < PVA < TEA < SDS ~ control < CTAB < SA < 1-decanol.

Table 4.2 Effects of surfactants on dispersion of modified MWCNT in n-hexadecane

Surfactant	Suspension time (min)	Surfactant	Suspension time (min)
Control	70	TEA	65
SDS	70	AcCOOH	20
CTAB	105	SA	140
PVA	40	1-decanol	290
PEG	25	Tween-80	17
TEMED	30	Triton X-100	15

It appears that the surfactants Tween 80 and Triton X-100 accelerated the aggregation and sedimentation of the modified and original MWCNT particles in the hexadecane, probably because the two surfactants were not very soluble in hexadecane and the density was higher, so the MWCNT particles sank to the bottom due to the density difference. The ionic surfactants, including SDS and CTAB, had better effects on the dispersion of the modified MWCNT particles than that of the original particles, but they were still not as good as expected since they could not be ionized in hexadecane and are only dependent on dipole-dipole interactions. The polymer dispersion using PVA and PEG had similar results to the original ones since they also interacted with MWCNT by physically wrapping them, and thus only twisted the particles with little chemical interaction. Although TEMED had a remarkable effect on the dispersion of the original MWCNT particles, its effects on the modified MWCNT particles were greatly weakened. This was because the electron-donating effect of amines on the original MWCNT no longer existed in the

modified MWCNT, and the new interaction between them was hydrogen bonding. The dispersion effect of TEMED might have been hindered by the di-amine forming a bridge-liked structure that linked the MWCNT particles together. Since using a long, straight carbon chain mono-amine might improve the situation, long straight carbon chain alcohol (1-decanol) and carboxylic acid (SA) were used as substitutes. The hydrogen bonding in these two molecules is believed to be stronger than in amines since the electronegativity of OH is stronger than that of NH. Polar molecule SA and 1-decanol showed huge improvements on the dispersion of the modified MWCNT, although AcCOOH had little effect on both modified and original MWCNT. This was because AcCOOH had little solubility in hexadecane, but the modified MWCNT had very good solubility in AcCOOH due to the hydrogen bonding. In contrast, the polar group of SA and 1-decanol could form hydrogen bonds in MWCNT, and the long carbon chain tail gave them good solubility in hexadecane, which leads to stable dispersion.

Of all the chemicals used, 1-decanol showed the best performance of dispersion for both original and modified MWCNT. It was therefore chosen for further investigation at increased concentrations in modified MWCNT. The dispersion effect was greatly increased since 1-decanol could completely coat the MWCNT particles. A schematic diagram of the interaction between 1-decanol and modified MWCNT particle is given in Figure 4.7. The visible aggregation was negligible even after seven days.

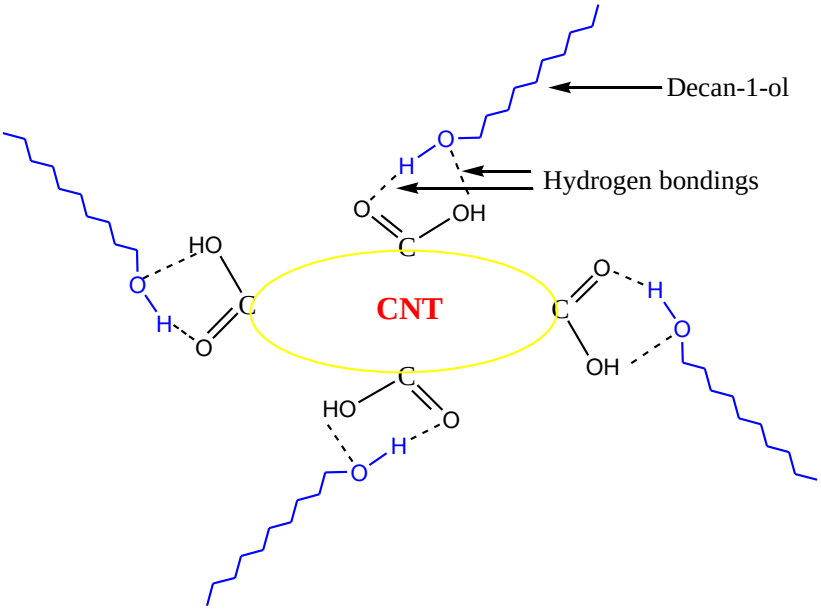

Figure 4.7 The schematic diagram of the interaction between 1-decanol and modified MWCNT.

Based on the dispersion analysis and comparison above, modified MWCNT assisted by 1-decanol (MWCNT-1-decanol) were well dispersed in liquid n-hexadecane to form a stable n-hexadecane / MWCNT-1-decanol slurry. A series of slurries with different MWCNT-1-decanol concentrations (0.1%-10% w/w) was prepared for further investigations into their effects on supercooling.

4.3.2 The Particle Size of MWCNT-1-decanol

The average hydrodynamic diameter of MWCNT-1-decanol in hexadecane was 2761.3 nm or 2.76 μm (Figure 4.8) as measured by dynamic light scattering analysis (Malven Zetasizer) with the count rate at 200.3 +6.6 kilo count per second (kcps) at 25 ℃. The range of difference between the repeated measurements was +36.1 nm,

which means the MWCNT particles were well dispersed. The polydisperse index was 0.585, which means the range of the distribution in particle size was medium.

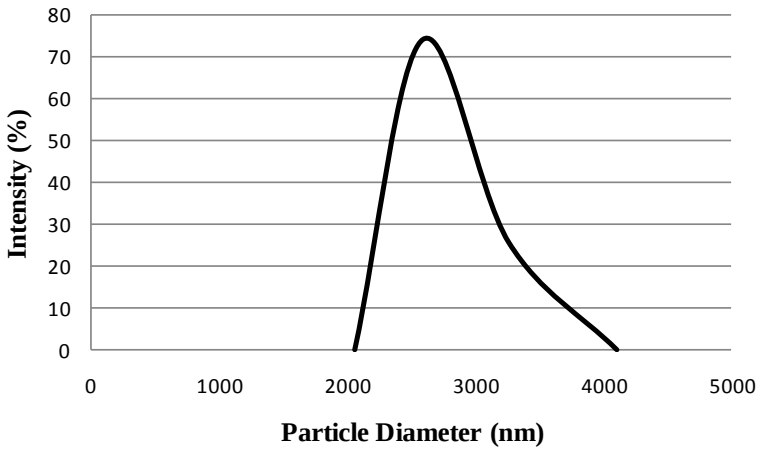

Figure 4.8 The size distribution of MWCNT-1-decanol in n-hexadecane

4.3.3 Morphology of MWCNT

TEM micrographs of the original MWCNT and MWCNT-1-decanol are presented in Figure 4.9 and Figure 4.10, respectively. The size and shape of the MWCNT particles can be observed clearly and are consistent with the parameters provided by the manufacturer, with an outer diameter of 10-20 nm and a length of 0.5-2 μm. Compared with the morphology of the original MWCNT, the surface of the MWCNT-1-decanol was rougher. There were some masses on the surface of the nano tubes, which may have been caused by surfactant modification and the addition of decan-l-ol. These can be observed more clearly in the TEM micrographs (Figure 4.11), which show the crystal structure of the nano tubes.

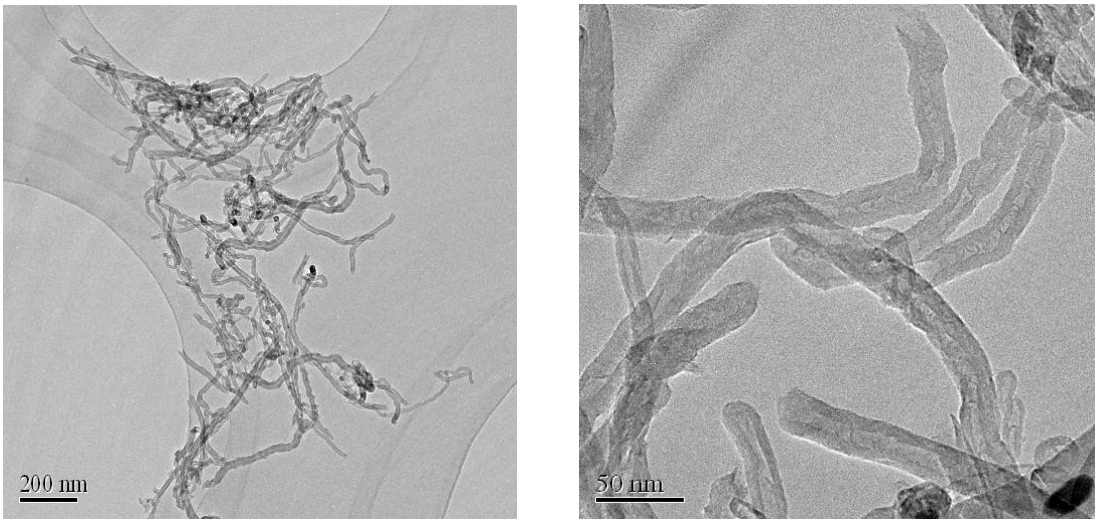

a) **b)**

Figure 4.9 TEM micrographs of original MWCNT on different scales showing the morphology: a) 200 nm and b) 50 nm

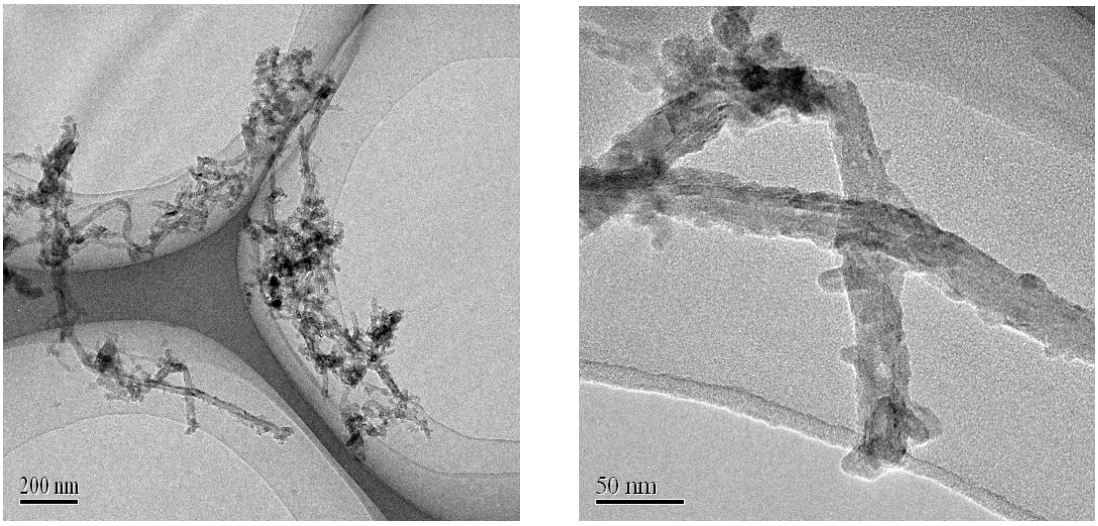

a) **b)**

Figure 4.10 TEM micrographs of well dispersed MWCNT-1-decanol on different scales showing the morphology: a) 200 nm and b) 50 nm

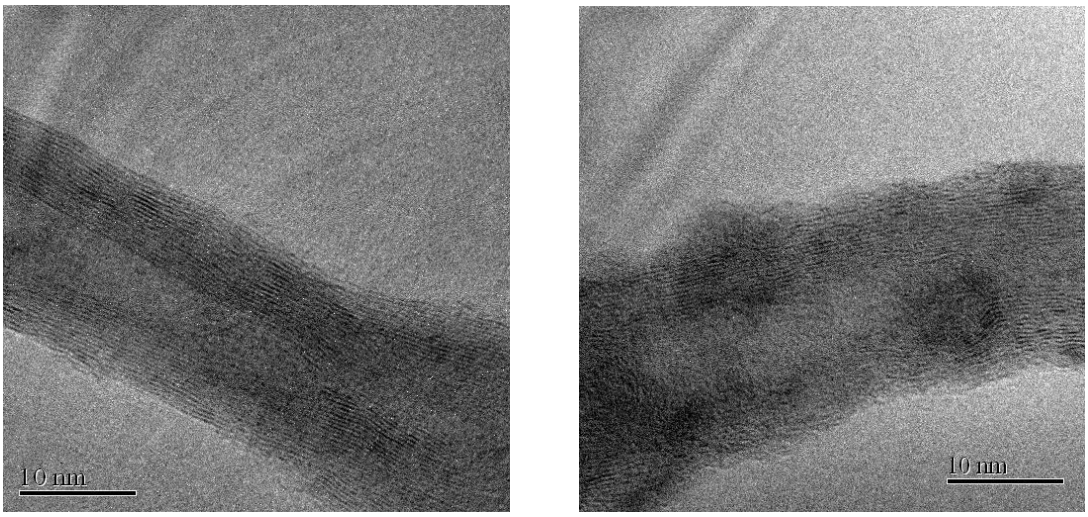

a) **b)**

Figure 4.11 TEM micrographs of different MWCNT showing the crystal structure of MWCNT: a) original MWCNT and b) MWCNT-1-decanol

4.3.4 Supercooling Reduction

In the nucleation process, the formation of the nuclei is associated with a change in the free energy of the system. At a given supersaturation and temperature, there is a critical value of free energy at which stable nuclei of critical size are formed. This behavior of the free energy change, ΔG, associated with the formation of the nucleus was shown in Figure 4.12 as a function of the nucleus radius r. When the radius r of the nuclei is smaller than r^* the nuclei dissolve; however, when $r > r^*$, the nuclei are stable and grow. ΔG^* is a barrier to nucleation, and only when $r > r^*$ is there a reduction in the free energy of the nucleus and an increase in its size. The higher the activation barrier ΔG^*, the more difficult it is to attain stable nuclei. The nucleation process may be homogeneous or heterogeneous. Homogeneous nucleation is possible when there is no external source, ideally in pure liquids, whereas heterogeneous

nucleation occurs when the system contains nanoparticles and/or impurity particles (Sangwal 2007).

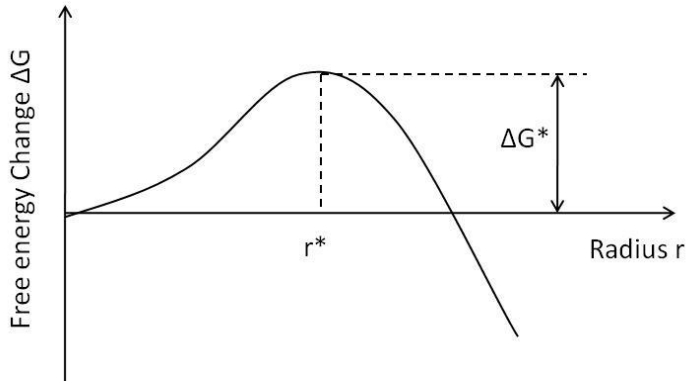

Figure 4.12 Change in Gibbs free energy ΔG as a function of radius r of nucleus formed in a supersaturated medium (Sangwal 2007)

According to the classical nucleation theory, well dispersed MWCNT particles are expected to act as seeds during the process of crystallization, and thus will be used as nucleating agents to reduce the supercooling of n-hexadecane. The DSC technique was used to analyze the thermal properties of the n-hexadecane / MWCNT-1-decanol slurry.

Figure 4.13 showed the DSC melting and freezing curves of the pure hexadecane at a 5 ℃/min scanning rate and the characteristic temperatures including the melting temperature T_m, melting peak temperature $T_{m.peak}$, freezing temperature T_f and freezing peak temperature $T_{f.peak}$. The difference between $T_{m.peak}$ and $T_{f.peak}$ is the supercooling ΔT. It can be observed that the melting/freezing peak temperature is 22.67 ℃ and 14.08 ℃ respectively, so the supercooling is 8.59 ℃.

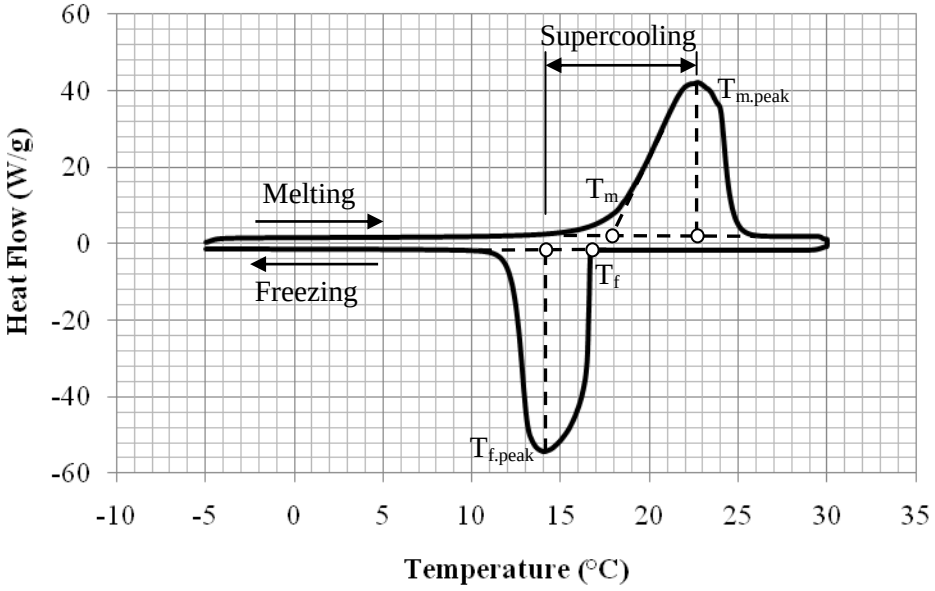

Figure 4.13 DSC melting and freezing curves of the pure n-hexadecane at 5 ℃/min scanning rate and the characteristic temperatures T_m, $T_{m.peak}$, T_f and $T_{f.peak}$.

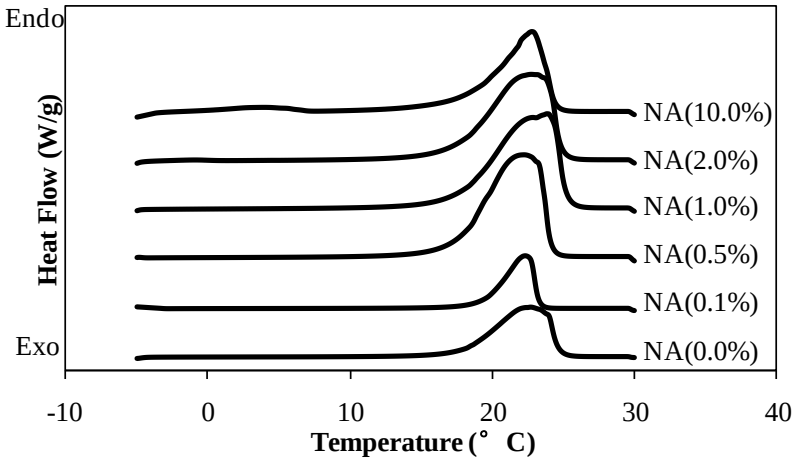

a)

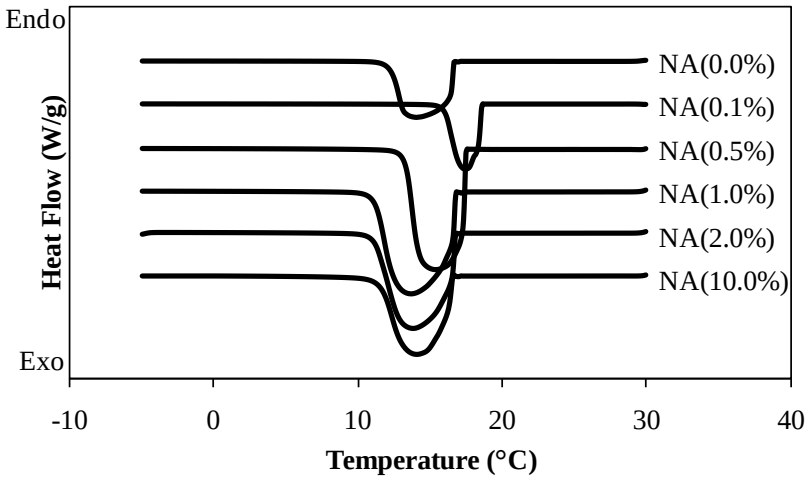

b)

Figure 4.14 DSC curves of the n-hexadecane with MWCNT of different fractions as the nucleating agent (NA): a) heating process and b) cooling process

Table 4.3 Melting and crystallization properties of n-hexadecane with MWCNT of different fractions as the nucleating agent (NA)

	ΔH_m	ΔH_f	$T_{m.peak}$	$T_{f.peak}$	ΔT
	J/g	J/g	℃	℃	℃
NA (0.0 wt %)	227.13	225.81	22.67	14.08	8.59
NA (0.1 wt %)	196.58	196.33	22.33	17.42	4.91
NA (0.5 wt %)	256.28	250.59	22.25	15.42	6.83
NA (1.0 wt %)	237.90	239.77	23.83	13.67	10.16
NA (2.0 wt %)	244.81	244.22	22.75	13.83	8.92
NA (10.0 wt %)	219.60	223.03	22.70	14.08	8.67

The DSC heating/cooling curves of the hexadecane/MWCNT-1-decanol slurry obtained at a heating and cooling rate of 5 ℃/min are presented in Figure 4.14, and the melting and crystallization properties calculated from the DSC tests are presented

in Table 4.3. It can be observed that the freezing temperature of the hexadecane/MWCNT-1-decanol slurry varied with the MWCNT concentration while the melting temperature remained fundamentally unchanged. With the addition of the nucleating agent of 0.1 wt%, the freezing temperature clearly increased from 14.08 ℃ to 17.42 ℃, and the supercooling of hexadecane decreased by 43%, from 8.59 ℃ to 4.91 ℃. With the addition of the nucleating agent of 0.5 wt%, the supercooling reduction effect was also significant, but weaker than at the lower concentration. When the concentrations of the nucleating agent exceeded 1.0 wt%, no reduction in supercooling was not seen. Judging from these results, it appears that there exists an optimal or most-effective concentration range of the nucleating agent and this agrees with experimental research reported by other researchers (Liu 2005; Tomura and Kawasaki-shi 2010). The fact that the mass concentration required is small has positive practical implications.

4.3.5 Discussion

The crystal structure of n-hexadecane (even-carbon n-alkanes with n<26) is a triclinic structure (Sangwal 2007), while that of MWCNT particles with a diameter of 10-20 nm (more than 25Å) is a honeycomb structure (Tersoff and Ruoff 1994). The similar crystal structure of MWCNT and n-hexadecane is the basis for MWCNT to be used as the nucleating agent. The experimental results help to confirm this hypothesis. Without any foreign additives, the formation of stable nuclei relying on homogeneous nucleation is a “sluggish” process, which is the main cause of large supercooling. In this experimental investigation, the well-dispersed nanoparticles provided stable foreign nuclei of the proper size to promote the heterogeneous

nucleation process and accelerate the crystallization process, thus the crystallization temperature was raised and the supercooling was significantly reduced.

The small concentration of additives required has a number of positive implications for potential engineering applications of the technology. Firstly, it will have negligible impact on the volumetric latent heat of the PCM; and secondly, the cost of the nano materials will be much reduced.

4.4 Conclusions

It was difficult to disperse the original MWCNT particles in a hexadecane liquid. The surfactant used to disperse the MWCNT must be soluble in the hexadecane, and the results showed that the functional group in the surfactants that are supposed to react with the acid groups in MWCNT should be as exposed as possible, otherwise the branch near the functional group would produce hindrance and lower the dispersion effect. Modified MWCNT particles, with the addition of 1-decanol as a surfactant, were successfully dispersed in hexadecane. It can be expected that using 1-decanol to disperse MWCNT in other higher molecular alkanes that are similar to hexadecane, such as pentadecane and heptadecane, is possible. The results may also imply that using other fatty alcohols with similar structures to 1-decanol, such as nonadecan-1-ol and undecan-1-ol, to assist in dispersing MWCNT in hexadecane is also possible.

It is encouraging that well-dispersed MWCNT at a relatively low concentration had a significant effect in reducing the supercooling of hexadecane. With the addition of

0.1wt% MWCNT, the supercooling of hexadecane decreased by 43%, which was the most significant effect from among the test samples. It is also interesting to note that there was an effective concentration range of nanoparticles for supercooling reduction, and better results cannot be obtained by continuously increasing nanoparticle concentration.

For thermal cooling storage in air conditioning systems and other building applications, reducing supercooling as much as possible is essential. High levels of supercooling will decrease the COP of the cooling storage process in electricity-driven cooling storage systems, and reduce the utilization hours or the per-volume storage capacities of natural cooling systems, such as evaporative cooling systems.

Chapter 5

Utilization Potential of Nocturnal Radiative Cooling Combined with MPCM Slurry Storage and Cooled Ceiling

In Chapters 3 and 4, the study exposed the potential for utilizing MPCM slurry in thermal storage applications, accounting for its decent thermal performance while preventing supercooling by adding nucleus agents. MPCM slurry provides a better kind of media for thermal energy storage in air conditioning systems compared to the conventional media, ice, due to its relatively higher working temperature. Furthermore, it has thermal properties that are appropriate for further applications of nature cooling sources and passive cooling. In this chapter, a novel MPCM slurry storage system is investigated by combining it with a nocturnal radiative cooling system. An integrated model is developed for a simulation study of the cooling ability, the energy consumption and the energy-saving potential. The application potential of the novel hybrid system is analyzed based on the simulation results for five typical cities in China. The optimization and proper usage of the hybrid system are also suggested at the end of this chapter.

5.1 Introduction

Various passive cooling applications in building heating and cooling systems have been investigated extensively in recent years and are expected to relieve the situation of high energy consumption in the rapidly developing world. Several natural heat sinks have

been utilized to improve the indoor environment, including water evaporation, under-surface cooled soil and ambient air. Sky radiation is one such technique that can be effectively applied to replace conventional cooling strategies and it has been investigated by many researchers (Hamza H. Ali, Taha et al. 1995; Mihalakakou, Ferrante et al. 1998; Saitoh and Fujino 2001). Because the upper atmosphere is near absolute zero, about 4 K (Bliss 1961), it can be utilized as a heat sink. Therefore the sky radiator is the critical component of the radiant cooling system, the surface of which is exposed to the sky at night to give out heat. The media commonly used to carry the radiative cooling include water and air.

Saitoh and Fujino (2001) indicated that sky radiation cooling appears most significant under certain weather conditions, namely clear weather with low relative humidity and low wind speeds. The efficiency depends on there being a large temperature difference between the sky and the cooling collector, the nocturnal radiator. Therefore, evaluation of the performance of natural cooling techniques for actual application design should be based on detailed local climatic data (Argiriou, Santamouris et al. 1994). The weather in summer in tropical cities such as Hong Kong is not suitable for the application of sky radiation because of high ambient temperature and high humidity (80–90%). In contrast, cities in northern China are ideal places for the technique due to the relatively low temperature and low humidity there.

The demand for thermal storage systems is rooted in the fact that heat rejection between the intermediate medium and the sky occurs at night, while that between the intermediate

medium and the room occurs during office hours. Because the efficiency and the energy consumption saving of nocturnal sky radiator system depend on the weather conditions, MPCM slurry with its relative high melting temperature is of great potential to be combined with the nocturnal radiation system. Conventionally, using ice as the storage medium requires a working temperature below 0 °C for the heat transfer media in the radiator. The available operating time will obviously be reduced because the sky temperature seldom falls below 0 °C. Therefore, using ice as the storage media for the nocturnal radiator system has significant difficulties and shortcomings. In contrast, using MCPM slurry as a storage media can sustain a much higher working temperature of the heat transfer media in radiators up to 15°C. It makes it possible for cooling to still be obtained in the summer, because the radiator used with a relatively high temperature, 15 °C, and the temperature difference still exists when the sky temperature rises, depending on the ambient temperature and humidity around the radiator.

In this chapter, an integrated system containing an MPCM slurry storage, a coiled ceiling system, and a nocturnal sky radiator system is studied. The MPCM slurry is used to store the cooling energy generated by the nocturnal radiative cooling system and to provide cooling for the cooled ceiling system in the room during the daytime for sensible heat removal. In addition, a mechanical chiller is used as a supplemental cooling source for both when there is insufficient radiative cooling ability during the MPCM slurry storage charging process, and under peak load at the end-user side under extreme conditions. There is also a dedicated fresh air handling unit that provides dehumidified fresh air for the ventilation purposes. A feasibility analysis of radiative cooling applications was

conducted for five typical cities across China, namely, Hong Kong, Shanghai, Beijing, Lanzhou and Urumqi, based on local meteorological data and supported by detailed assessment of the annual occurrence of sky temperatures and the potential cooling capacity of nocturnal radiators. On this basis, the loads shifted by the hybrid system and the energies saved by using nocturnal radiative cooling technology in the five typical cites are investigated and compared based on the hour-by-hour simulation results. Finally, because the cooling capacity of the nocturnal radiator is directly restricted by the area of radiator, the utilization potential of the hybrid system in different types of buildings, low-rise building or high-rise building, are discussed.

5.2 Simulation Model

5.2.1 Simulation Tool

The thermal performance of a hybrid system is evaluated using a previously validated building energy simulation program called ACCURACY (Chen and Kooi 1988; Niu and Kooi 1994; Niu, Kooi et al. 1995) and MATLAB. ACCURACY is a room-energy-balance method, in which the ceiling panels are treated as individual surfaces which exchange heat convectively with the room air and radiantly with other surfaces. Heat conduction within the ceiling panels is treated in a one dimensional way by using a three-nodal-point model. The program calculates not only the cooling load, but also the required supply water or air temperature for different panel installation areas. Adopting this dynamic building simulation model, the hour-by-hour data of heating/cooling loads,

room air temperature and other components of the room with ceiling panels running with water can be calculated.

In this study, the cooling load of the end user, the energy consumption of the primary equipment such as the compressor and the fans, is calculated using a form of semi-empirical model in ACCURACY, based on the work of Wang, Niu et al. (2008; 2009). Adopting these building simulation techniques, the hour-by-hour cooling/heating loads of the room under the proposed hybrid system can be calculated. The nocturnal radiator calculation program is built by MATLAB to simulating the outlet water temperature and the effective cooling capacity according to weather condition data and ACCURACY simulation results.

5.2.2 Structure and Operating Strategy of Hybrid System

The hybrid system (Figure 5.1) is a combination of a nocturnal radiative cooling system, a cooled ceiling system, and an MPCM slurry storage system. A conventional vapor compression refrigeration system is also used to provide auxiliary cooling water generation when the cooling energy stored in the MPCM slurry is not sufficient to provide the cooling for the ceiling panels and the nocturnal radiative cooling is not sufficient to charge the MPCM slurry tank. The cooled ceiling panels are installed to extract the sensible heating load in the room. The cooling water circulated in the ceiling panels is firstly cooled by the MPCM slurry storage tank, and then by the conventional vapor compression refrigeration. For ventilation purposes, a conventional fresh air

handling unit provides minimum cooled and dehumidified fresh air, which can also avoid possible condensation on the ceiling panel surface at the same time.

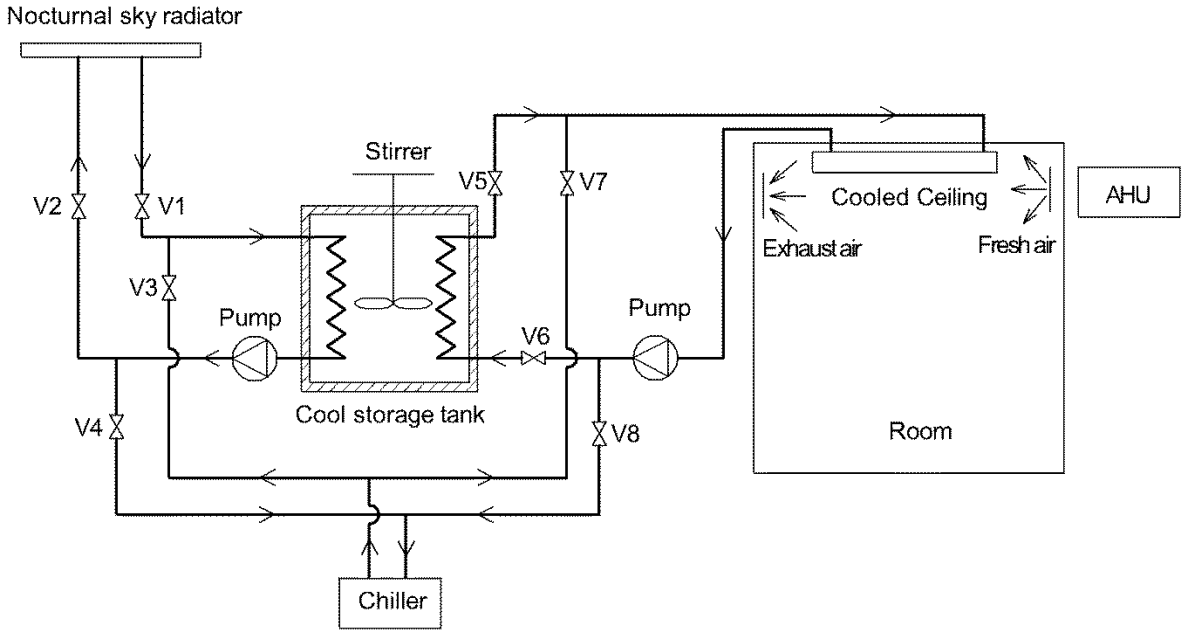

Figure 5.1 Schematic diagram of the hybrid system

As shown in Figure 5.1, two heat exchangers are immersed in the slurry tank to store or release the cooling energy, a variable speed stirrer is used to keep the slurry homogeneous and to generate forced convective heat transfer. In order to improve the efficiency of the hybrid system, the operation of the hybrid system is designed to maximize the use of the nocturnal radiative cooling energy and cooling storage energy. For the slurry tank charging process, when the cooling water outlet temperature from the nocturnal radiator is lower than the MPCM melting temperature in the slurry tank, valves 1 and 2 are open and valves 3 to 8 are closed, thereby the cooling water is controlled to

flow into the heat exchanger to cool the MPCM slurry until the slurry is completely charged. The MPCM particle cores change the state from liquid to solid and store the cooling energy in the form of latent heat during the cooling charging process. If the nocturnal radiative cooling is not sufficient for charging the slurry tank, which means the slurry tank is not completely charged, but the cooling water outlet temperature from the nocturnal radiator has already risen higher than the MPCM slurry melting temperature, the slurry tank will continued to be charged by the supplemental chiller system. In this situation, valves 1, 2, 5 to 8 are closed, and valves 3 and 4 are opened to change the flow path. During the working period of the room, the cooling energy storage in the slurry tank is first used for the space cooling application. When the MPCM slurry temperature is lower or equal to the PCM melting temperature, the valves 5 and 6 are open and the other valves are closed, so the cooling water is controlled to transfer cooling energy in the slurry tank to the water through heat exchange. Then the cooling energy in the cooling water is released to the office room to remove the sensible heat by means of the ceiling panels. The MPCM particle cores in the tank then change state from solid to liquid and release the cooling energy in the form of latent heat during the discharging process. When the MPCM slurry temperature is higher than the MPCM melting temperature, the chiller system is switched on to supply cooling to the room, then valves 7 and 8 are open and valves 1 to 6 are closed to change the cooling water flow path.

5.2.3 System Design Description

To evaluate and compare the efficiency and energy saving potential of the novel hybrid system in five typical Chinese cities, a south-facing room is simulated with the hybrid

system. The outside conditions are based on the local typical meteorological year (TMY) weather data of Hong Kong, Shanghai, Beijing, Lanzhou and Urumqi with a 1982 – 1997 period of record obtained from the U.S. National Climatic Data Center (U.S. Department of Energy website)

A one floor building is employed in the simulation to thoroughly evaluate the performance of the hybrid system. The further discuss about the application potential in high-rise building is based on the simulation result of the one floor building. The standard room is 5.1 m long, 3.6 m wide and 2.6 m high, situated in an intermediate story, and the adjacent rooms are all identical. The main construction of the external wall is 180 mm thick concrete slab inside, 200 mm thick brick outside and 60 mm insulation in between. Double glazing windows are used on the south facing façade, with center-of-glass U value of 1.31 W/ (m^2. ^oC) and the area is 2.88 m^2. The combined heat transmission coefficient of the façade is 1.28 W/(m^2.^oC) . The south wall is the external wall and the north wall is adjacent to a corridor. The partition walls are made of 26 mm gypsum board. The floor and ceiling are 320 mm thick concrete slab bases with 70 mm thick outside cement layers. It is determined that about 60 % of the ceiling is covered with cooled ceiling panels when the cooled ceiling system is applied.

In working hours, from 9:00 to 18:00, the building is occupied with constant internal sensible loads of 800 W of equipment and lighting, or about 44 W/m^2 floor area. There is no air infiltration in the calculation of the cooling load. The operating hours of the ceiling panels and ventilation system are also scheduled from 9:00 to 18:00, which means the

MPCM discharging process. The operating hours of the nocturnal sky radiator are from 19:00 to 8:00, which means the MPCM charging process.

The processed air is supplied at a rate of 100 m^3/ h, which is about 2 ach in terms of the room volume. This flow rate will meet the ventilation requirement for three persons according to the ASHREA standard. To keep the air dew point temperature below the ceiling panel surface temperature, the outside air is first cooled and dehumidified, and then reheated to 15 ^oC. The design value of the inlet and outlet temperature of cooling water to the cooled ceiling is 16.7 ^oC, with 1 ^oC temperature difference with the slurry melting temperature 15.7 ^oC, and 20 ^oC respectively. Hence the cooling water rate to the ceiling is about 0.38 m^3/h, which results in a temperature rise of the cooling water of about 3.3 ^oC at the estimated peak load conditions. The overall control strategy of the combined terminal system for the end user is that the air supply rate and temperature are kept constant, and further cooling requirement are met by ceiling panels.

For the nocturnal sky radiator cooling water system, the design value of the inlet and outlet temperature of the cooling water is 14.7 ^oC, with also 1 ^oC temperature difference with the slurry melting temperature 15.7 ^oC, and 12 ^oC, respectively. The peak cooling capacity of the nocturnal radiator is estimated under typical weather data in spring and fall, when the temperature difference between sky and nocturnal radiator is large enough and the cooling supply for the room is required. Therefore, the cooling water rate to the nocturnal radiator is determined about 0.48 m^3/h under such design conditions.

The radiator panel is similar to a conventional solar collector. Hamza H. Ali, Taha et al. (1995) indicated that the nocturnal sky radiator with simple metal surface has obvious economic benefit and is easy to install and maintain as well. In addition, wind screen is not used in this system, because of the limited effect, high cost and short life (Argiriou, Santamouris et al. 1994). Therefore, a typical horizontal flat-plate radiator is selected in this study. The radiator panel consists of one or several standard panels as shown in Figure 5.2. The standard panel consists of several copper pipes, which are connected to each other by a segregator. Each pipe is installed at the center of a thin galvanized stainless steel plate used for the radiation collector. The galvanized steel panel is selected because it has a high emissivity in 8~14 μm infrared transmission, which is equal to about 0.9 (Khedari, Waewsak et al. 2000), and is widely used with a relatively low price. In addition, there is a 25 mm polyurethane form insulation coated with a metal frame box installed below the collector to reduce unnecessary heat loss from the ambient air. For radiation dimension determination, the radiator is designed as 5 m long and 3 m wide, which is under the assumption that the entire surface of the roof of either low-rise building or high-rise building is occupied by nocturnal radiators.

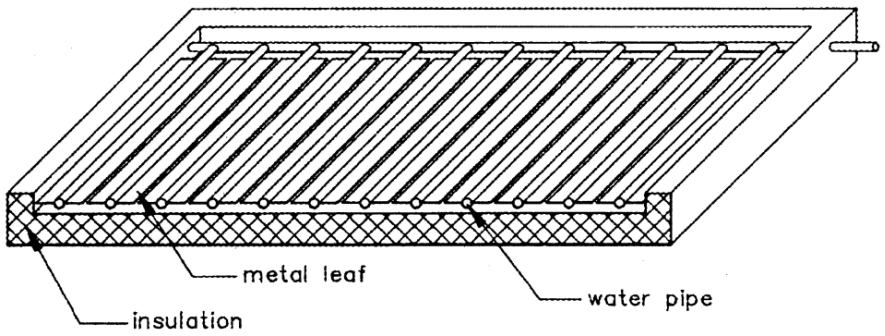

Figure 5.2 Construction of the nocturnal sky radiator (Erell and Etzion 2000)

The capacity of the slurry tank is selected to be able to supply 80% of daily load in the day with the largest cooling load demand. Based on such design conditions, a slurry tank of 0.2 m^3 containing 192kg MPCM slurry is used in the system. The capacity of the additional chiller is determined by the larger one of the supplementary cooling supply for the storage tank at peak daily load and the supply for the nocturnal sky radiator at night in the summer heat.

5.3 Mathematical Model

5.3.1 Nocturnal Sky Radiator Model

When the nocturnal sky radiator is activated at night, the circulating water flows in pipes and releases its heat from the nocturnal sky radiator to sky and ambient air. There are two major ways for a radiator to reject heat to the external environment, radiant heat transfer and convective heat transfer, as shown in Figure 5.3.

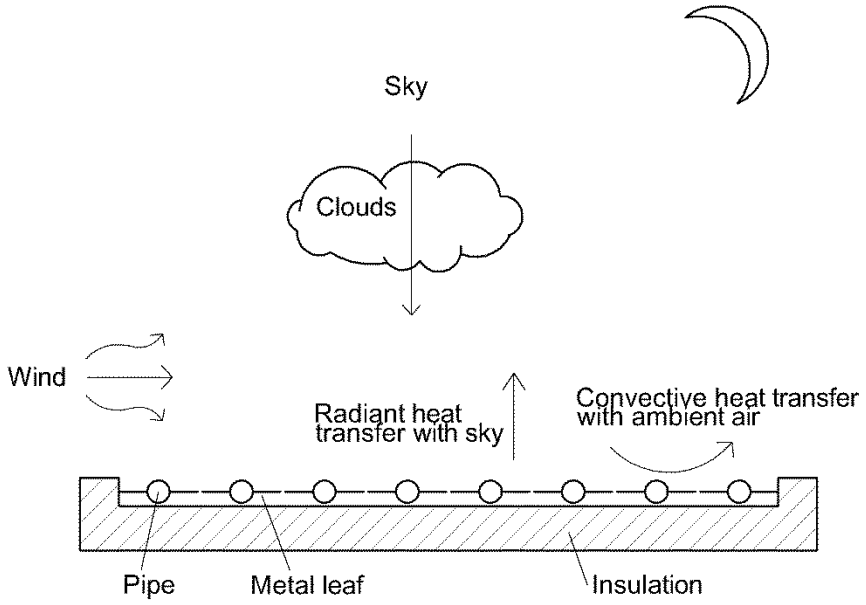

Figure 5.3 A schematic diagram of nocturnal sky radiator

The objectives of establishing the mathematical model of the nocturnal sky radiative cooling techniques can be described as follows:

- Calculation of the climatic potential for the net radiant heat transfer as a function of the ambient air temperature, relative humidity, cloudiness and wind speed.
- Calculation of the outlet water temperature of the nocturnal sky radiator according to the inlet water temperature, the mass flow rate and the TMY weather data.
- Calculation of the cooling energy delivered to the building hour-by-hour for a whole year, as a function of the design details of the radiator and hybrid system.

In order to consolidate the radiator model and the hybrid system model during the simulation and to enhance the simulation efficiency, the model is developed based on such assumptions as follows:

- The nocturnal sky radiator is placed horizontally toward the sky.
- The operation of the radiator is assumed to be a steady state process.
- The water and heat flow inside the radiator panel is one-dimensional along its length direction. There is no temperature gradient in the width direction.
- Heat loss from the back and edges of the radiator panel can be negligible (Hamza H. Ali, Taha et al. 1995).
- The thermal capacity of the construction of the radiator plate is neglected.

5.3.1.1 Radiator Plate Model

Radiant heat transfer and convective heat transfer are the two major ways for a radiator to reject heat into the external environment. The percentages of those two parts depend largely on the specific weather conditions. The detailed heat transfer principle of the nocturnal sky radiator is plotted in Figure 5.4.

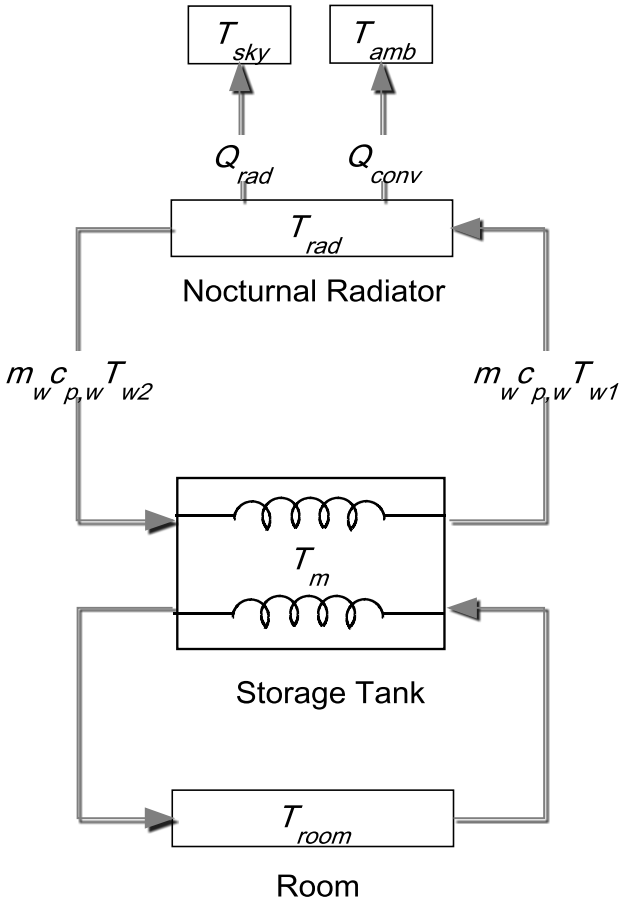

Figure 5.4 Heat transfer mechanism of nocturnal sky radiator

The overall energy balance of the nocturnal radiator is shown in Equation (5.1).

$$\dot{Q}_{cool} = \dot{Q}_{rad} + \dot{Q}_{conv} \tag{5.1}$$

where $\dot{Q}_{cool}$ is the cooling capacity of the nocturnal sky radiator (W); $\dot{Q}_{rad}$ is the radiative heat transfer rate from the radiator to the sky (W); and $\dot{Q}_{conv}$ is the convective heat transfer rate from the radiator to the surrounding environment (W).

The radiative heat transfer rate from the radiator to the sky can be calculated with the following equations (Clark and Allen 1978; Ito and Miura 1989):

$$\dot{Q}_{rad} = A_{rad}\varepsilon_{rad}\sigma({T_{rad}}^4 - {T_{sky}}^4) \tag{5.2}$$

$$T_{sky} = (C_a\varepsilon_{sky})^{0.25}T_{amb} \tag{5.3}$$

$$C_a = 1 + 0.0224n - 0.0035n^2 + 0.00028n^3 \tag{5.4}$$

where A_{rad} is the area of radiator plate exposed to the sky (m^2); ε_{rad} is the emissivity of white painted metal radiator plate, 0.90 (Khedari, Waewsak et al. 2000); σ is the Stefan-Boltzmann constant ($5.67x10^{-8} W\ m^{-2}\ K^{-4}$); T_{rad} is the absolute temperature of the radiator plate (K); T_{sky} is the absolute temperature of the sky (K); C_a is the cloudiness coefficient; n is the total opaque cloud amount (0 for clear sky, 10 for overcast sky); and T_{amb} is the absolute dry bulb temperature of ambient air (K); ε_{sky} is the emissivity of the clear sky.

Many different long wave radiation parameterization methods have been used in order to calculate clear sky emissivity (Clark and Allen 1978; Berdahl and Martin 1984; Duffie and Beckman 2006). In this study, Equations (5.5) and (5.6) (Berdahl and Martin 1984) are used for the calculation of sky emissivity calculation.

$$\varepsilon_{sky} = 0.711 + 0.56\left(\frac{T_{dew} - 273.15}{100}\right) + 0.73\left(\frac{T_{dew} - 273.15}{100}\right)^2 \tag{5.5}$$

$$T_{dew} = C_3 \cdot \frac{\ln(RH) + C_1}{C_2 - [\ln(RH) + C_1]} \tag{5.6}$$

where T_{dew} is the absolute dew point temperature of ambient air (K); RH is the relative humidity (0-1); and C_1 to C_3 can be calculated as the following equation (5.7).

$$\begin{cases} C_1 = C_2 \cdot T_{amb} / (C_3 + T_{amb}) \\ C_2 = 17.08085 \\ C_3 = 234.175 \end{cases} \tag{5.7}$$

The absolute temperature of the radiator surface T_{rad} is assumed to be equal to the average temperature of water flowing across the panel as follows:

$$T_{rad} = (T_{w1} + T_{w2}) / 2 \tag{5.8}$$

where T_{w1} and T_{w2} are the inlet and outlet temperatures of the nocturnal radiator (K).

Convective heat transfer from the radiator to the surrounding environment is calculated as Equation (5.9):

$$\dot{Q}_{conv} = A_{rad} h_{conv} (T_{rad} - T_{amb}) \tag{5.9}$$

where h_{conv} is the convective heat transfer coefficient (W $\cdot$m^{-2} $\cdot$K^{-1}).

For surfaces without wind screen, the coefficient for convection h_{conv} is in the first order a linear function of the wind speed V which has the form $h_{conv} = a + b \cdot V$. There are some previous studies which show a large variety in assigning values to a and b. Relations applied by Mitchell (1976), modified for forced convection over buildings by Duffie and Beckam (1991), and McAdams (1954), have been used to fit the experimental data. The best fit, by using h_{conv}, was reported and discussed by Clark and Berdahl (1980), and was used in several pieces of researches on radiators (Erell and Etzion 2000; Dobson 2005; Heidarinejad, Farmahini Farahani et al. 2010):

$$h_{conv}(V) = 1.8 + 3.8V \quad (1.35 < V < 4.5) \tag{5.10}$$

where V is the wind speed (m/s).

As the radiator plate model Equation (5.2) shown, the radiation heat transfer rate from the radiator to the sky $\dot{Q}_{rad}$ is a function of the temperature of the nocturnal radiator front surface and the sky temperature. When the temperature of the radiator surface is higher than the sky temperature, usually at midnight, $\dot{Q}_{rad}$ is positive and the radiator can be cooled by the sky, an infinite cooling source, until the radiator temperature is approximate to the sky temperature. In addition, Equation (5.9) shows the convective heat transfer from the radiator to the surrounding environment. When the temperature of the nocturnal radiator is higher than the surrounding temperature, the convective heat transfer $\dot{Q}_{conv}$ is positive and is beneficial for the cooling gain of the radiator. However,

in fact the building's cooling applications combined with the radiator system usually operate at hot weather conditions, and the surrounding temperature is higher than the radiator temperature, even at night. Consequently, the convective heat transfer is usually the heat loss of the radiator for nocturnal sky cooling collection applications. The detailed heat gain of nocturnal radiator from radiation heat transfer, convective heat transfer, and eventually the total heat gain amount, should be simulated synthetically to evaluate the potential cooling ability of the nocturnal radiator.

5.3.1.2 Cooling Water Model

As the analysis of the heat transfer principle of the nocturnal sky radiator (which is shown in Figure 5.4) demonstrates, the cooling obtained by the nocturnal radiator is used to charge the MPCM slurry in the cooling storage tank, and the cooling water capacity can be calculated as Equation (5.11):

$$\dot{Q}_{cool} = \dot{m}_w c_{p,w}(T_{w1} - T_{w2}) \tag{5.11}$$

where $\dot{m}_w$ is the mass flow rate of water through the radiator (g/s) and $c_{p,w}$ is the heat capacity of the water, 4.2kJ ŀkg^{-1} ŀK^{-1}.

5.3.1.3 Integrated Model

The radiator plate and the cooling water model can be integrated to get a new thermal energy balance model of the cooling capacity of the radiator $\dot{Q}_{cool}$ based on the Equations (5.1) to (5.11) shown as follows:

$$\begin{aligned}\dot{Q}_{cool} &= A_{rad}\varepsilon_{rad}\sigma[(\frac{T_{w1}+T_{w2}}{2})^4 - T_{sky}{}^4] + A_{rad}h_{conv}(\frac{T_{w1}+T_{w2}}{2} - T_{amb}) \\ &= \dot{m}_w c_{p,w}(T_{w1} - T_{w2})\end{aligned} \qquad (5.12)$$

In Equation (5.12), there are three variables need to be defined, T_{w1}, T_{w2} and $\dot{m}_w$. The nocturnal radiator side of the cooling water system is a constant flow system, hence $\dot{m}_w$ equals 0.13kg/s, which is determined under design conditions. In this study, to simplify the calculation, the heat exchangers of the thermal storage tank at both the nocturnal radiator side and the cooled ceiling side are assumed to be ideal ones, and the heat transfer between the outside and inside of the heat exchanger tube is almost sufficient. Under such an assumption, the temperature difference between the MPCM slurry and the outlet of the heat exchanger at the nocturnal radiator side, which is also the inlet temperature of the radiator, is assumed to be 1 °C. The melting temperature of MPCM slurry T_m in the tank is 15.7 °C, so the inlet temperature of radiator T_{w1} can be assumed to be 14.7 °C. Therefore, the outlet temperature of radiator T_{w2} is the only variable of Equation (5.12), which can be expressed as the new formula (5.13) shown below. This nonlinear equation can be solved by using Newton's method (Moler 2004).

$$f(T_{w2}) = A_{rad}\varepsilon_{rad}\sigma[(\frac{T_{w1}+T_{w2}}{2})^4 - T_{sky}{}^4] + A_{rad}h_{conv}(\frac{T_{w1}+T_{w2}}{2} - T_{amb}) - \dot{m}_w c_{p,w}(T_{w1} - T_{w2}) = 0 \quad (5.13)$$

The principle of Newton's method for solving $f(x) = 0$ is drawing the tangent to the graph of $f(x)$ at any point and determining where the tangent crosses the *x*-axis. Using the definition of the slope of a function, at $x = x_i$, the formula of Newton's method can be shown as follows:

$$x_{i+1} = x_i - \frac{f(x_i)}{f'(x_i)} \quad (5.14)$$

The solution of the equation starts from an initial guess value x_i, then the next guess value, x_{i+1}, can be obtained by using Equation (5.14). The absolute relative approximate error $|\varepsilon_a|$ can be calculated as follows:

$$|\varepsilon_a| = \left|\frac{x_{i+1} - x_i}{x_{i+1}}\right| \times 100\% \quad (5.15)$$

Compare the absolute relative approximate error with the pre-specified relative error tolerance, ε_s. The root x can finally be found by repeating this process until $|\varepsilon_a| < \varepsilon_s$.

Finally, after the solution of $T_{w,2}$, the accurate cooling capacity of the radiator, can be calculated by Equation (5.11).

In this simulation, the thermal properties of the nocturnal radiator, including the outlet temperature and the effective cooling capacity, are evaluated by the calculation program built by MATLAB in which the cooling load and the energy consumption of the primary equipment is simulated by the building energy simulation code ACCURACY. Figure 5.5 demonstrates the work flow of the nocturnal radiator calculation based on the main algorithm listed as below:

- Assume the initial outlet water temperature $T_{w2,i}$ of the nocturnal sky radiator.
- Calculate the outlet water temperature $T_{w2,i+1}$ based on Equation (5.13) and (5.14) by using Newton's method, and find the absolute relative approximate error $|\varepsilon_a|$ based on Equation (5.15).
- Get the accurate outlet water temperature T_{w2} by repeating the previous step until the absolute relative approximate error is less than the pre-specified relative error tolerance, ε_s.
- Calculate the radiator cooling capacity by Equation (5.11).

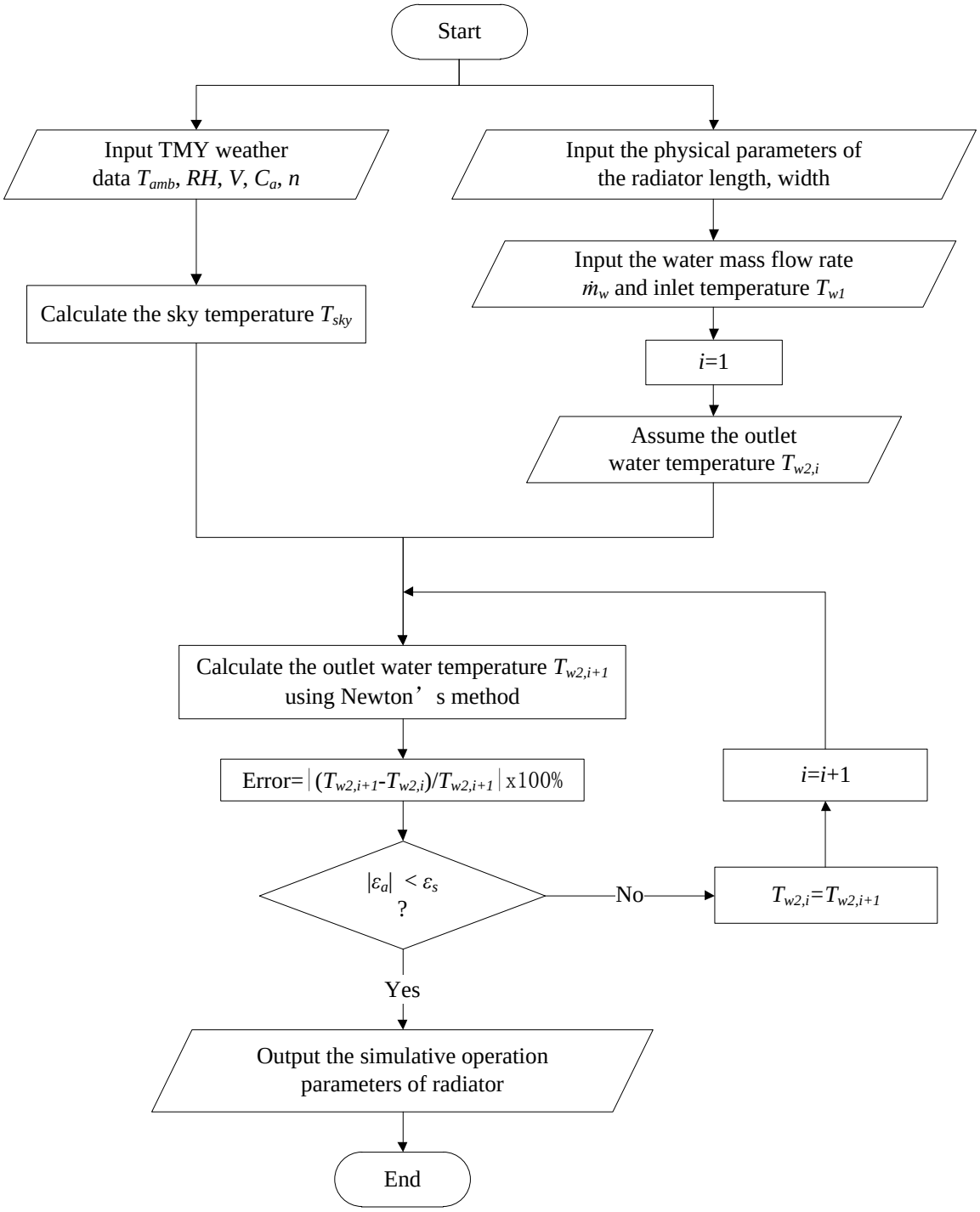

Figure 5.5 Flow chart of nocturnal sky radiator calculation

5.3.2 Storage Tank Model

The slurry tank is filled with the MPCM slurry which is made by microencapsulated n-hexadecane ($C_{16}H_{34}$) with a thin Amino Plastics film as shell and dispersed into water as a carrier fluid. The core-shell ratio was controlled to be about 7:1 by weight during the preparing process. The thickness of shell was approximately 0.3μm. The solid content of the emulsion used in this study is about 23%. The thermal property derived from the DSC experiment result is listed in Table 5.1

Table 5.1 Thermal Property of the MPCM

Melting Temperature (°C)	Latent Heat (kJ/kg)
15.7	178

In this study, the MPCM slurry in the storage tank is assumed to be ideally mixed by the stirrer during the operation of the system, so the MPCM material is supposed to remain in the two-phase condition with a fixed temperature of 15.7°C, and the cooling gained from the nocturnal sky radiator is the same as the cooling stored in the storage tank and the cooling supplied for the cooled ceiling.

As mentioned in section 5.2.1, the latent heat of MPCM slurry is first supplied by the nocturnal sky radiator, then by chiller if the amount supplied by the radiator is not enough. In the sky radiator model description, section 5.3.1, the heat transfer exchanger is assumed to be an ideal one, so the inlet water temperature of nocturnal radiator T_{w1} is

14.7°C, and outlet temperature of radiator T_{w2} can be obtained by the MATLAB calculation program. So the latent heat stored in the tank can be calculated as follows:

$$\dot{Q}_{cool} = \dot{m}_w c_{p,w}(T_{w1} - T_{w2}) = \Delta m_{PCM} h_l \quad (5.16)$$

where Δm_{PCM} is the phase change rate of the MPCM slurry (g/s); h_l is the latent heat capacity of the MPCM slurry (kJ/kg).

5.4 Results and Discussion

5.4.1 Feasibility Analysis of Radiative Cooling Applications

5.4.1.1 Weather Condition Analysis

The typical monthly average weather data in Hong Kong is shown in Figure 5.6. Relative humidity (*RH*) and ambient dry bulb temperature (T_{amb}) are obtained based on TMY weather data in Hong Kong. Sky temperature (T_{sky}) is calculated by Equations (5.3) to (5.6). Hong Kong lies within the tropics and experiences a maritime climate. The monthly average ambient temperature is distributed from the lowest 15.7 °C in January to the highest 28.9 °C in August. It is worthwhile to note that Hong Kong is also a humid city with very high humidity, above 70%, all year round, and it experiences extreme humidity during the rainy season. Sky temperature is a function related to ambient temperature, dew point temperature and cloud cover. The results in Figure 5.6 show that

monthly average sky temperature in Hong Kong is distributed from the lowest 5.4 °C in January to the highest 27.4 °C in July. For building passive cooling applications, the sky temperature in Hong Kong in summer, from May to September, is really high and hard to use in an air conditioning system.

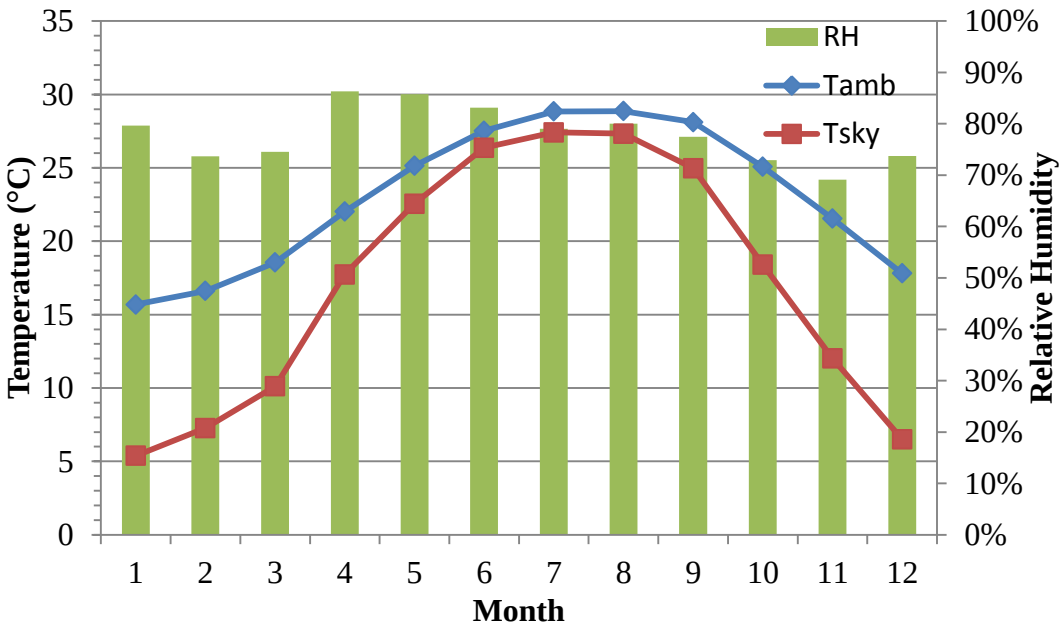

Figure 5.6 Typical monthly average weather data in Hong Kong

The sky radiation depends on atmospheric temperature, water vapor pressure, and the apparent fractional cloudiness. Hitherto, many empirical equations have been presented that correlate the apparent emittance of the atmosphere and the meteorological factors (Saitoh and Ono 1984). Its intensity increases as these factors increase. Hence, a preliminary inference can be drawn that a nocturnal sky radiator system has a greater potential in dry and cool regions such those in northern China.

Figure 5.7 shows the monthly average sky temperature of five cities calculated based on the local weather data record. It is clear that, unlike hot and humid Hong Kong, there is a large annual variation of the sky temperature for the other four cities. In Shanghai and Beijing, the sky temperature in summer is relatively high just like Hong Kong, but it obviously decreases in the other seasons. The sky temperature of almost 10 months over the year is below 20°C and even below 0°C in winter. In Lanzhou and Urumqi, all the monthly average sky temperatures are below 10°C, which is extremely attractive for nocturnal radiator cooling applications in building passive cooling applications.

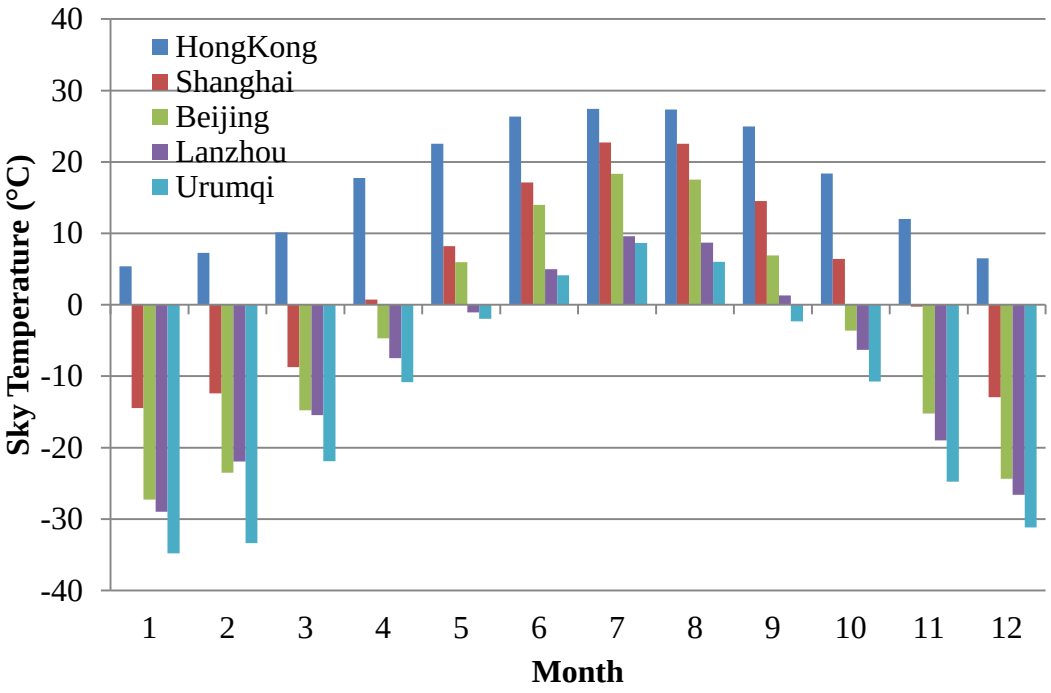

Figure 5.7 Monthly average sky temperature of five cities in China

5.4.1.2 Annual occurrence of sky temperature

The annual occurrence of sky temperature of five cities in China is shown in Figure 5.8. The annual occurrence shows the percentage of accumulated hourly amounts that are above the temperatures shown in the *x*-axis, which effectively helps to analysis the potential of the free cooling source for sky radiation utilization. It can be shown in Hong Kong that the sky temperature is below 20°C for about 55% of the hours. This means that in this period, sky radiation can be used in building cooling applications. In addition, compared with Hong Kong, Shanghai and Beijing have more potential for using a nocturnal radiative cooling source, because the percentage of hours below 20°C are above 80% in both cities. It is more attractive that in Lanzhou and Urumqi the sky temperature is below 20°C almost all year. It is indeed positive evidence that there is great potential for using a nocturnal sky radiator in the northern cities of China.

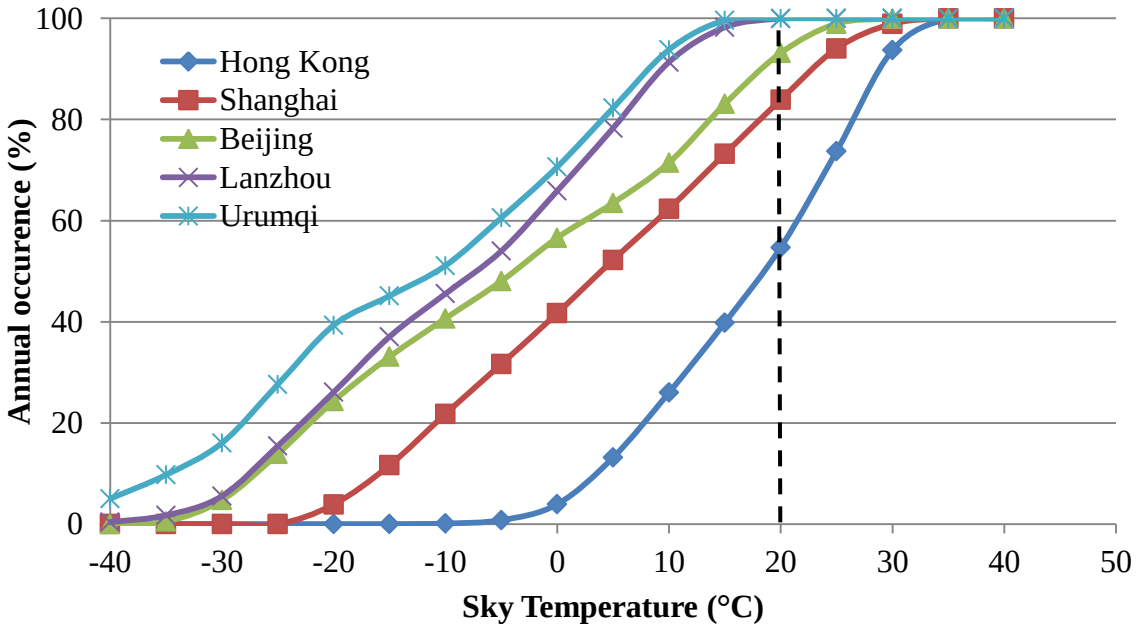

Figure 5.8 Percentage annual occurrence of sky temperature of five cities in China

5.4.1.3 Potential Cooling Capacity of Nocturnal Radiator

Figure 5.9 shows the monthly average potential cooling capacity per unit area of radiator in Hong Kong and Urumqi. The calculation assumes the radiator operates all 24 hours in 365 days without further air conditioning controls, so the results can describe the radiator capacity dependent on weather conditions. The columns show the convective and radiative cooling capacity of the radiator, and the line shows the total potential cooling capacity of the radiator in a whole year.

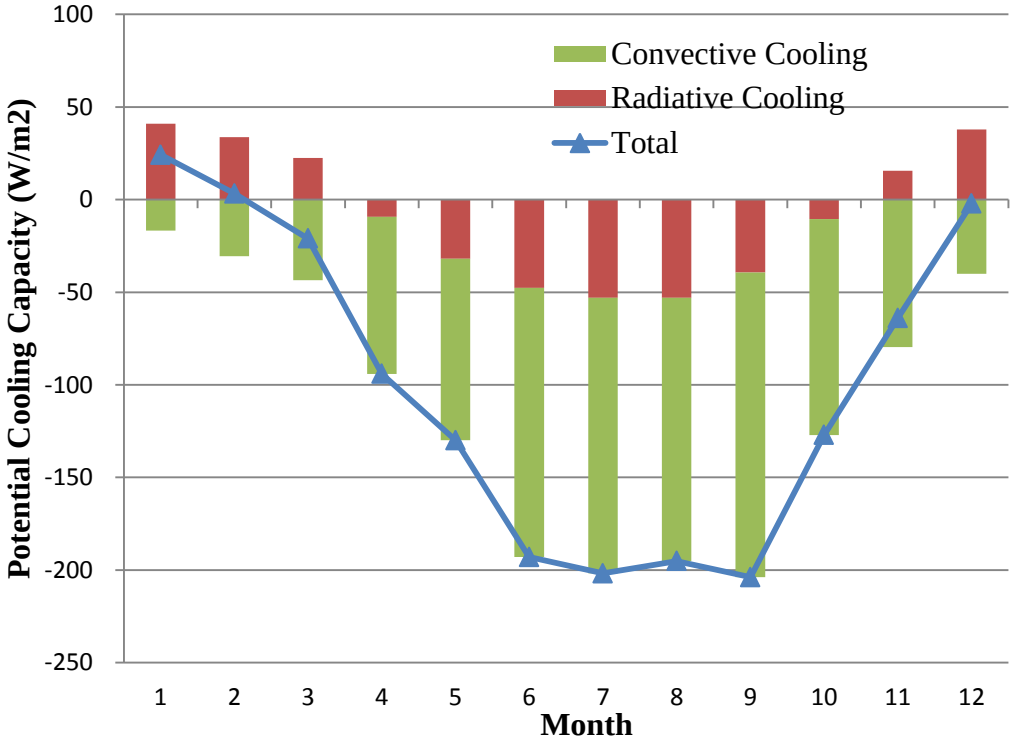

a)

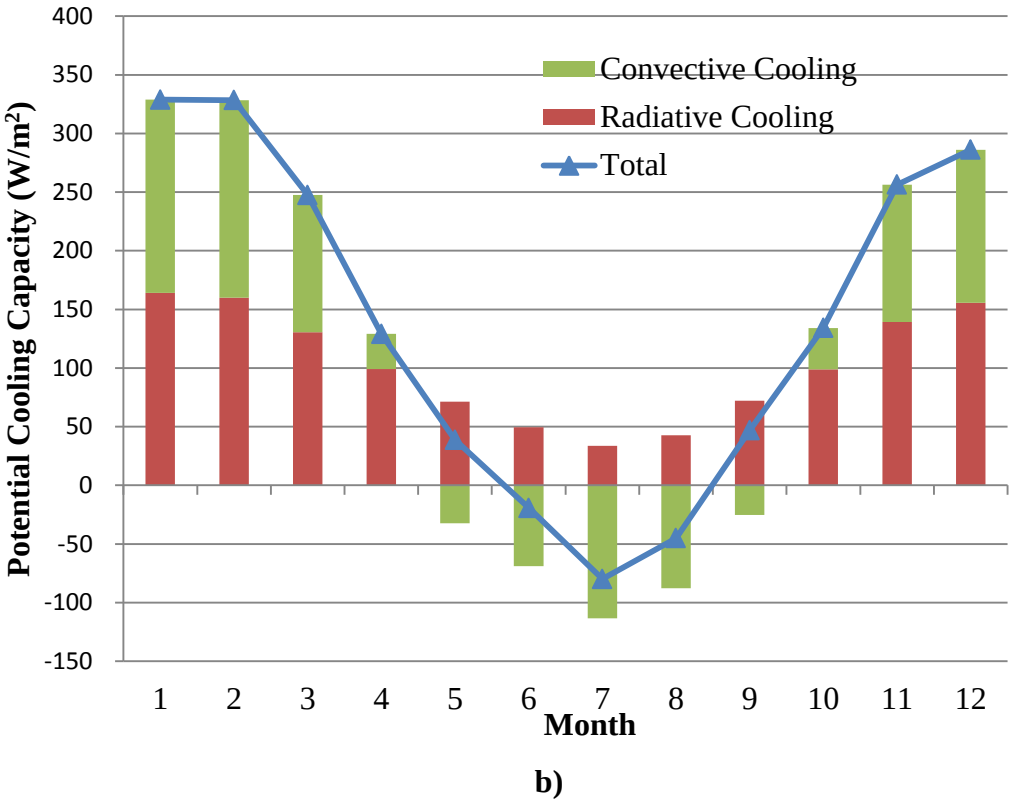

b)

Figure 5.9 Monthly average potential cooling capacity of nocturnal sky radiator: a) in Hong Kong and b) in Urumqi

In hot and humid Hong Kong, the sky temperature is very high throughout the year, so the nocturnal radiation can just be used in winter, from November to May. Because of the high ambient temperature, the path of convective heat transfer is from ambient to radiator throughout the year, so the convective heat transfer phenomenon is not conducive to the application of sky radiation and decreases the cooling capacity of the radiator most of time. The total cooling obtained by the nocturnal radiator can only be used in three months, from December to February, and cannot meet the large cooling demand in the summer.

In contrast to Hong Kong, the weather conditions in Urumqi are the most attractive of the five cities based on the analysis above. In Figure 5.9, it is clearly shown that the radiative cooling obtained by the nocturnal radiator is positive throughout the year because of the relatively low sky temperature. But in summer, the convective cooling obtained by the radiator is negative because of high ambient temperature. The total cooling capacity of the radiator is even negative from June to August, because the amount of convective heat transferred from the radiator to the surroundings is larger than the amount obtained through sky radiation. In the other seasons, convective heat transfer is positive because of the low ambient temperature. The amount of the convection is very large and almost equal to the amount from sky radiation. A conclusion can be drawn that convective heat transfer plays an important role in nocturnal sky radiation and cannot be ignored during the analysis of utilization potential. In general, the nocturnal sky radiation can be utilized almost year round in Urumqi. In addition, the cooling capacity of a radiator in Urumqi can reach 300W/m^2, a considerable cooling capacity for the practical utilization to decrease the additional area for the radiator. The utilization of a nocturnal radiator in Urumqi is much more attractive than in Hong Kong.

5.4.2 Load Shifting by the Hybrid System

Table 5.2 and Table 5.3 show the detailed results of the cooling load of the hybrid system in Urumqi focused on the charging/discharging process of the cooling energy storage system and load shifting in spring and summer respectively. The temperature calculation,

and the radiative and convective heat transfer calculations are also listed for the analysis of the load shifting process.

The results in Table 5.2 show a typical operation condition with partial loading in spring. For working hours, sensible heat load is extracted by cooling panels, of which the cooling demand can be totally supplied by the charged MPCM slurry in the cooling storage tank, and the percentage of MPCM in solid phase gradually decreases with the storage cooling energy supplied from 100% to 42%. For night time, the operation of the cooling energy storage system changes from a discharging process to a charging process. According to the operation strategy, the MPCM slurry is first charged by the nocturnal sky radiator. In spring, the sky temperature is very low, almost below -5 °C during the whole day, and the ambient temperature is also at a low level. Therefore, the nocturnal sky radiation is abundant and the convective heat transfer is beneficial for the cooling supply. The charging process for the storage tank actually starts from 19:00, and stops at 23:00 when the storage tank has already been fully charged. The nocturnal radiator could provide total cooling capacity of 25 kWh at night, in which 5.6 kWh is finally used for the cooling tank storage.

The results of Table 5.3 show a typical operation condition with full load in summer. For working hours, a sensible load is first extracted by the cooling storage in MPCM slurry, from 10:00 to 17:00. At 18:00, the percentage of MPCM in solid phase reduces to 0%, which indicates the cooling storage in MPCM slurry is completely exhausted. Then, the additional chiller runs to meet the other cooling load demand. For the nocturnal charging

process, the cooling capacity of the nocturnal sky radiator is extremely limited, mainly caused by the large amount of negative convective heat transfer from the radiator. This is easy to understand in a hot summer climate. Therefore, up to the end of the charging process, the nocturnal sky radiator can only provide 1.2 kWh cooling energy, which shows a large span to meet the cooling energy storage demand of 9.6 kWh. Based on this situation, the additional chiller runs for the remaining cooling energy charging supply, a total of 8.4 kWh.

Table 5.2 Hourly operational parameters of cooling storage system with nocturnal radiator in Urumqi in spring

Date	Hour	T_{amb}	T_{dew}	T_{sky}	Sensible Load	Load Extraction		Nocturnal Radiator			Cooling Storage Charging		Percentage of MPCM in solid phase	Note
						By MPCM slurry	By Chiller	Radiative Cooling	Convective Cooling	Cooling Power	By Radiator	By Chiller		
		℃	℃	℃	W	W	W	W	W	W	W	W		
30.Apr.	10	8.8	-3.6	-12.3	619	619	0	0	0	0	0	0	94%	Discharging Process
30.Apr.	11	10.2	-4.7	-11.5	824	824	0	0	0	0	0	0	85%	
30.Apr.	12	11.8	-3.9	-9.6	806	806	0	0	0	0	0	0	77%	
30.Apr.	13	13.3	-2.7	-7.7	779	779	0	0	0	0	0	0	68%	
30.Apr.	14	14.4	-1.8	-6.2	700	700	0	0	0	0	0	0	61%	
30.Apr.	15	15.3	-2.7	-5.8	596	596	0	0	0	0	0	0	55%	
30.Apr.	16	16.0	-4.5	-6.0	485	485	0	0	0	0	0	0	50%	
30.Apr.	17	16.5	-6.4	-6.5	397	397	0	0	0	0	0	0	46%	
30.Apr.	18	16.9	-6.7	-6.2	393	393	0	0	0	0	0	0	42%	
30.Apr.	19	16.8	-6.8	-6.4	0	0	0	1321	-441	880	880	0	51%	Charging Process
30.Apr.	20	16.3	-4.8	-5.9	0	0	0	1286	-295	992	992	0	61%	
30.Apr.	21	15.1	-3.3	-6.3	0	0	0	1301	-189	1111	1111	0	73%	
30.Apr.	22	13.2	-1.7	-7.3	0	0	0	1339	38	1377	1377	0	87%	
30.Apr.	23	11.4	-0.1	-8.1	0	0	0	1369	295	1664	1238	0	100%	
30.Apr.	24	10.4	0.7	-8.6	0	0	0	1388	435	1824	0	0	100%	
1.May	1	10.2	0.5	-8.9	0	0	0	1402	462	1864	0	0	100%	
1.May	2	10.6	0.1	-8.7	0	0	0	1397	406	1803	0	0	100%	
1.May	3	10.9	-0.2	-8.6	0	0	0	1393	364	1756	0	0	100%	
1.May	4	10.8	-0.3	-8.8	0	0	0	1400	377	1777	0	0	100%	
1.May	5	10.1	0.2	-9.2	0	0	0	1416	446	1862	0	0	100%	
1.May	6	8.8	0.8	-10.1	0	0	0	1453	615	2069	0	0	100%	
1.May	7	7.9	1.3	-10.6	0	0	0	1476	733	2210	0	0	100%	
1.May	8	8.3	1.0	-10.4	0	0	0	1471	635	2106	0	0	100%	
1.May	9	10.6	0.6	-8.5	0	0	0	1391	278	1668	0	0	100%	
Total (kWh)					5.6	5.6	0.0	20.8	4.2	25.0	5.6	0.0		

Table 5.3 Hourly operational parameters of cooling storage system with nocturnal radiator in Urumqi in summer

Date	Hour	T_{amb}	T_{dew}	T_{sky}	Sensible Load	Load Extraction		Nocturnal Radiator			Cooling Storage Charging		Percentage of MPCM in solid phase	Note
						By MPCM slurry	By Chiller	Radiative Cooling	Convective Cooling	Cooling Power	By Radiator	By Chiller		
		℃	℃	℃	W	W	W	W	W	W	W	W		
29.Aug.	10	24.3	7.9	8.6	1195	1195	0	0	0	0	0	0	88%	Discharging Process
29.Aug.	11	27.8	8.2	12.1	1210	1210	0	0	0	0	0	0	75%	
29.Aug.	12	30.2	7.4	13.9	1196	1196	0	0	0	0	0	0	62%	
29.Aug.	13	31.3	7.1	14.7	1193	1193	0	0	0	0	0	0	50%	
29.Aug.	14	31.5	5.9	14.2	1180	1180	0	0	0	0	0	0	38%	
29.Aug.	15	31.8	5.4	14.1	1135	1135	0	0	0	0	0	0	26%	
29.Aug.	16	32.6	5.2	14.8	955	955	0	0	0	0	0	0	16%	
29.Aug.	17	33.5	5.1	15.5	864	864	0	0	0	0	0	0	7%	
29.Aug.	18	34.2	4.8	16.0	827	671	156	0	0	0	0	0	0%	
29.Aug.	19	33.8	4.5	15.5	0	0	0	231	-4500	-4269	0	0	0%	Charging Process
29.Aug.	20	32.4	4.3	14.0	0	0	0	321	-4382	-4061	0	0	0%	
29.Aug.	21	29.9	4.5	11.8	0	0	0	412	-3460	-3048	0	0	0%	
29.Aug.	22	26.9	4.7	9.1	0	0	0	531	-2533	-2002	0	0	0%	
29.Aug.	23	24.2	5.1	6.8	0	0	0	625	-1691	-1066	0	0	0%	
29.Aug.	24	22.6	5.5	5.5	0	0	0	667	-1102	-434	0	0	0%	
30.Aug.	1	22.1	6.4	5.6	0	0	0	636	-662	-26	0	0	0%	
30.Aug.	2	22.2	6.4	5.7	0	0	0	602	-212	390	390	0	4%	
30.Aug.	3	22.1	6.4	5.6	0	0	0	633	-622	11	11	0	4%	
30.Aug.	4	21.4	5.3	4.3	0	0	0	733	-921	-188	0	0	4%	
30.Aug.	5	20.2	4.3	2.6	0	0	0	846	-1052	-206	0	0	4%	
30.Aug.	6	18.6	3.7	0.7	0	0	0	940	-798	143	143	0	6%	
30.Aug.	7	17.5	3.4	-0.5	0	0	0	1000	-622	378	378	0	10%	
30.Aug.	8	17.9	3.8	0.1	0	0	0	969	-684	284	284	0	13%	
30.Aug.	9	20.2	4.7	2.8	0	0	0	817	-808	9	9	8384	100%	
Total (kWh)					9.8	9.6	0.2	10.0	-24.0	-14.1	1.2	8.4		

5.4.3 Energy Saving Potential of the Hybrid System

5.4.3.1 Potential Cooling Energy Storage of MPCM Slurry by Radiative Cooling

The potential monthly cooling energy storage by the nocturnal radiator in five typical Chinese cities is shown in Figure 5.10. The whole positive cooling capacity of the radiator is accumulated by month, and results reveal the maximum cooling capacity of the radiator during the charging period without the cooling storage demand.

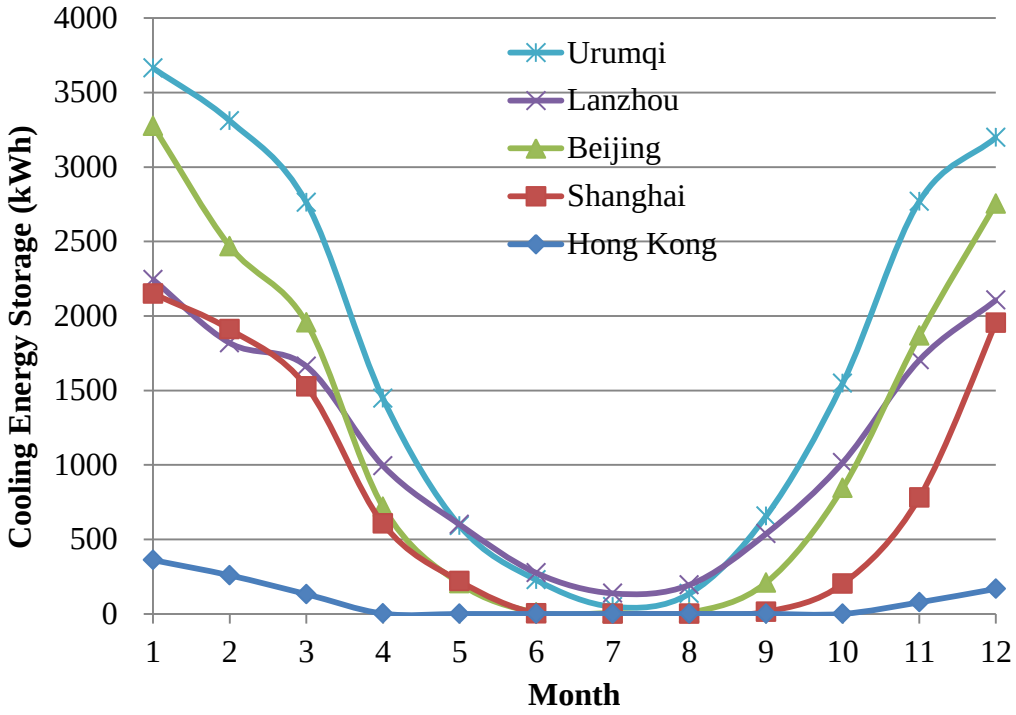

Figure 5.10 Potential monthly cooling energy storage supplied by nocturnal sky radiator

In Urumqi and Lanzhou, the nocturnal radiator could be used during the whole year. Although the cooling capacity used for charging the cooling storage tank is limited in June to August, it is also extraordinarily attractive in the other months. In the other

two cities, Beijing and Shanghai, the free cooling source cannot be effectively used in summer, but in the other seasons it still offers an exciting application prospect. Finally, it is necessary to mention that in Hong Kong the sky radiation utilization potential is limited through the year because of the hot and humid climate conditions.

5.4.3.2 Annual Chiller Energy Saving Potential by Nocturnal Radiator Applications

Based on the simulation result of the hybrid system, more results can be further obtained such as the cooling storage demand, the cooling capacity of the nocturnal radiator and the actual operation energy consumption. The detailed results are shown in Figure 5.11 and Table 5.4.

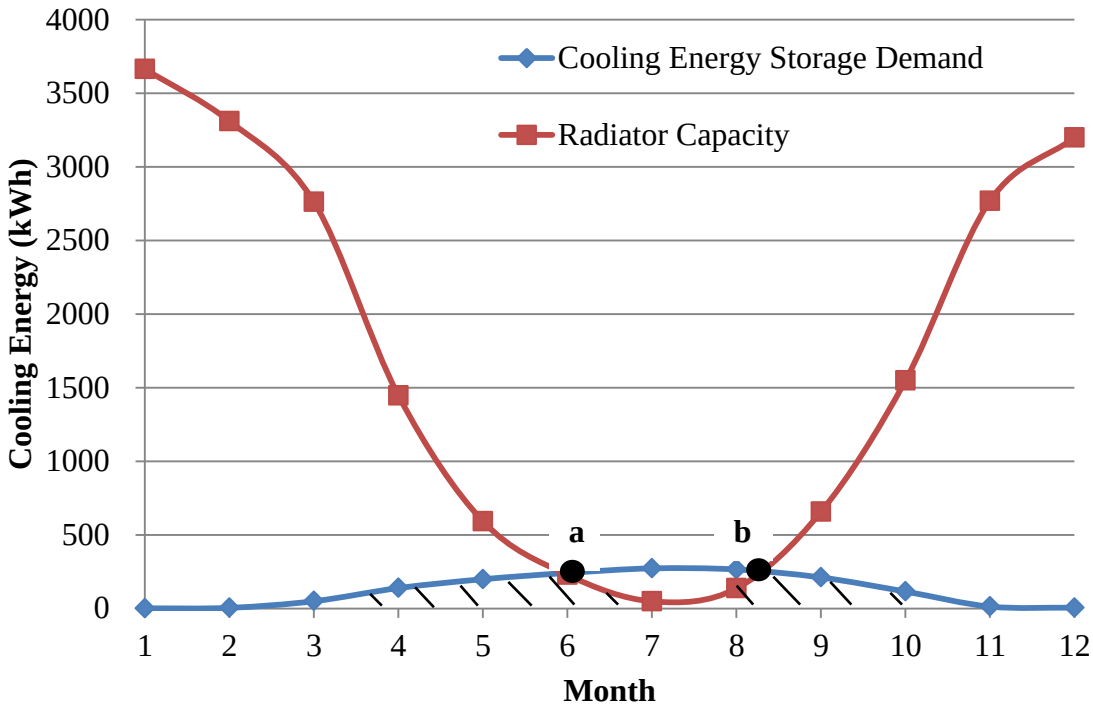

Figure 5.11 Supply-demand relationship of nocturnal sky radiator system in Urumqi

Figure 5.11 illustrates the relationship between the cooling storage demand and the radiator capacity. The cooling storage demand is big in summer and small in winter, and the variation of radiator capacity is just the polar opposite. Therefore, the demand curve and the ability curve cross at two points, a and b, when the radiator can satisfy the cooling demand of the cooling storage tank. The shadow area is thus enclosed to show the actual cooling storage charged by the nocturnal radiator, and the other blank area enclosed by two curves indicates the actual cooling storage charged by the chiller.

Table 5.4 Monthly cooling energy storage by radiator and chiller in Urumqi

Month	Cooling Energy Storage Demand	Radiator Capacity	Actual Storage Charging by Radiator	Actual Storage Charging by Chiller
	kWh	kWh	kWh	kWh
1	1	3664	1	0
2	4	3310	4	0
3	49	2762	49	0
4	138	1446	134	4
5	198	592	175	23
6	241	228	107	134
7	272	48	36	236
8	265	136	103	161
9	210	656	188	22
10	115	1548	115	0
11	13	2769	13	0
12	5	3198	5	0
Total	1511	20359	930	581

Table 5.4 show the detailed data of monthly cooling energy storage in Urumqi. Besides the variation of storage demand and radiator capacity, which have already been expounded in Figure 5.11, the results also show that the cooling energy storage demand is finally satisfied by both the radiator and the chiller, and the cooling energy charging by the radiator reflects the electric power saving. Based on Table 5.4, the annual cooling demand for the storage tank is 1511 kWh, and the nocturnal sky radiator can offer 930 kWh, which means 62% cooling energy of the whole demand. This means a respectable amount of energy savings due to the use of a natural cooling source.

Similar to Urumqi, the actual cooling energy storage from a nocturnal radiator of the other four cities is also analyzed based on the relationship of storage demand and radiator capacity, and the results can be shown in Figure 5.12. In Hong Kong, there is a relatively high cooling load demand throughout the year and the average ambient temperature is generally high, so the utilization of sky radiation cooling applications only offers a limited attraction in the winter because of the relatively low sky temperature. In contrast with Hong Kong, the utilization rate of nocturnal sky radiation in the other four northern and central cities in China reveals a different trend. In winter, although the cooling capacity of the radiator is very high, the cooling storage charging demand is relatively low, so the actual cooling energy supplied by the radiator for cooling charging is limited. In spring and fall, there is a balance of cooling storage demand and radiator cooling capacity, so a large amount of cooling obtained by the radiator can be used. In summer, the cooling capacity of the radiator is reduced because of the high ambient temperature, so the utilization of nocturnal radiation is reduced again. In general, the four northern and central

Chinese cities reveal attractive application potential for using nocturnal radiation in building cooling applications in the transition seasons.

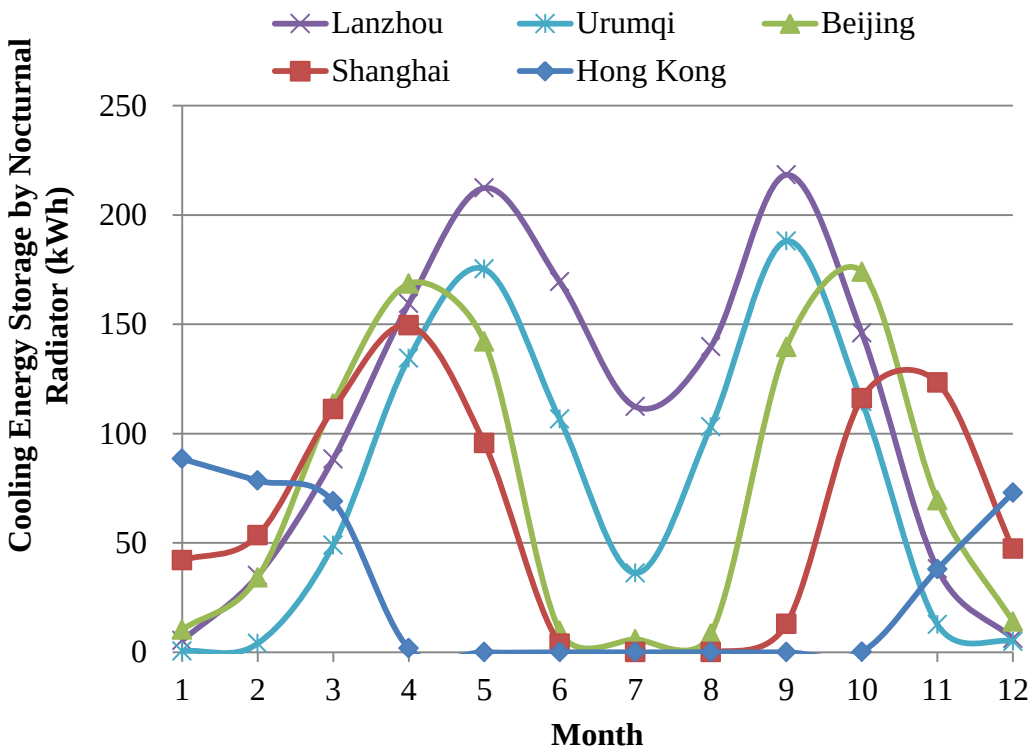

Figure 5.12 Actual monthly cooling energy storage by the nocturnal radiator

Figure 5.13 shows the annual cooling energy storage and the application hours of the nocturnal radiator. It clearly shows that the cooling energy demand in Hong Kong is the largest, but the cooling storage amount of the nocturnal radiator is the smallest, and the utilization hours of the nocturnal radiator are only 891 hrs, because of the hot and humid weather conditions. In Lanzhou, there is a good balance between cooling storage demand and radiator utilization. Therefore, the utilization hours and the amount of cooling storage supplied by the radiator are both the largest of the five cities. There are 1,945 effective hours in a year to utilize the nocturnal radiation in Lanzhou. In Urumqi, although the potential cooling capacity of the radiator is the

highest of the five cities, an extremely large amount of radiation cooling sources occurs in winter and the transition seasons, which cannot match the air conditioning demand in the summer. For such reasons, the actual effect of applying nocturnal radiation as a passive cooling method in building cooling applications is most noticeable in Lanzhou, then in Urumqi, and modest in Hong Kong.

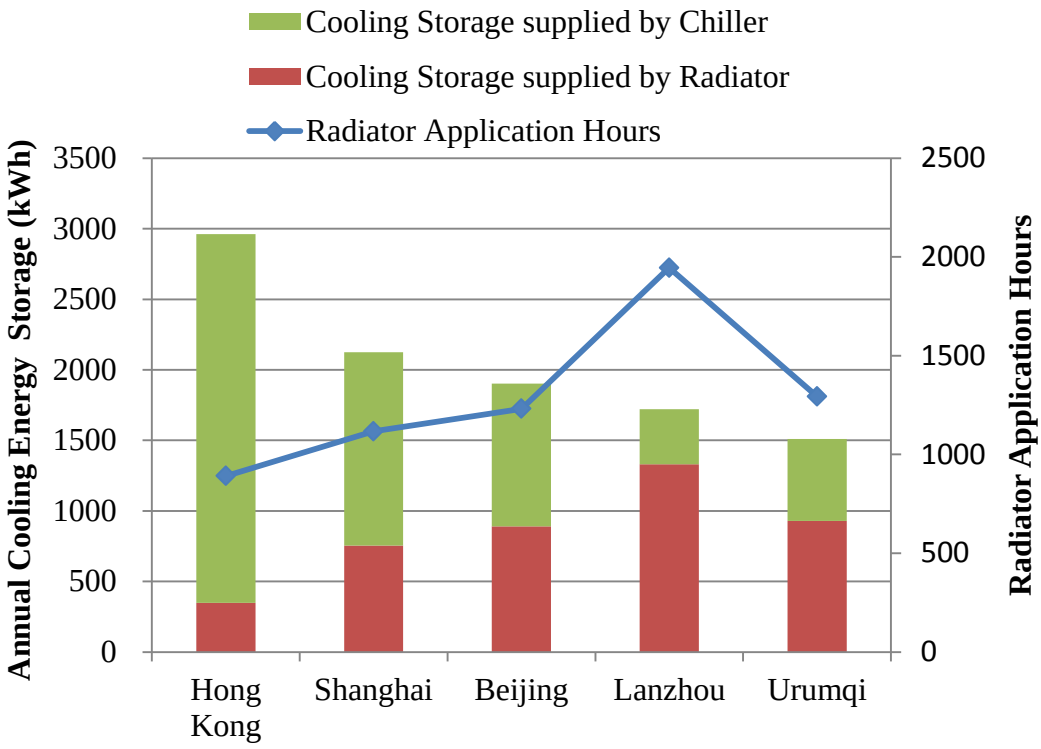

Figure 5.13 Annual cooling energy storage and radiator application hours

With the introduction of the new nocturnal radiation concept, the load of charging the MPCM slurry at night is mainly participated by the nocturnal sky radiator, which means the chiller energy consumption greatly reduced at night. Due to the huge difference of the climate conditions among the five cities across China, which strongly influence the utilization of the nocturnal radiation, there is a foreseeable difference of the energy saving efficiency of the chiller in different cities. To evaluate the energy saving efficiency after using the hybrid system, two indexes of

percentage of chiller energy saving and ratio of radiator application hours are introduced, which are defined as:

$$\begin{aligned}&\text{Percentage of chiller energy saving}\\&= \frac{\text{Annual reduced energy by nocturnal sky radiator}}{\text{Annual chiller energy consumption of the tradiational system}} \times 100\% \end{aligned} \quad (5.17)$$

$$\begin{aligned}&\text{Ratio of radiator application hours}\\&= \frac{\text{Annual effective cooling hours by radiator}}{\text{Annual radiator working hours}} \times 100\% \\&= \frac{\text{Annual effective cooling hours by radiator}}{15(hr) \times 365(days)} \times 100\%\end{aligned} \quad (5.18)$$

In Figure 5.14, the annual chiller energy saving percentage by using the hybrid system and the utilization hour ratio of the nocturnal radiator are described. Similar to the previous conclusions, nocturnal sky radiation is comparatively hard to utilize in Hong Kong. The ratio of radiator application hours is only 16%, and the percentage of the amount saved by using a nocturnal radiator is even lower at 12%. It can be clearly seen that the cooling capacity of the radiator per unit time is lower than the other cities. In Lanzhou, 36% of hours in the whole year are effective hours to employ clean and free nocturnal radiation to replace the conventional electric resource. It is important to point out that 77% energy can be saved by using a nocturnal radiator system, which is very exciting for energy saving purposes. The outstanding effect can also be observed in Urumqi, and the energy saving percentage reaches 62%. All four northern and central Chinese cities, Lanzhou, Urumqi, Beijing and Shanghai, show enormous energy saving potential by utilizing nocturnal radiation technology.

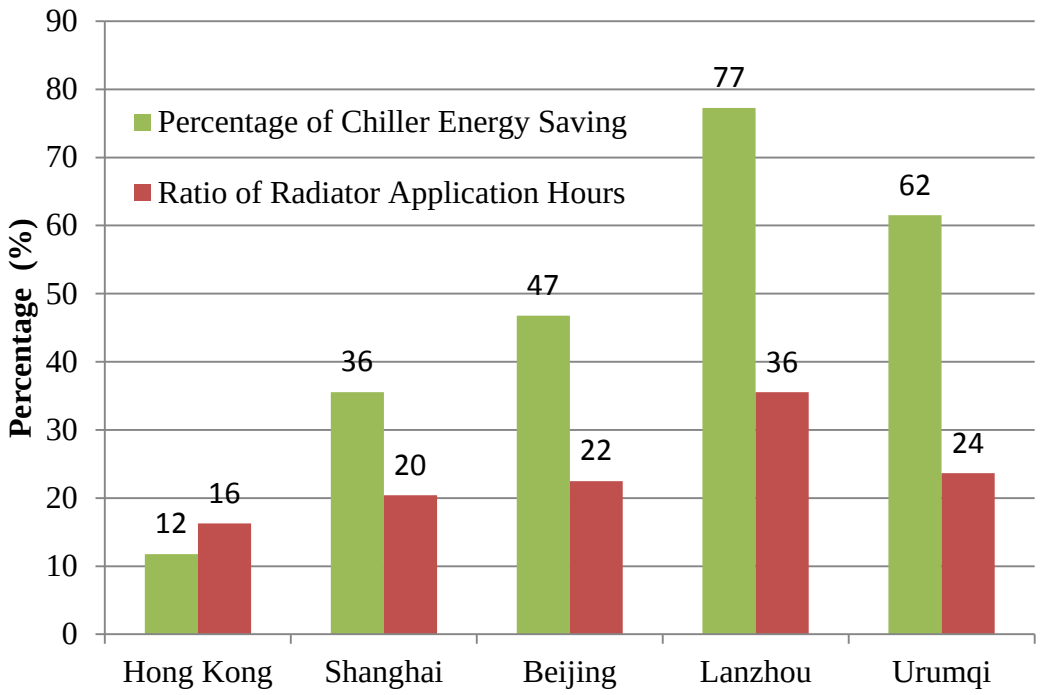

Figure 5.14 Percentage of chiller energy saving and the utilization ratio of nocturnal radiator

5.4.3.3 Nocturnal Radiator Application in Different Types of Buildings

The area of radiator is one of the key parameters affecting the cooling capacity. In the practical building design, especially in big cities, there is usually not spacious place for the radiator installation. Limited to the deficiency of the site, roof is ordinarily the best choice for the radiator setting. In previous research in this study, the calculation and analysis focus on a one floor building, for which the area of radiators is almost the same as the roof area. When the technology utilized in high-rise buildings, the situation is different from low-rise buildings. For high-rise buildings, the load demand increases at the double rate of the floor number, but the radiator area remains the same, which means the radiative cooling capacity cannot

increase with the load demand. Therefore, in general, the nocturnal radiative cooling can only supply partial cooling load for high-rise building due to the room limit.

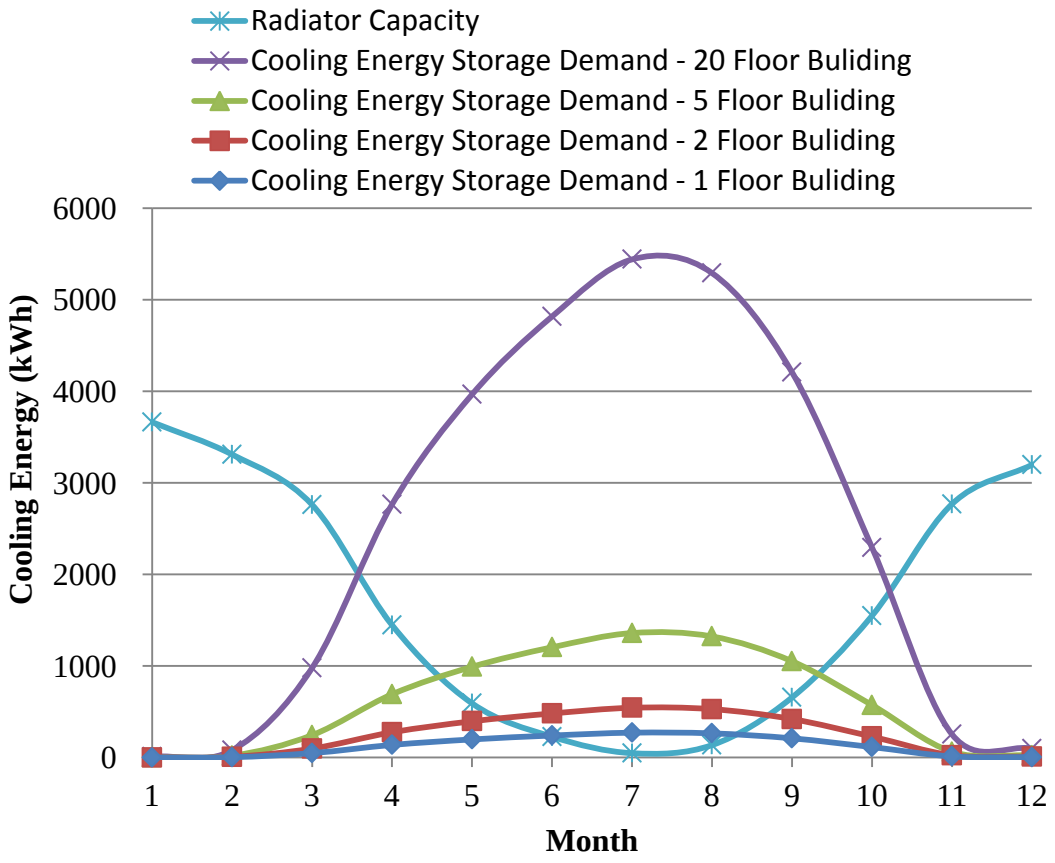

Figure 5.15 Supply-demand relationship of nocturnal sky radiator system for different types of buildings in Urumqi

Figure 5.15 shows the supply-demand relationship of nocturnal sky radiator system for different types of buildings in Urumqi. The standard floor of the multi-floor building is the same as the one floor building, so the monthly cooling load demand of the multi-floor building is simply calculated through multiplying the one floor building load by floor number, and the radiator area, which means the radiator capacity, is the same of all the buildings according to the same roof area. Similar

with the one floor building result in Figure 5.11, the cooling energy storage demand of multi-floor building cross the radiator capacity with two points respectively, which represent two points when the radiator supply capacity can just satisfy the cooling demand. The area enclosed by x-axis and the minimum value of the capacity and the cooling demand shows the situation that the cooling energy storage demand can be satisfied by nocturnal sky radiator, which mainly occurs in transition season. In winter, although the radiator capacity is large, the cooling demand is very limited, so the nocturnal radiation, the natural cooling source, cannot be fully utilized. On the other hand, in summer, the radiator capacity is so limited that it cannot meet the rapid increasing of the cooling load demand, especially in high-rise building. In such situation, the residual cooling energy storage demand has to be satisfied by supplemental mechanical chiller. Furthermore, it is noted that the two cross points gradually move from the central to the two sides with the increasing of the floor number. For one floor building, the radiator capacity can just meet the cooling demand in June and August, but it happens in March and October for the 20 floor building, which verifies the previous primary analysis that the limited room for radiator setting leads to the scantly cooling supply especially for high-rise buildings. Thus, it is necessary to employ annual dynamic simulation method to analysis such hybrid system in individual practical system design to increase the utilization ratio of natural cooling source.

To further evaluate the relationship of the natural cooling source utilization efficiency and the limitation situation of multi-floor building, an index, radiator area ratio, is employed in this study and defined as follows:

$$\text{Radiator area ratio} = A_{rad} / A_b \quad (5.19)$$

where A_b is the building area (m^2). On the assumption in this study that the radiator area is equal to the roof area, for one floor building, the radiator area ratio is 1, and for 20 floor building, it is 0.05.

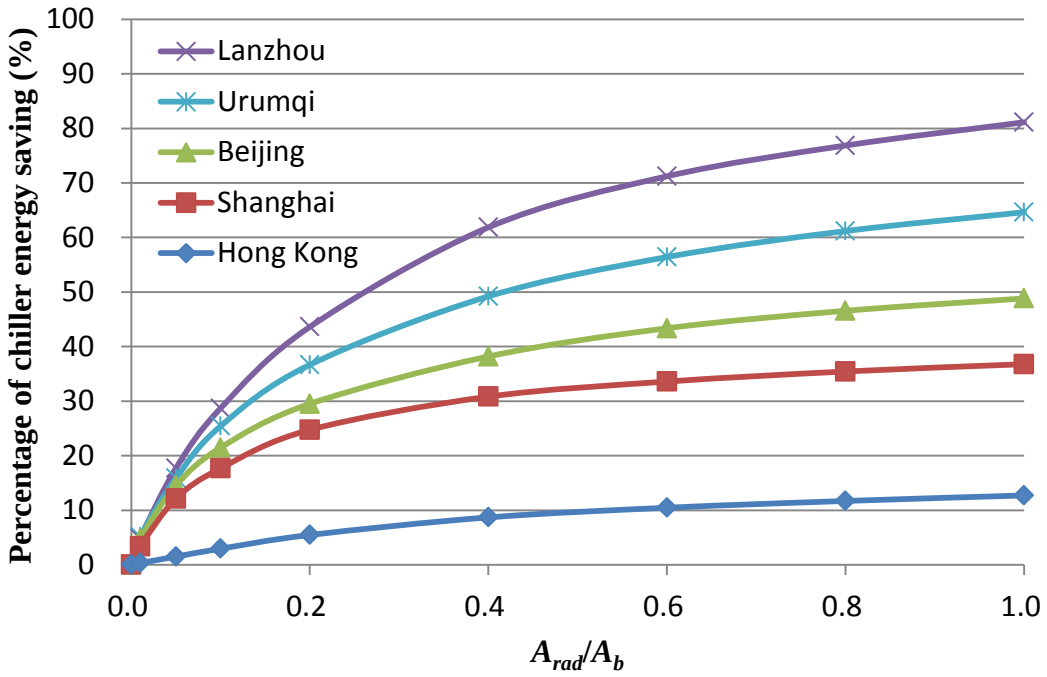

Figure 5.16 Chiller energy saving percentage of the hybrid system for different types of buildings

Figure 5.16 shows the percentage of chiller energy saving of the hybrid system for different types of buildings in the five cities across China. The percentage of chiller energy saving decreases as A_{rad}/A_b decreases, and it decreases faster as the A_{rad}/A_b becomes smaller. The change of the percentage of chiller energy saving shows the same trend in all the five cities. For low-rise building in Lanzhou, one floor building (A_{rad}/A_b=1), for instance, percentage of chiller energy saving can reach to 81%, a relatively high level. It is illustrated that nocturnal radiator can afford most of the

demand of MPCM slurry storage, and only small amount of the load demand is supplied by the electric chiller, which results in a high reduction of chiller electricity consumption. For high-rise building in Lanzhou, 20 floor building (A_{rad}/A_b=0.05), for instance, the percentage of chiller energy saving rapidly decreases to 18%, which indicates the nocturnal radiative cooling cannot satisfy the rapidly increasing cooling load demand as the floor number increases. The major problem to estimate the life cycle cost of the system is the MPCM slurry has not been produced in industry, which significantly increases the initial cost of the system. Therefore, detailed economic assessment is recommended when using nocturnal radiative cooling technology, especially for high-rise buildings.

5.5 Conclusions

A new design of hybrid system consisting of an MPCM slurry storage tank and a nocturnal sky radiator is proposed and mathematically modeled in this chapter. MPCM slurry appears to be a good medium for the combined application of passive cooling technology and nocturnal radiation in an air conditioning system due to its relatively high working temperature. During night time, cooling absorbed by the nocturnal sky radiator and generated by an electrically powered chiller for supplementary is stored in MPCM slurry in latent heat. During daytime, the stored cooling is released to remove sensible heat in the room, and the supplementary chiller is used to provide the peak load in case of demand. For ventilation purpose, fresh air treated by an AHU is supplied to the room at a flow rate to fulfill health and thermal comfort requirements.

The cooling energy consumption and the effect of an energy-free nocturnal radiation application are simulated by using the energy simulation code ACCURACY and the MATLAB model based on hour-by-hour calculations. A systematic analysis of the cooling capacity and energy saving potential of the hybrid system combined with the nocturnal radiation and cooling energy storage system has been conducted for five typical cities across China, from north to south, Urumqi, Beijing, Lanzhou, Shanghai and Hong Kong based on the local meteorological records. In general, Lanzhou and Urumqi have the most evident annual energy saving effect and largest cooling capacity of utilizing nocturnal sky radiative cooling system. The energy saving potential can reach 77% and 62% in the two cities, which exhibits a strong attractions for building energy conservation and emission reduction. Hong Kong has the weakest effect in the five typical cities under the same operating conditions due to the hot and humid climate conditions. The utilization potential in Shanghai and Beijing is also considerable and cannot be ignored. In addition, low-rise building reflects sufficient preponderance in utilizing the nocturnal radiative cooling technology compared with high-rise building, because it is easier for the ratio of the radiator area to the building area to reach a desired value. The following issues are necessary to be studied to enhance the cooling capacity of nocturnal radiator, which help to overcome the limitation of room shortage for radiator installation, including increasing radiation emissivity of the radiator surface and reducing heat gain by convective heat transfer.

The present hybrid system is recommended to be used in Northern, west and central Chinese cities where the weather is dry and the ambient temperature is low at night. The utilization of storing cooling absorbed through nocturnal radiation is based on

the development of novel phase change material and an optimized system design. A good energy saving potential is expected to be fulfilled by proper system configuration and strict control strategy.

Chapter 6

Conclusions and Suggestions for Future Research

With respect to the identified research questions as presented in the first chapter, i.e. the effect of supercooling on the effective cooling storage capacity of MPCM slurry as TES medium, how to effectively prevent supercooling of MCPM slurry and how to combined nocturnal sky radiator with MCPM slurry, the main objectives of this thesis were focused on the three research outputs, including obtaining empirical equation describing the relationship of supercooling and the effective cooling storage capacity of MPCM slurry, obtaining proper nucleating agent with effective concentration range and operating process for supercooling decreasing of MPCM, and building an simulation model to evaluate the potential of energy saving of the hybrid system combined with nocturnal sky radiator and MPCM slurry TES. The main findings of this research are translated into the following conclusions and future research activities.

6.1 Conclusions

6.1.1 Effect of Supercooling on MCPM Slurry as TES Medium

Thermal characterization of PCM and MPCM were investigated by using DSC. The DSC results showed the latent heat of fusion, melting and solidification temperatures and supercooling degree of the material.

A novel hybrid air conditioning system combined with MCPM slurry TES and cooled ceiling system were designed and used to measure the dynamic heat transfer performance of the hybrid system under the practical operation scheme. Heat balance method was used to calculate the heat loss and to verify the accuracy of the test system is satisfactory. The water slurry of microencapsulated n-hexadecane with a melting temperature of 15.7 ℃ was cooled to 5 ℃ and heated to 25 ℃ cyclically in a storage tank of 230 litre. Melting and crystallization behaviours of MPCM slurry running in a thermal storage test system under different mixer speed were investigated experimentally. Supercooling and effective latent heat of MPCM slurry were also investigated.

The results from tests with the MPCM slurry described the practical operating status of using MPCM slurry as TES medium in a hybrid air conditioning system. It proved that, when the temperature of charging and discharging are respectively at 5 °C and 20 °C, the chiller efficiency compares well with chilled water storage and the volumetric storage capacity is 2.2 times that of liquid water. The impact of the supercooling phenomenon on the storage capacity was experimentally assessed. For the specific MPCM investigated, the effective latent heat relates to the end temperature, and is around 80% of the thermodynamic latent heat when cooled to around 8 ^{o}C. However, to utilize natural cooling sources such as evaporative cooling for building cooling, a higher storage temperature of around 17 ℃ would be desirable. In this respect, the MPCM used in this study would offer very limited cooling storage capacity at this temperature due to the supercooling that occurred, but it would work effectively in climates where natural cooling, such as nocturnal sky radiative cooling, can cool the slurry to around 7 ℃. This analysis demonstrates that developing a PCM

working at a temperature of around 17℃ with small supercooling can greatly maximise the opportunities for using natural cooling sources for building cooling applications.

Finally, two correlation equations in the form of polynomial regression, accounting for the hysteresis associated with the melting and solidification processes were obtained. The empirical equations described the relationship between the effective latent heat and the charging temperature, which can be used for determining the medium mass needed for a specified working temperature range. The experiments also demonstrated that a PCM working at the temperature of 17°C can greatly maximize the opportunities of using natural cooling sources for building cooling applications.

6.1.2 Prevention of Supercooling

In this study, MWCNT particles were dispersed in an organic liquid n-hexadecane used to decrease supercooling. Various surfactants were tested as additives to overcome the rapid aggregation and sedimentation of the nanoparticles in the organic liquid, and the morphology of nano-additives was observed by TEM. Moreover, the dispersion and stability of nano-additives in PCM was measured under DLS analysis. The average particle size and the polydispersity index were also analyzed by the Zetasizer Advanced Software. Finally, Thermal performance of the n-hexadecane with well dispersed MWCNT particles at concentrations ranging from 0.1%-10% w/w was measured by DSC to evaluate the supercooling prevention effect of n-hexadecane.

It was difficult to disperse the original MWCNT particles in an n-hexadecane liquid. The surfactant used to disperse MWCNT must be soluble to the n-hexadecane, and the results showed that the functional group in the surfactants that are supposed to react with the acid groups in MWCNT should be as exposed as possible, otherwise the branch near the functional group would produce hindrance and lower the dispersion effect. Stable and homogenous dispersion was attained through surface modification of the MWCNT particles with strong acids H_2SO_4 and HNO_3, plus the addition of 1-decanol as a surfactant to the organic liquid. Among all chemicals used, 1-decanol showed the best performance of dispersion for both original and modified MWCNT. The average hydrodynamic diameter of MWCNT-1-decanol in n-hexadecane was 2.76 μm as measured by DLS analysis. The range difference within the repeated measurements was +36.1 nm, therefore the MWCNT particles were well dispersed. The visible aggregation was negligible even after seven days.

Thermal analysis of the n-hexadecane with well dispersed MWCNT particles by DSC indicated with the addition of 0.1wt% MWCNT, the supercooling of n-hexadecane was significantly decreased by 43%, which produced the most significant effect among the test samples. There was an effective concentration range (<0.5wt%) of nanoparticles for supercooling reduction, and better results cannot be obtained by continuously increasing nanoparticle concentration. It appears that well dispersed nanoparticles provided stable foreign nuclei of proper size to promote the heterogeneous nucleation process and accelerate crystallization process, thus the supercooling was significantly reduced. The obvious effects of MWCNT particles on the decrease of supercooling of n-hexadecane provide promising way of improving

the performance of system energy efficiency in building cooling and heating applications.

In terms of the crystal structure, the crystal structure of n-hexadecane is triclinic structure, and that of MWCNT particles with a diameter of 10-20 nm is honeycomb structure. The similar crystal structure of MWCNT and n-hexadecane is the basis for MWCNT to be used as the nucleating agent. The experimental results help to confirm this hypothesis: without any foreign additives, formation of stable nuclei relying on homogeneous nucleation is a "sluggish" process, which is the main cause of large supercooling.

The small concentration of additives required has a number of positive implications for the potential engineering application of the technology. Firstly, it will have negligible impact on the volumetric latent heat of the PCM; secondly, the cost of the nano materials can be much reduced.

6.1.3 Nocturnal Radiative Cooling Potential with MPCM slurry Storage

The previous study about the thermal performance of MPCM slurry in thermal storage applications and the prevention of supercooling by nucleus agents provide proper medium with relative high working temperature and well thermal properties to utilize natural cooling source in air conditioning system more easily. Based on such investigation result, a mathematical model of the hybrid system combined with nocturnal sky radiator and MPCM slurry TES was built. The cooling energy consumption and the effect of energy-free nocturnal radiation application were

simulated by using the energy simulation code ACCURACY and MATLAB model based on hour-by-hour calculations.

It can be drawn that MPCM slurry appears to be a good medium for the combined application of passive cooling technology and the nocturnal radiation in air conditioning system due to its relatively high working temperature. During night time, cooling absorbed by the nocturnal sky radiator is stored in MPCM slurry in latent heat. During daytime, the stored cooling is released to remove sensible heat in the room. PCMs with different melting temperature as the working temperature can be chosen as the core material of MCPM slurry to satisfy various demands in different application situations.

A systematic analysis about cooling capacity and energy saving potential of the hybrid system combined with nocturnal radiation and cooling energy storage system of a low-rise building has been conducted for five typical cities across China, from north to south, Urumqi, Beijing, Lanzhou, Shanghai and Hong Kong based on the local meteorological records. In general, Lanzhou and Urumqi have the most evident annual energy saving effect and largest cooling capacity of utilizing of nocturnal sky radiative cooling system. The energy saving potential can reach 77% and 62% in the two cities for low-rise buildings, which exhibits strong attractions for building energy conservation and emission reduction. Hong Kong has the weakest effect in the five typical cities under the same operating condition due to the hot and humid climate condition. The utilization potential in Shanghai and Beijing is also considerable and cannot be ignored.

It can be also drawn that, in such nocturnal radiative cooling system, radiator area is one of the most important factors impacting the nocturnal radiation capacity directly, which is subject to different building types. On the assumption that the whole roof is full of nocturnal radiator, the nocturnal radiative cooling utilization efficiency and energy saving of the hybrid system of traditional low-rise building is distinctly superior to high-rise commercial building. This conclusion is demonstrated graphically and convincingly by comparing the relations between nocturnal radiative cooling supply and building cooling demand under different ratios of roof to building area. Increasing radiation emissivity of the radiator surface and reducing heat gain by convective heat transfer are two effective methods help to overcome the limitation of room shortage for radiator installation.

The present hybrid system is recommended to be used in Northern west and central China cities where the weather is dry and the ambient temperature is low at night. The utilization of storing cooling absorbed through nocturnal radiation is based on the development of novel phase change material and optimized system design. A good energy saving potential is expected to be fulfilled by proper system configuration and strict control strategy.

6.2 Suggestions for Future Research

Some of the techniques used in this study can be deepened and expanded, for instant, looking for other type particles as nucleating agent and the optimization of the hybrid system to fully utilize the natural cooling resources. Moreover, the present work can also be further extended to better understanding of the flow and heat transfer

behaviors of the MPCM emulsion, and experimental investigations of the MPCM emulsion storage. Thus, the following recommendations can be given.

- For nanoparticle dispersion, it can be expected that using 1-decanol to disperse MWCNT in other higher molecular alkanes that are similar to hexadecane such as pentadecane and heptadecane is possible. The experimental results in this study may also imply that it is also possible using other fatty alcohols, such as nonadecan-1-ol and undecan-1-ol, which have similar structures to 1-decanol to assist to disperse MWCNT in hexadecane.

- Other types of nano materials such as ZnO and TiO_2, spherical nano particles, can also be tested as seeds, namely nucleating agents, for crystallization, and thereby reduce the supercooling of the PCM. Special recipes will be developed to formulate PCM medium which achieve good functional performances.

- Following the classical theory of nucleation, the formation of the nuclei is associated with a change in Gibbs free energy, as a function of nucleus radius. There is a critical value of free energy as a barrier for nucleation, and only when the nucleus radius is larger than the critical value, the free energy of the nucleus will reduce with an increase in its size, which means stable nuclei of critical size can be formed. Based on this theory, the effect of the nucleation agent particle size on the supercooling prevention can be further investigated and discussed. Proper and effective range of the additive size is proposed for different PCM.

- The method in this study, using nanoparticles as nucleating agent to prevent supercooling, focus on the bulk PCM hexadecane at this stage. The similar application can be expanded to PCM microcapsule/water slurry. The size of capsules with PCM in it is of micrometer range, so the nanoparticles size cannot be neglected compare to the capsule. It is important to investigate about the homogeneous distribution and foreseeable amount of nanoparticles in every capsule. Furthermore, the nucleation progress in such small space is need to be investigated, and weather the nanoparticles can still have the same effect on the MCPM slurry is also need to be verified.

- For the performance evaluation of the hybrid system, some models of the system component are simplified, such as the heat exchanger and the primary equipment. In addition, an elementary control scheme is employed in this study to evaluate the energy saving potential of using MPCM slurry TES and nocturnal sky radiative cooling technology. The simulation model can be further refined to describe the practical operation of the system more reliably. The system composition and the control strategy can be optimized to improve the operation efficiency and exploit greater energy saving potential applying the constructal law (Bejan and Lorente 2008).

- In the present study, the performance of nocturnal sky radiator system running with MPCM slurry was investigated by the dynamic simulation model. To gain more insight into the dynamic thermal behaviors of the MPCM slurry in the ceiling panels and MPCM slurry storage tank, an experimental investigation is recommended to implement for a combined system.

- It became clear that an alternative medium form, PCM/water emulsions, namely PCM droplets dispersed in water with the assistance of emulsifiers (Inaba 2000), can be an attractive option enrolled in the TES technology for building energy saving applications (Inaba and Morita 1995). It is expected all the heat transfer and fluid flow advantages of MPCM/water slurry can be retained while the potential cost of the microencapsulation, i.e., the polymerization of the shell, as well as the potential abrasion loss or mechanical damage due to the stirring in applications can all be avoided. The emulsion as a storage medium appears to be the compromise between the bulk PCM and MPCM slurry form, in which the supporting or coating materials cause additional costs and often increase the viscosity as well as the heat transfer resistance.

- The previous limited work about PCM/water emulsion by Inaba and Morita (1995) and Yang, Xu et al. (2003) indicated that instability and supercooling are the two major problems of using paraffin dispersions, although stabilization of emulsions have long been proved in the food industry (Binks 1998; Sangwal 2007). In the very recent work reported by Huang et al (Huang, Petermann et al. 2009; Huang, Doetsch et al. 2010; Huang, Günther et al. 2010; Huang and Weidner 2010)and Gunther et al (Günther, Schmid et al. 2010; Günther, Huang et al. 2011), it was found that subcooling worsens with decreasing emulsion droplet size, and the supercooling of hexadecane emulsions can be decreased with the addition of a paraffin of a higher-melting temperature as the nucleating agent. In addition, there is also some significant studies should be followed up. For instance, virtually no studies have been done on the heat transfer rates under

actual thermal storage conditions, and there is obviously a need for study leading to the optimized droplet sizes for the dispersed PCM phase, taking into account subcooling avoidance, viscosity reduction and heat transfer enhancement.

References

Abu-Nada, E. (2008). "Application of nanofluids for heat transfer enhancement of separated flows encountered in a backward facing step." International Journal of Heat and Fluid Flow **29**(1): 242-249.

Agafonov, I. A., I. K. Garkushin, et al. (1999). "Patterns of phase diagram changes in series of n-alkane binary systems." Journal of Physical Chemistry **73**(5): 681-685.

Ai, Y., Y. Jin, et al. (2007). "Microencapsulation of n-hexadecane as phase change material by suspension poly merization." e-Polymers **September**(98): 1-9.

Alvarado, J., C. Marsh, et al. (2006). "Characterization of supercooling suppression of microencapsulated phase change material by using DSC." Journal of Thermal Analysis and Calorimetry **86**(2): 505-509.

Annex14 Cooling in all climate with thermal energy storage. Annex 14, Subtask 3 Report from Japan.

Argiriou, A., M. Santamouris, et al. (1994). "Assessment of the radiative cooling potential of a collector using hourly weather data." Energy **19**(8): 879-888.

Athienitis, A. K., C. Liu, et al. (1997). "Investigation of the thermal performance of a passive solar test-room with wall latent heat storage." Building and Environment **32**(5): 405-410.

Banu, D., D. Feldman, et al. (1998). "Evaluation of thermal storage as latent heat in phase change material wallboard by differential scanning calorimetry and large scale thermal testing." Thermochimica Acta **317**(1): 39-45.

Bejan, A. and S. Lorente (2008). Design with Constructal Theory. Hoboken, Wiley.

Berdahl, P. and M. Martin (1984). "Emissivity of clear skies." Solar Energy **32**(5): 663-664.

Binks, B. P. (1998). Emulsions - recent advances in understanding. Modern Aspects of Emulsion Science. B. P. Binks. Cambridge, The Royal Society of Chemistry**:** 1-55.

Bliss, R. W. (1961). "Atmospheric radiation near the surface of the ground: A summary for engineers." Solar Energy **5**(3): 103-120.

Broadhurst, M. (1962). "An analysis of the solid phase behaviour of the normal paraffins." Research of the National Bureau of Standards – A. Physics and Chemistry **66A**(3): 241-249.

Butala, V. and U. Stritih (2006). "Cold storage with phase change material for building ventilation." Vincenc Butala and Uroš Stritih **5**(2): 189-198.

Butala, V. and U. Stritih (2009). "Experimental investigation of PCM cold storage." Energy and Buildings **41**(3): 354-359.

Byung Chul, S., K. Sang Done, et al. (1989). "Phase separation and supercooling of a latent heat-storage material." Energy **14**(12): 921-930.

Cai, Y. B., L. Song, et al. (2008). "Preparation, thermal and flammability properties of a novel form-stable phase change materials based on high density polyethylene/poly(ethylene-co-vinyl acetate)/organophilic montmorillonite nanocomposites/paraffin compounds." Energy Conversion and Management **49**(8): 2055-2062.

Charunyakorn, P., S. Sengupta, et al. (1991). "Forced convection heat transfer in microencapsulated phase change material slurries: flow in circular ducts." International Journal of Heat and Mass Transfer **34**(3): 819-833.

Chen, B., X. Wang, et al. (2008). "An experimental study of convective heat transfer with microencapsulated phase change material suspension: Laminar flow in a circular tube under constant heat flux." Experimental Thermal and Fluid Science **32**(8): 1638-1646.

Chen, Q. and J. V. D. Kooi (1988). "ACCURACY — A computer program for combined problems of energy analysis, indoor airflow, and air quality." ASHRAE Transactions **94**(2): 196-214.

Clark, E. and P. Berdahl (1980). Radiative cooling: resource and applications. the passive cooling workshop, the fifth national passive solar conference. M. Harry. mherst, Massachusetts, US Department of Energy Publication**:** 219-254.

Clark, G. and C. Allen (1978). The Estimation of Atmospheric Radiation for Clear and Cloudy Skies. Proceedings 2nd National Passive Solar Conference (AS/ISES)**:** 675-678.

Clausse, D., J. P. Dumas, et al. (1987). "PHASE TRANSFORMATIONS IN EMULSIONS. I PHASE TRANSFORMATIONS IN EMULSIONS : PART I : EFFECTS OF THERMAL TREATMENTS ON NUCLEATION PHENOMENA : EXPERIMENTS AND MODEL." Journal of Dispersion Science and Technology **8**(1): 1 - 28.

Din çer, I. and M. A. Rosen (2010). Thermal energy storage : systems and applications Chichester ; New York : Wiley.

Ding, Y., H. Alias, et al. (2006). "Heat transfer of aqueous suspensions of carbon nanotubes (CNT nanofluids)." International Journal of Heat and Mass Transfer **49**(1-2): 240-250.

Dirand, M., M. Bouroukba, et al. (2002). "Normal Alkanes, Multialkane Synthetic Model Mixtures, and Real Petroleum Waxes: Crystallographic Structures, Thermodynamic Properties, and Crystallization." Journal of Chemical & Engineering Data **47**(2): 115-143.

Dobson, R. T. (2005). "Thermal modelling of a night sky radiation cooling system." Journal of Energy in South Africa **16**(2).

Duffie, J. A. and W. A. Beckman (1991). Solar Engineering of Thermal Processes. NY, Wiley.

Duffie, J. A. and W. A. Beckman (2006). Solar Engineering of Thermal Processes. NY, Wiley.

Erell, E. and Y. Etzion (2000). "Radiative cooling of buildings with flat-plate solar collectors." Building and Environment **35**(4): 297-305.

Evers, A. C., M. A. Medina, et al. (2010). "Evaluation of the thermal performance of frame walls enhanced with paraffin and hydrated salt phase change materials using a dynamic wall simulator." Building and Environment **45**(8): 1762-1768.

Fan, Y. (2003). Fabrication, Thermal Stability and Super-cooling of Nano and Microencapsulated Phase Change Materials (in Chinese), MSc Thesis. MSc, Tianjin Polytechnic University.

Farid, M. M., A. M. Khudhair, et al. (2004). "A review on phase change energy storage: materials and applications." Energy Conversion and Management **45**(9-10): 1597-1615.

Feldman, D., D. Banu, et al. (1993). Energy storage building materials with organic PCM's. Proceedings of the 28th Intersociety Energy Conversion Engineering Conference **2:** 143-148.

Günther, E., L. Huang, et al. (2011). "Subcooling in PCM emulsions – Part 2: Interpretation in terms of nucleation theory." Thermochimica Acta **522**(1-2): 199-204.

Günther, E., T. Schmid, et al. (2010). "Subcooling in hexadecane emulsions." International Journal of Refrigeration **33**(8): 1605-1611.

Garg, H. P., S. C. Mullick, et al. (1985). Solar Thermal Energy Storage, D. Reidel Publishing Company.

Genovese, A., G. Amarasinghe, et al. (2006). "Crystallisation, melting, recrystallisation and polymorphism of n-eicosane for application as a phase change material." Thermochimica Acta **443**(2): 235-244.

Givoni, B. (2011). "Indoor temperature reduction by passive cooling systems." Solar Energy **85**(8): 1692-1726.

Gschwander, S., P. Schossig, et al. (2005). "Micro-encapsulated paraffin in phase-change slurries." Solar Energy Materials and Solar Cells **89**(2-3): 307-315.

Hamza H. Ali, A., I. M. S. Taha, et al. (1995). "Cooling of water flowing through a night sky radiator." Solar Energy **55**(4): 235-253.

Hatakeyama, T. and F. X. Quinn (1999). Thermal analysis : fundamentals and applications to polymer science. New York, John Wiley and Sons Inc.

He, B. (2004). High-Capacity Cool Thermal Energy Storage for Peak Shaving - A Solution for Energy Challenges in the 21st Century. PhD, Royal Institute of Technology.

He, B., V. Martin, et al. (2003). "Liquid–solid phase equilibrium study of tetradecane and hexadecane binary mixtures as phase change materials (PCMs) for comfort cooling storage." Fluid Phase Equilibria **212**(1-2): 97-109.

He, B., V. Martin, et al. (2004). "Phase transition temperature ranges and storage density of paraffin wax phase change materials." Energy **29**(11): 1785-1804.

He, B. and F. Setterwall (2002). "Technical grade paraffin waxes as phase change materials for cool thermal storage and cool storage systems capital cost estimation." Energy Conversion and Management **43**(13): 1709-1723.

He, Q., W. Tong, et al. (2007). "Experimental study on super-cooling degree of nanofluids for cryogenic cool storage (in Chinese)." Journal of Refrigeration **28**(4): 33-36.

Heidarinejad, G., M. Farmahini Farahani, et al. (2010). "Investigation of a hybrid system of nocturnal radiative cooling and direct evaporative cooling." Building and Environment **45**(6): 1521-1528.

Hu, X. and Y. Zhang (2002). "Novel insight and numerical analysis of convective heat transfer enhancement with microencapsulated phase change material slurries: laminar flow in a circular tube with constant heat flux." International Journal of Heat and Mass Transfer **45**(15): 3163-3172.

Huang, L., C. Doetsch, et al. (2010). "Low temperature paraffin phase change emulsions." International Journal of Refrigeration **33**(8): 1583-1589.

Huang, L., E. Günther, et al. (2010). "Subcooling in PCM emulsions--Part 1: Experimental." Thermochimica Acta **509**(1-2): 93-99.

Huang, L., P. Noeres, et al. (2010). "Experimental study on heat capacity of paraffin/water phase change emulsion." Energy Conversion and Management **51**(6): 1264-1269.

Huang, L., M. Petermann, et al. (2009). "Evaluation of paraffin/water emulsion as a phase change slurry for cooling applications." Energy **34**(9): 1145-1155.

Huang, L. and E. Weidner (2010). Paraffin/water phase change emulsion for cold storage and distribution applications, Laufen, Oberhausen.

Hwang, Y., J. K. Lee, et al. (2007). "Stability and thermal conductivity characteristics of nanofluids." Thermochimica Acta **455**(1-2): 70-74.

Hwang, Y., H. S. Park, et al. (2006). "Thermal conductivity and lubrication characteristics of nanofluids." Current Applied Physics **6**(Supplement 1): e67-e71.

IEA (2002). Optimization of Cool Thermal Storage and Distribution. IEA District Heating and Cooling - Programme of Research, Development and Demonstration on District Heating and Cooling, Including the Integration of CHP, International Energy Agency (IEA). **5**.

Inaba, H. (2000). "New challenge in advanced thermal energy transportation using functionally thermal fluids." International Journal of Thermal Sciences **39**(9-11): 991-1003.

Inaba, H., M.-K. Kim, et al. (2004). "Melting heat transfer characteristics of microencapsulated phase change material slurries with plural microcapsules having different diameters." Journal of Heat Transfer **126**(4): 558-565.

Inaba, H. and S. Morita (1995). "Flow and cold heat-storage characteristics of phase-change emulsion in a coiled double-tube heat exchanger." Journal of Heat Transfer **117**(2): 440-446.

Ito, S. and N. Miura (1989). "Studies of Radiative Cooling Systems for Storing Thermal Energy." Journal of Solar Energy Engineering **111**(3): 251-256.

Kakaç S. and A. Pramuanjaroenkij (2009). "Review of convective heat transfer enhancement with nanofluids." International Journal of Heat and Mass Transfer **52**(13-14): 3187-3196.

Kasza, K. E. and M. M. Chen (1985). "Improvement of the performance of solar energy or waste heat utilization systems by using PHASE-CHANGE slurry as an enhanced heat-transfer storage fluid." Journal of Solar Energy Engineering, Transactions of the ASME **107**(3): 229-236.

Kaygusuz, K. (1999). "Investigation of a combined solar-heat pump system for residential heating. Part 1: Experimental results." International Journal of Energy Research **23**(14): 1213-1223.

Khedari, J., J. Waewsak, et al. (2000). "Field investigation of night radiation cooling under tropical climate." Renewable Energy **20**(2): 183-193.

Khudhair, A. M. and M. M. Farid (2004). "A review on energy conservation in building applications with thermal storage by latent heat using phase change materials." Energy Conversion and Management **45**(2): 263-275.

Kim, Y. J., H. M. and, et al. (2010). "Plasma nanocoated carbon nanotubes for heat transfer nanofluids." Nanotechnology **21**(29): 295703-295703.

Kimball, B. A. (1985). "Cooling performance and efficiency of night sky radiators." Solar Energy **34**(1): 19-33.

Kissock, J., J. Hannig, et al. (1998). Testing and simulation of phase change wallboard for thermal storage in buildings. Proceedings of 1998 International Solar Energy Conference. J. M. Morehouse and R. E. Hogan. New York, USA**:** 45-52.

Lane, G. A. (1983). Solar heat storage : latent heat materials; V1: Background and Scientific Principles, CRC Press,Inc. Boca Raton,Florida.

Lee, T., D. W. Hawes, et al. (2000). "Control aspects of latent heat storage and recovery in concrete." Solar Energy Materials and Solar Cells **62**(3): 217-237.

Lee, W.-m. (2004). Microcapsule containing phase change material and article having same. United States.

Li, Y. and Q. Zhu (2004). "A Model of Heat and Moisture Transfer in Porous Textiles with Phase Change Materials." Textile Research Journal **74**(5): 447-457.

Lin, K., Y. Zhang, et al. (2005). "Experimental study of under-floor electric heating system with shape-stabilized PCM plates." Energy and Buildings **37**(3): 215-220.

Liu, Y. (2005). Study on Preparation and Thermal Properties of Phase Change Nanocomposites for Cool Storage (in Chinese), PhD Thesis. PhD, Chongqing University.

MacCracken, M. (2010). "Energy Storage: Provding for a Low-Carbon Future." ASHRAE Journal **52**(9): 28-36.

Marie, E., Y. Chevalier, et al. (2005). "Control of n-alkanes crystallization by ethylene–vinyl acetate copolymers." Journal of Colloid and Interface Science **290**(2): 406-418.

Marinković, M., R. Nikolić, et al. (1998). "Thermochromic complex compounds in phase change materials: Possible application in an agricultural greenhouse." Solar Energy Materials and Solar Cells **51**(3-4): 401-411.

McAdams, W. H. (1954). Heat Transmission. New York, McGraw-Hill.

Mehling, H. and L. F. Cabeza (2008). Heat and cold storage with PCM. Berlin ; London, Springer.

Michell, D. and K. L. Biggs (1979). "Radiation cooling of buildings at night." Applied Energy **5**(4): 263-275.

Mihalakakou, G., A. Ferrante, et al. (1998). "The cooling potential of a metallic nocturnal radiator." Energy and Buildings **28**(3): 251-256.

Mitchell, J. W. (1976). "Heat transfer from spheres and other animal forms." Biophysical Journal **16**(6): 561-569.

Mnyukh, Y. (1960). "The structure of normal paraffins and of their solid solutions." Journal of Structural Chemistry **1**(3): 346-365.

Moler, C. B. (2004). Numerical computing with MATLAB, Chapter 4.2, Philadelphia SIAM, Soc. for Industrial and Applied Math.

Mostrel, M. and B. Givoni (1982). "Windscreens in radiant cooling." Passive Solar Journal: 229-238.

Niu, J. and J. V. D. Kooi (1994). "Indoor climate in rooms with cooled ceiling systems." Building and Environment **29**(3): 283-290.

Niu, J., J. v. d. Kooi, et al. (1995). "Energy saving possibilities with cooled-ceiling systems." Energy and Buildings **23**(2): 147-158.

Niu, J. L., L. Z. Zhang, et al. (2002). "Energy and humidity performance of a system combining chilled-ceiling with desiccant cooling." ASHRAE Transactions **108**(2): 195-201.

Okada, K., K. Watanabe, et al. (2007). "Supercooling ([Delta]T) dependence of nano-nucleation of PE by SAXS and proposal of a new nucleation theory." Polymer **48**(4): 1116-1126.

Oliver, M. J. and P. D. Calvert (1975). "Homogeneous nucleation of n-alkanes measured by differential scanning calorimetry." Journal of Crystal Growth **30**(3): 343-351.

Parker, D. S. (2005). Theoretical Evaluation of the NightCool Nocturnal Radiation Cooling Concept, Florida Solar Energy Center

University of Central Florida.

Rady, M. (2009). "Study of phase changing characteristics of granular composites using differential scanning calorimetry." Energy Conversion and Management **50**(5): 1210-1217.

Rastogi, R., R. Kaushal, et al. (2008). "Comparative study of carbon nanotube dispersion using surfactants." Journal of Colloid and Interface Science **328**(2): 421-428.

Regin, A. F., S. C. Solanki, et al. (2008). "Heat transfer characteristics of thermal energy storage system using PCM capsules: A review." Renewable and Sustainable Energy Reviews **12**(9): 2438-2458.

Ryu, H. W., S. A. Hong, et al. (1991). "Heat transfer characteristics of cool-thermal storage systems." Energy **16**(4): 727-737.

Saitoh, T., H. Matsuhashi, et al. (1985). "An energy-independent house combining solar thermal and sky radiation energies." Solar Energy **35**(6): 541-547.

Saitoh, T. and T. Ono (1984). "Utilization of Seasonal Sky Radiation Energy for Space Cooling." Journal of Solar Energy Engineering **106**(4): 403-407.

Saitoh, T. S. and T. Fujino (2001). "Advanced energy-efficient house (HARBEMAN house) with solar thermal, photovoltaic, and sky radiation energies (experimental results)." Solar Energy **70**(1): 63-77.

Sakamoto, M., A. Ohba, et al. (2004). "Influences of fatty acid moiety and esterification of polyglycerol fatty acid esters on the crystallization of palm mid fraction in oil-in-water emulsion." Colloids and Surfaces B: Biointerfaces **37**(1-2): 27-33.

Salyer, I. O. (2002). Phase change composition containing a nucleating agent. United States, Energy Storage Technologies Inc. (Dayton, OH).

Saman, W., F. Bruno, et al. (2005). "Thermal performance of PCM thermal storage unit for a roof integrated solar heating system." Solar Energy **78**(2): 341-349.

Sangwal, K. (2007). Additives and Crystallization Processes: From Fundamentals to Applications. West Sussex, John Wiley & Sons Ltd.

Santamouris, M. (2006). Passive cooling – the state of the art. Advances in Solar Energy. London, James and James Science Publishers.

Sarı, A., C. Alkan, et al. (2009). "Microencapsulated n-octacosane as phase change material for thermal energy storage." Solar Energy **83**(10): 1757-1763.

Sari, A. and K. Kaygusuz (2001). "Thermal Energy Storage System Using Some Fatty Acids as Latent Heat Energy Storage Materials." Energy Sources **23**(3): 275-285.

Sharma, A., V. V. Tyagi, et al. (2009). "Review on thermal energy storage with phase change materials and applications." Renewable and Sustainable Energy Reviews **13**(2): 318-345.

Sohn, C. W. and M. M. Chen (1981). "Microconvective thermal conductivity in disperse two-phase mixtures as observed in a low velocity Couette flow experiment." Journal of Heat Transfer. Transactions of the ASME **103**(1): 47-51.

Song, X., N. Jiang, et al. (2008). "Synthesis of CeO2-coated SiO2 nanoparticle and dispersion stability of its suspension." Materials Chemistry and Physics **110**(1): 128-135.

Stovall, T. K. and J. J. Tomlinson (1995). "What are the potential benefits of including latent storage in common wallboard?" Journal of Solar Energy Engineering, Transactions of the ASME **117**(4): 318-325.

Sun, G., G. Chen, et al. (2009). "A facile gemini surfactant-improved dispersion of carbon nanotubes in polystyrene." Polymer **50**(24): 5787-5793.

Suppes, G. J., M. J. Goff, et al. (2003). "Latent heat characteristics of fatty acid derivatives pursuant phase change material applications." Chemical Engineering Science **58**(9): 1751-1763.

Tersoff, J. and R. S. Ruoff (1994). "Structural Properties of a Carbon-Nanotube Crystal." Physical Review Letters **73**(5): 676.

Thumann, A. and D. P. Mehta (2008). Handbook of energy engineering, Taylor & Francis Ltd.

Tomura, K. and J. Kawasaki-shi (2010). Heat storage substance, heat storage agent, heat reservoir, heat transport medium, cold insulation agent, cold insulator, melting point control agent for heat storage agent, supercooling preventive agent for heat storage agent and method for producing main agent of heat storage agent heat transport medium, or cold insulation agent.

Tomura, K. and J. Kawasaki-shi (2010). Heat storage substance, heat storage agent, heat reservoir, heat transport medium, cold insulation agent, cold insulator, melting point control agent for heat storage agent, supercooling preventive agent for heat storage agent and method for producing main agent of heat storage agent heat transport medium, or cold insulation agent. United States.

Turner, W. R. (1971). "Normal Alkanes." Industrial Engineering Chemistry Product Research and Development **10**(3): 238-260.

U.S. Department of Energy website. from http://energy.gov/heating-cooling.

U.S. Department of Energy website. "Energy Efficiency and Renewable Energy." from http://apps1.eere.energy.gov/buildings/energyplus/weatherdata_about.cfm.

U.S. Energy Information Administration (2003). Commercial Buildings Energy Consumption Survey, U.S. Energy Information Administration.

Vaisman, L., H. D. Wagner, et al. (2006). "The role of surfactants in dispersion of carbon nanotubes." Advances in Colloid and Interface Science **128-130**: 37-46.

W.M, M. (1957). "Thermal analysis of normal alkanes." Analytica Chimica Acta **17**(0): 97-106.

Wang, J. F., H. Q. Xie, et al. (2009). "Thermal properties of paraffin based composites containing multi-walled carbon nanotubes." Thermochimica Acta **488**(1-2): 39-42.

Wang, X. and J. Niu (2009). "Performance of cooled-ceiling operating with MPCM slurry." Energy Conversion and Management **50**(3): 583-591.

Wang, X., J. Niu, et al. (2007). "Flow and heat transfer behaviors of phase change material slurries in a horizontal circular tube." International Journal of Heat and Mass Transfer **50**(13-14): 2480-2491.

Wang, X., J. Niu, et al. (2008). "Heat transfer of microencapsulated PCM slurry flow in a circular tube." AIChE Journal **54**(4): 1110-1120.

Wang, X., J. Niu, et al. (2008). "Raising evaporative cooling potentials using combined cooled ceiling and MPCM slurry storage." Energy and Buildings **40**(9): 1691-1698.

Weinläder, H., A. Beck, et al. (2005). "PCM-facade-panel for daylighting and room heating." Solar Energy **78**(2): 177-186.

Yamagishi, Y., T. Sugeno, et al. (1996). An evaluation of microencapsulated PCM for use in cold energy transportation medium. Energy Conversion Engineering Conference, 1996. IECEC 96. Proceedings of the 31st Intersociety, Washington, DC, USA.

Yamagishi, Y., H. Takeuchi, et al. (1999). "Characteristics of microencapsulated PCM slurry as a heat-transfer fluid." AIChE Journal **45**(4): 696-707.

Yamaha, M. (1997). A simulation model for thermal response of PCM installed in air distribution system. Proceedings of IEA Annex 10 "Phase change materials and chemical reactions for thermal energy storage", 1st workshop. Adana, Turkey.

Yamazaki, M., C. Sasaki, et al. (2002). "Thermal and structural characterization of trimethylolethane trihydrate." Thermochimica Acta **387**(1): 39-45.

Yang, R., H. Xu, et al. (2003). "Preparation, physical property and thermal physical property of phase change microcapsule slurry and phase change emulsion." Solar Energy Materials and Solar Cells **80**(4): 405-416.

Zalba, B., J. M. Marin, et al. (2003). "Review on thermal energy storage with phase change: materials, heat transfer analysis and applications." Applied Thermal Engineering **23**(3): 251-283.

Zalbaa, B., J. M. Marína, et al. (2004). "Free-cooling of buildings with phase change materials." International Journal of Refrigeration **27**(8): 839-849.

Zeng, R., X. Wang, et al. (2009). "Heat transfer characteristics of microencapsulated phase change material slurry in laminar flow under constant heat flux." Applied Energy **86**(12): 2661-2670.

Zhang, J., H. Zou, et al. (2003). "Effect of Chemical Oxidation on the Structure of Single-Walled Carbon Nanotubes." The Journal of Physical Chemistry B **107**(16): 3712-3718.

Zhang, X.-x., Y.-f. Fan, et al. (2005). "Crystallization and prevention of supercooling of microencapsulated n-alkanes." Journal of Colloid and Interface Science **281**(2): 299-306.

Zhang, X. J., P. Wu, et al. (2010). "Analysis of the nucleation of nanofluids in the ice formation process." Energy Conversion and Management **51**(1): 130-134.

Zhang, Y. and A. Faghri (1995). "Analysis of forced convection heat transfer in microencapsulated phase change material suspensions." Journal of Thermophysics and Heat Transfer **9**(4): 727-732.

Zhang, Y., H. Hu, et al. (1996). The theory and application of using phase change materials for energy storage (in Chinese). Heifei, University of Science and Technology of China Press.

Zhang, Y. P., K. P. Lin, et al. (2006). "Preparation, thermal performance and application of shape-stabilized PCM in energy efficient buildings." Energy and Buildings **38**(10): 1262-1269.

Zhou, G., Y. Zhang, et al. (2008). "Thermal analysis of a direct-gain room with shape-stabilized PCM plates." Renewable Energy **33**(6): 1228-1236.

Zhu, N., Z. Ma, et al. (2009). "Dynamic characteristics and energy performance of buildings using phase change materials: A review." Energy Conversion and Management **50**(12): 3169-3181.